AGARD-R-572-70

AGARD-R-572-70

AGARD

ADVISORY GROUP FOR AEROSPACE RESEARCH & DEVELOPMENT

7 RUE ANCELLE 92 NEUILLY-SUR-SEINE FRANCE

AGARD REPORT No. 572

on

Effect of Loading Frequency on the Strain Behaviour and Damage Accumulation in Low-cycle Fatigue

by

D.E. Gücer and M. Çapa

6/1970

NORTH ATLANTIC TREATY ORGANIZATION

DISTRIBUTION AND AVAILABILITY
ON BACK COVER

AGARD Report No.572

NORTH ATLANTIC TREATY ORGANIZATION

ADVISORY GROUP FOR AEROSPACE RESEARCH AND DEVELOPMENT

(ORGANISATION DU TRAITE DE L'ATLANTIQUE NORD)

EFFECT OF LOADING FREQUENCY ON THE STRAIN BEHAVIOR AND DAMAGE ACCUMULATION IN LOW-CYCLE FATIGUE

by

D.E.Gücer and M.Çapa

This Report was prepared at the request of the
Structures and Materials Panel of AGARD

Published June 1970
539.451:539.382

Printing by Technical Editing and Reproduction Ltd
Harford House, 7-9 Charlotte St. London, W1P 1HD

SUMMARY

In this report low cycle fatigue phenomenon is investigated in total strain ranges from 1 to 2 per cent, and frequencies from 0.2 to 100 cpm. Changes in endurance life under varying strain and frequency conditions were determined. During the endurance tests changes in the moment and strain values at the critical minimum section of the specimens were recorded. From the continuous time recordings of these parameters, elastic and plastic time ratios of specimen lives were defined and their dependence on strain and frequency levels found. Change of crack propagation rate with frequency was also studied. Finally a cumulative fatigue hypothesis, incorporating both frequency and strain parameters, was formulated and shown to be valid under varying strain and frequency conditions.

RESUME

Le présent Rapport étudie le phénomène de la fatigue à faible cycle dans toute la gamme des déformations allant de 1 à 2% et des fréquences comprises entre 0,2 et 100 cpm. Les modifications de la durée de vie dans différentes conditions de déformation et de fréquence ont été déterminées. Au cours des essais d'endurance on a enregistré les modifications des valeurs de moment et de déformation se produisant à la section minimale critique des éprouvettes. Les enregistrements continus de ces paramètres dans le temps ont permis de définir les rapports élastiques et plastiques dans le temps des durées de vie des éprouvettes et de constater jusqu'à quel point ils sont fonction des niveaux de déformation et de fréquence. La modification de la vitesse de propagation de fissures avec la fréquence a été également étudiée. On finit par formuler une hypothèse concernant la fatigue cumulative, qui comporte des paramètres tant de fréquence que de déformation, et qui s'est révélée applicable dans différentes conditions de déformation et de fréquence.

FOREWORD

In no category of applications are fatigue and its potential for damage of greater importance than in aerospace vehicles. It is to be expected, therefore, that the Structures and Materials Panel of the NATO Advisory Group for Aerospace Research and Development devote itself, as it has for years, to the many forms of damage that might be incurred as a result of fatigue, in terms of both a better fundamental understanding of the various phenomena and a better appreciation and knowledge of the effects under various situations. Particular attention has been devoted to developing an improved capability for predicting the effects of given load spectra on cumulative damage. Experimental data defining the effects of load frequencies on fatigue behavior are definitely inadequate. These effects are manifested in various ways to various degrees, sometimes in a contradictory manner, depending on the type and level of loading and on the range of frequencies concerned.

The present report, therefore, is a welcome addition to the existing literature, in that it deals with very high strain ranges in low cycle fatigue at low frequencies. It was solicited by the Panel for presentation as a tutorial lecture at its semi-annual meeting in Istanbul, in September 1969. It is hoped that the strain results reported, together with the proposed cumulative fatigue hypotheses, will provide a better insight to this subject and stimulate further discussion and research in this timely and important field.

N.E.Promisel Chairman,
AGARD Structures and Materials Panel

CONTENTS

EFFECT OF LOADING FREQUENCY ON THE STRAIN BEHAVIOR AND DAMAGE ACCUMULATION IN LOW-CYCLE FATIGUE

D.E. Gücer* and M. Çapa*

1. INTRODUCTION

Machine components and structural members which fail by fatigue are nearly always subjected to load changes of varying frequencies. In practice these frequency changes range from thousands of cycles per minute down to thousands of minutes per cycle. An understanding of the frequency effects in fatigue is not only important because it may throw light on the basic mechanism or mechanisms of fatigue failure; but also because of the need of the designer for such data in designing structures itself or in designing accelerated tests for decreasing the testing time of these structures.

In recent years, attention has increasingly been drawn to this problem. However, most of the work has been carried out in the range of frequencies of conventional fatigue machines, which is roughly 500 to 10,000 cycles per minute (cpm), and under loads giving long endurance lives. Under these conditions frequency effects have been found to be small, usually of the order of a few percent. In the investigations above this range, a continuous increase in fatigue strength, with or without a maximum depending on the type of material and test conditions, was observed. Below this range results are more conflicting and sometimes contradictory. Study of existing information shows that there is a need for extending the investigations to very low and very high frequency regions. There appears that frequency effects originate from specimen heating due to high damping; physical changes taking place in the structure of the material as a result of strain aging or other phenomena, corrosive influence of air or other media, and finally from rheological effects related with strain rate or creep. Reviews of literature dealing with the effect of frequency on fatigue have been given by Van Leeuwen[1], Forrest[2], Stephenson[3], Bradshaw[4] and Weller[5].

The present investigation studies the frequency effects in the low-cycle fatigue field. Since endurance lives in this field are below 10^4 or 10^5 cycles, machines with high frequency load application are not suitable. Usually fatigue tests of axial, rotating bending or direct bending type are carried out at frequencies below 500 cpm. Existing information indicates that mechanism of failure in low cycle fatigue is, most probably, different from failure at long endurances, as evidenced from the appearance of the fracture surface which resembles more that of the static tensile fracture than that of the typical fatigue fracture. Also at low cycle fatigue endurance is more related to ductility[6,7] and strain hardening capacity[8], whereas high-cycle fatigue is better correlated with tensile strength of the material. Information on the effect of frequency in low cycle field is limited and fragmentary. Eckel's work[9], based on his investigations on lead, to correlate frequency with endurance life and subsequent efforts[10,11] to extend this relationship to other materials and its adaptation by Harris[12] to include the effect of corrosion as a parameter should be mentioned.

2. EXPERIMENTAL ARRANGEMENT

The tests were made by direct reversed bending of a cantilever beam specimen under constant deflection conditions. The testing machine, shown in Figure 1, was constructed to enable continuous frequency changes by means of a mechanical variator. Frequencies chosen for tests were 0.2, 1, 10, 100 cpm. The test specimen in Figure 2, was developed during previous investigations[8,13,14]. It has biaxial state of stress at the center of its slightly notched critical section. All specimens were cut from the same plate with their longitudinal axis in the direction of rolling. Chemical composition and mechanical properties of the test steel are given in Table 1. Specimens were cut by oxygen, planed, and normalized at 900°C for 50 minutes. They were then grooved by milling, and a stress relief treatment at 600°C for 50 minutes was performed. Final operation was grinding of the groove surface by a specially prepared sand belt to 2/0 finish. Although the stress concentration factor of the groove is small (1.001) it helps localize the cracks. A transverse groove at the end of the specimen helps fix the moment arm at the same length at each test. Endurance life is taken as the number of cycles to the formation of a crack of 3 mm length. Triplicate tests were run for each testing condition. Strains were recorded by means of inductive strain gages of 40 mm gage length, throughout the endurance life of the specimen. These gages had a sensitivity of 10^{-6} mm/mm. Deflections were changed by means of an eccentric. For the calibration of eccentric settings (and deflections) with the longitudinal strains, deformation of a 500 micron size Vickers indentation on the critical section was followed by an optical microscope. An inductive gauge placed at the elastically bent section of the specimen gave a signal proportional to the bending moment at the plastically bent critical section which was also continuously recorded. Figure 3 shows this arrangement. Leads from these gages are connected to a multi-channel recorder over dynamic bridges and pre-amplifiers for continuous time recordings. For obtaining the hysteresis loops the same leads were connected to an X-Y oscilloscope over dynamic bridges. The loops were photographed from the screen of the X-Y oscilloscope. A microscope equipped with traveling ocular was used to measure the crack lengths.

* Prof. Dr Doğan E. Gücer and Dr Mehmet Çapa are both connected with the Technical University of Istanbul. Prof. Gücer is also the Director of the Materials Research Unit of the Turkish Scientific and Technical Research Council (T.B.T.A.K.)
This paper is based on part of the research project MAG-104 sponsored by the T.B.T.A.K.

3. EXPERIMENTAL RESULTS

3.1 Effect of Frequency on the Strain Behavior

Simultaneous time recordings of moment (above) and total strain (below) are reproduced in Figure 4, starting with the initial loading of a virgin specimen. Initial yield phenomenon is observed in the moment curve as a plateau in the first half-cycle, and as an increase in the corresponding strain values. The range between extreme values of moment is called the moment range and denoted by ΔM. Strain records represent the total strain (i.e. elastic plus plastic strain) values. Range of total strain between a maximum tension and a maximum compression state will be called total strain range and will be denoted by $\Delta\epsilon_t$. Figure 4 shows that there is a continuous increase in the moment range and a continuous decrease in the total strain range due to strain hardening of the initially annealed and stress relieved specimen. These ranges stabilize after nearly 5 cycles. It has been observed that these stabilized values remain unchanged until appreciable cracking occurs in the critical test section, and after which $\Delta\epsilon_t$ increases due to opening of crack sides and ΔM decreases due to loss of the load carrying capacity of the critical section. It was also found out that these changes start when the size of the cracks reaches about 3 mm length; and the criterion for the end of the test was determined on this basis. When frequency was changed during a test run between fixed deflection levels, magnitude of the total strain range did not change. The same result was also seen on the hysteresis curves (Fig.10). For this reason $\Delta\epsilon_t$ was taken as the measure of the severity of loading; rather than plastic strain range, which, as will be shown later, changes with frequency. It should also be remarked that, since the strain values stabilize at the very early cycles, constant deflection tests become equivalent to the constant strain tests for the remainder of the endurance life.

Neglecting any anelastic contribution to the strains, which was found to be negligeable in the range studied, one can write for the instantaneous values

$$\epsilon_t = \epsilon_e + \epsilon_p , \tag{1}$$

where ϵ_e shows the elastic, ϵ_p the plastic component of the total strain ϵ_t. For the range values of the same components

$$\Delta\epsilon_t = \Delta\epsilon_e + \Delta\epsilon_p \tag{2}$$

is valid, In Figure 5 time recordings of moment and total strain at the $\Delta\epsilon_t = 1.571\%$ level and at the frequency $f = 10$cpm are drawn systematically after stabilization is complete, in strict faithfulness to the original recordings. Approximate cyclic changes in the elastic and plastic components of the total strain were also shown in broken curves with the following considerations. Obviously when $M = 0$ the component $\epsilon_e = 0$ and $\epsilon_t = \epsilon_p$, and when M has an extremum value, ϵ_t, ϵ_e and ϵ_p have the corresponding extremum values. Also when $\epsilon_t = 0$, the components $\epsilon_e = -\epsilon_p$. When a bent specimen springs back from an extremum position only elastic deformation takes place, that is, ϵ_e alone changes from its extremum value to zero and ϵ_p remains constant. With these considerations fairly approximate ϵ_e and ϵ_p curves were inserted to the figure and $\Delta\epsilon_e$ and $\Delta\epsilon_p$ were indicated. During this investigation deflections were determined by the fixed eccentric angles. Therefore stabilized values of total strain ranges which show the strain levels are not round figures, but values obtained by calibration tests. Table II gives these stabilized values over a gage length l_o, equal to 500 microns, and 40 mms. This latter figure is the gage length of the inductive gages. Although the periods of all these changes are equal, they are not simple harmonic in character. A systematic study of these curves recorded at various total strain levels and frequencies revealed that time intervals following each extremum value of the total strain, during which plastic strains remain constant and only elastic strains change until the instantaneous value of moment becomes equal to zero, are easily measurable and reproducable quantities. There are two such intervals during a period, equal in magnitude, one following the maximum and the other the minimum point. If one such interval is denoted by t, then 2t becomes the time interval at each period T during which the specimen deforms only elastically. One can define then the ratio

$$\theta_e = \frac{2t}{T}\,100\% \tag{3}$$

as the elastic time ratio, and the ratio

$$\theta_p = \frac{T-2t}{T}\,100\% = (100-\theta_e)\% \tag{4}$$

as the plastic time ratio of endurance life. That means that during the θ_e per cent of its life, given in time units, the specimen will undergo elastic deformation only; and during θ_p per cent of its life plastic deformation will take place along with elastic deformation. Table III gives these values. It will be seen that at all strain levels, as frequency increases, specimens undergo more elastic deformation and less plastic deformation. If it is assumed that fatigue damage takes place, to a larger degree, during plastic deformation and increases with its magnitude, these results correlate very well with the effect of frequency on the endurance life, as will be seen at a later section. Thus, a quantitative measure is obtained for the generally qualitatively expressed statement, that as frequency increases materials behave more elastically and there is less time for plastic deformation.

Instantaneous changes of bending moment M and total strain ϵ_t shown in Figures 4 and 5 can better be interpreted by means of the M-ϵ_t hysteresis shown in Figures 6, 7 and 8. In Figure 6 each loop is slightly shifted on the screen in order to record the successive cycles without overlapping. Figure 7 shows the same changes systematically. After an initial yield, there is a gradual increase in bending moment range and a gradual decrease in the total and plastic strain ranges and an increase in the elastic strain range due to strain hardening. Finally a stabilized hysteresis loop is obtained after approximately 5 cycles (inner loop on Fig.7). Stabilized values of moment range ΔM, and total strain range $\Delta\epsilon_t$, plastic and elastic strain ranges $\Delta\epsilon_p$ and $\Delta\epsilon_e$ are shown on the stabilized curve. The changes in these parameters between the initial and stabilized values are denoted by δM, $\delta\epsilon_t$, $\delta\epsilon_p$ and $\delta\epsilon_e$. As will be seen from the figure, total changes in the range values are made up from changes on the tension side (indicated by prime signs) and on the compression side (indicated by double primes. Thus $\delta M = \delta M' + \delta M''$, etc) On either side these changes are measured from the first to the stabilized extremum values. The changes on the tension and compression sides are not necessarily equal, because the material changes continuously due to strain hardening. Only in the stabilized loop corresponding tension and compression values are equal. Obviously also

$$\delta\epsilon_t = \delta\epsilon_e + \delta\epsilon_p . \tag{5}$$

These changes can be obtained directly from the photograph of Figure 8, in which the hysteresis loops were allowed to overlap. In this figure, curves denoted by (a) show the changes from initial to stabilized conditions; in order to show a loop separately, the image on the screen was shifted towards the end of the test, and the curve (b) was recorded. It has been shown[8, 13] that these changes are important in themselves in determining the relative performance of steels in the low cycle range. It was found that, regardless of the strength properties of the steels, at a certain $\Delta\epsilon_t$ level, the steel with lower $\delta\epsilon_t$, that is with lower strain hardening capacity, gave a higher endurance. Since only one steel was studied in the present investigation, further evaluation of these range changes was not undertaken.

In Figure 9, an analysis of the stabilized total strain-bending moment hysteresis into its elastic and plastic components is given. These curves were obtained by direct strain readings. The specimen was strained by turning the machine manually in successive steps of loading-unloading-reloading; and strain readings were taken at each step. These values are indicated on the systematic curve. Elastic hysteresis is a straight line. Plastic loop shows that during elastic spring-back plastic strains remain constant. It will also be seen that when $\epsilon_t = 0$ the values of $\epsilon_e = -\epsilon_p$ as expected. However, these curves were obtained manually and with short periods of rest for strain readings; therefore they may be compared with recorded hysteresis loops for 0.2 or 1 cpm frequencies only.

3.2 Effect of Frequency on the Total Strain-Bending Moment Hysteresis

Figure 10 shows these effects. The scale on the screen was magnified in order to make the changes more clearly visible. Figure 10a shows the upper corner of the stabilized hysteresis; 10b the changes on the strain axis. Curves a, b and c on Figure 10a correspond to 1, 10 and 100 cpm respectively. That the stabilized moment range increases with frequency while the total strain range remains constant is visible and corroborates the observations made on continuous time recordings of these parameters. In Figure 10b corresponding curves show a decrease in the stabilized plastic range. Since total strain range remains constant with changes in frequency within the accuracy of measurements, obviously elastic strain range increases and the specimen behaves more elastically, as would be expected.

These results indicate that a correlation of endurance life with plastic strain range has to take loading frequency into account. A preliminary analysis, to find out whether observed changes in plastic strain range could explain the dependence of endurance life on frequency, will be undertaken during the discussion of the results.

3.3 Effect of Loading Frequency on the Crack Propagation Rate

In order to determine the effect of frequency on the crack propagation in 1 to 2 per cent total strain range, a crack was deliberately started at the corner of a 4 mm diameter hole drilled on the critical test section, at a quarter distance from the edge; since it was found that cracks in unnotched specimens started generally in this region. Growth of the crack was followed by means of a microscope equipped with a traveling ocular. Figure 11 shows that cracks propagated more rapidly at lower frequencies. This is presumably due to longer atmospheric exposure resulting in embrittlement of the material ahead of crack tip or in contamination of newly formed crack surfaces and consequent prevention of rewelding. It is found that a 3 mm crack length, which was taken as life criterion, is reached after a smaller number of cycles at lower frequencies. Therefore crack propagation rate is one of the factors bearing on the frequency dependence of endurance life.

It is seen that when the crack is small growth rate is also small. After approximately 0.5 mm growth is rapid at all frequencies. It will be also remarked that endurance life found by these curves is shorter than the life at regular tests, because in these tests cracks were initiated at an earlier stage due to deliberately introduced hole.

The same type of dependence of crack propagation rate on frequency was reported by other authors[18,19] for different materials and testing conditions.

3.4 Effect of Frequency on Endurance Life

In order to determine this effect, triplicate tests were run at three total strain levels and at four frequencies at each level. During a test, several cracks form on the test section and when their sizes reach 3 mm length load carrying capacity of the section begins to decrease. For this reason 3 mm crack length was adopted as a criterion of life. Test results, together with per cent decrease in life with decrease in frequency, are given in Table IV.

It will be seen that decreases in life from 100 to 0.2 cpm can be as high as 50 per cent (which also corresponds to an increase in life close to 100 per cent when frequency is increased from 0.2 to 100 cpm). These changes cannot be attributed to any temperature effect since temperatures at the surface or in the bulk of the test section do not rise above 50°C as will be seen from Table V. Due to damping specimens gradually heat up to temperatures in the table and temperature remains constant thereafter. At frequency 0.2 cpm temperature changes were negligeable and these values were not included in the table.

Strain ageing can also be discounted in this steel. The remaining factors, such as corrosive effect of air, crack propagation rate and rheological factors (changes in strain ranges, rates, etc.) may be responsible singly or jointly in affecting the endurances. However it is clear that, in the strain-frequency field investigated, the effect of frequency on endurance life is comparable in magnitude to that of strain. Similar effects of smaller magnitude were found, by Mann[16] and Wade and Grootenhuis[17] on the endurance lives correlated with stress range values. A plot of these values on a log-log scale is given in Figure 12, together with the least squares regression lines of log N on log f. Obviously an Eckel[9] type relationship is obeyed. The equations of the regression lines can be written as

$$\log N = \log N_1 + \mu \log f , \qquad (6)$$

where μ and N_1 are constants. The least squares values of μ and N_1 are given below at three strain levels.

Total strain range $\Delta\epsilon_t$, %	μ	N_1 (Calc.)
1.083	0.0926	1960
1.571	0.0923	1240
1.919	0.0914	705

It will be seen that the slopes of the lines (μ values) differ of the order of one percent. It may therefore be assumed that, in the strain ranges investigated, μ values are not dependent on the strain range. This result does not agree with the conclusions of Gohn and Ellis[14] for lead and lead alloys; and McKeown[15] for heavy non-ferrous alloys; who reported different values for different strain levels.

3.5 Cumulative Effects of Frequency

Two series of tests were conducted to find out the cumulative effects of frequency. First, keeping total strain level constant, specimens were run for various cycle ratios at different frequency levels, and the cumulative cycle ratios were determined. Secondly, specimens were subjected to cycle ratios with varying strain and frequency levels, and cumulative cycle ratios were found. Results of these two series of tests are given below.

(a) *Cumulative cycle ratios at constant strain level and varying frequencies.* The results of these tests are given in Table VI. At a fixed total strain level $\Delta\epsilon_t$, specimens were first cycled at f_1 initial frequency level where endurance was N_1 , for a predetermined n_1 cycles, or a cycle ratio $r_1 = n_1/N_1$; then frequency was changed to f_2 level, where endurance was N_2 , and the remaining life cycle n_2 or the cycle ratio $r_2 = n_2/N_2$ was determined; r_1 plus r_2 gives the cumulative cycle ratio. Endurance lives N_1 and N_2 are taken from Table IV. A high (100 cpm) and a low (1 cpm) frequency were chosen for initial cycling; followed by final cycling at 3 other frequencies. In the low-high frequency tests cumulative cycle ratios of 1.03 and 0.99 were found at the $\Delta\epsilon_t = 1.571\%$ and $\Delta\epsilon_t = 1.919\%$ levels respectively. In the high-low tests cumulative cycle ratios were 1.02 and 0.96 for these strain levels. Since all the values are very close to 1.00, test results suggest a linear damage law. By the assumptions,

(1) Total damage, D, at failure is 100 per cent or 1;

(2) Partial damage d_i received by the specimen during the cycle ratio r_i is numerically equal to the latter, i.e. $d_i = r_i$;

(3) A certain state of damage is independent of the path followed;

we can formulate the following hypothesis for the accumulation of damage at various frequencies at a certain strain level

$$D = \sum_i d_i = \sum_i \frac{n_i}{N_i} = \sum_i r_i \qquad (7)$$

where (i = 1, 2, 3, ...), indicate the frequency levels.

This is similar to the cumulative damage law proposed by Miner[15] for varying stress levels. Hypothesis put forward in Equation (7) is verified by the two-step tests summarized in Table VI.

(b) *Cumulative Cycle Ratios at Varying Strain and Frequency Levels* Two parallel series of tests were run according to the program given in the Table below.

$\Delta\epsilon_t$, %	*Frequencies, f, cpm*
1.571 1.083 1.919	100 → 10 → 1 ↓ 100 ← 10 ← 1 ↓ ↓ 100 → 1 → 10 (end)

In these tests the following notations were used. In a test at f_i frequency and $\Delta\epsilon_{tj}$ strain level, total endurance life was denoted by N_{ij}, a partial number of cycles run at this level by n_{ij}, and by partial cycle ratio $r_{ij} = n_{ij}/N_{ij}$. For the program given above, $f_1 = 100$, $f_2 = 10$, $f_3 = 1$ cpm and $\Delta\epsilon_{t1} = 1.571$, $\Delta\epsilon_{t2} = 1.083$, $\Delta\epsilon_{t3} = 1.919\%$. N_{ij} are to be taken out of Table IV. The partial cycle ratios in both tests are shown in Table VII. It will be seen that in these two tests, where all the cycle ratios, except the final r_{23}, are kept the same, cumulative cycle ratios give the values 0.990 and 1.134 or an average of 1.062 which again is close to 1. Therefore we can hypothesize that damage accumulation is linear and partial damage $d_{ij} = r_{ij}$. With further assumptions stated in the previous section we can generalize the relation (7) to the following form:

$$D = \sum_{ij} d_{ij} = \sum_{ij} \frac{n_{ij}}{N_{ij}} = \sum_{ij} r_{ij} = 1 . \qquad (8)$$

Preliminary tests of Table VII satisfy this hypothesis. However more data is needed to test its validity. Since specially low frequency tests need too much time, further tests could not be undertaken within the framework of the present investigation.

4. DISCUSSION OF THE RESULTS

In this investigation the effect of loading frequency on strain behavior and damage accumulation was studied. Although it is difficult to arrive at a fundamental relationship by means of bending tests, where the presence of stress and strain gradients complicate the analysis of the results, bending is a convenient way for introducing large amounts of plastic strains without endangering the stability of the specimen.

Continuous recordings of bending moments and total strains showed the expected stabilization of these parameters at early cycles. With frequency increase an increase in the stabilized moment range and the elastic strain range was observed, while the total strain range remained constant and the plastic strain range decreased. Constancy of the stabilized total strain range when the frequency changes is a significant result, in that it gives a reliable parameter for assessing the severity of loading in the low-cycle fatigue under changing frequencies. Since low-cycle fatigue seems to be dependent on ductility whereas long endurance (high-cycle) tests depend on stress values, the total strain range parameter could provide a link between these types of fatigue phenomena. In low cycle range, where $\Delta\epsilon_p$ component is large with respect to $\Delta\epsilon_e$, the behavior of the material should be determined by $\Delta\epsilon_p$ or the ductility. In high-cycle fatigue, on the other hand, where $\Delta\epsilon_e$ dominates and $\Delta\epsilon_p$ is negligible, $\Delta\epsilon_e$ which is proportional to stress should be the determining factor of the performance.

Since plastic fatigue range decreases with frequency there arises the necessity of examining correlations of fatigue life based on plastic fatigue range more closely. It would be worth-while to see whether the decrease in plastic range with frequency, when applied to the Coffin relationship, could explain the observed decrease in life with decreasing frequency. For low carbon steels this relationship can be written as

$$\Delta\epsilon_p \, N^{1/2} = C .$$

For two different frequencies we may write

$$\frac{N_2}{N_1} = \left(\frac{\Delta\epsilon_{p1}}{\Delta\epsilon_{p2}}\right)^2 .$$

At $\Delta\epsilon_t$ = 1.919% level for f_1 = 100 and f_2 = 1 cpm frequencies, from Fig.10b we obtain

$$\left(\frac{\Delta\epsilon_{p100}}{\Delta\epsilon_{p1}}\right)^2 = 0.91 ,$$

whereas $N_1/N_{100} \doteq 0.66$ from Table IV. Therefore decrease in N is not explained on the basis of the change in $\Delta\epsilon_p$ alone. According to Coffin formula life should decrease of 9% while it actually decreases about 34 percent. This result can be interpreted in two ways: (1) the said relationship does not hold in this case, or (2) the plastic strain increase is not the only factor determining the observed decrease of the endurance life; but other factors such as air corrosion and frequency dependence of crack propagation rate also make important contributions. Indeed, the observation made in this investigation, that at decreased frequencies the crack propagates faster (in term of load cycles) can make a positive contribution to close this gap. Increased corrosion time at lower frequencies also produces an effect in the direction of decreasing the life cycles.

Another observation made on the continuous strain records was that, as frequency increased the time during which the plastic strain component remained constant (that is specimen behaved solely elastically) increased. These times were expressed in ratio to one period of the strain cycle T and was called, for want of a better definition, elastic time ratio θ_e. In the rest of the period, plastic deformation takes place along with elastic deformation. This time expressed as a ratio of the period was called, plastic time ratio θ_p. It may be assumed that during the pure elastic deformation materials do receive less damage than when plastic deformation is also taking place with the elastic deformation. The fact that θ_e increases with increasing frequency, and decreasing strain level,. and θ_p increases with the decreasing frequency, an increasing strain level may provide quantitative parameters in explaining the effect of frequency on life.

Effect of frequency on the crack propagation rate seems to be an important factor in determining the fatigue life in low cycle fatigue. It has been observed that at high frequencies a crack propagates slower and at low frequencies faster presumably due to to corrosive and rheological effects. Since life criterion is taken usually as the number of cycles until the appearance of a crack of a certain length and since in low-cycle fatigue, life cycle values are small, contribution of this factor on life may be more important in this phenomenon than at high-cycle fatigue.

The effect of frequency changes from 0.2 to 100 cpm on the endurance life was found to be of the same order of magnitude as the effect of strains in the 1 to 2 per cent total strain range. As the frequency decreased from 100 to 0.2 cpm at all total strain levels life decreased between 40 to 50 per cent; whereas an increase in the total strain range from 1 to 2 percent decreased the life at all frequency levels between 60 to 80 per cent. The frequency effects may be attributed to the joint influences of increasing plastic strain range, increasing crack propagation rate and increasing air corrosion with decrease in frequency. Change of temperature was found negligible in this $\Delta\epsilon_t$-f field, as the increase in surface, where maximum amount of plastic deformation takes place, and in bulk temperatures, were between 2 to 30° above ambient temperature. This temperature increase cannot cause noticeable changes in the mechanical properties of the steels, but an effect on the air corrosion rate may be suspected.

In trying to evaluate the cumulative effects of frequency changes, two series of tests were carried out. In the first one, cumulative cycle ratios with changing frequency at constant strain levels were determined. In the second, cumulative cycle ratios during concurrent stepwise changes of strain and frequency levels were found. In both cases cumulative cycle ratios were close to one. Therefore linear cumulative damage hypothesis of the general form $\Sigma(n_{ij}/N_{ij}) = 1$ where $(i,j = 1,2,3...)$ was put forward. Here i indicates the frequency, j the strain levels. The hypothesis was tested and found to hold under j = constant conditions, and when both i and j were variable. Previous tests of similar nature had shown[13] that it also holds under i = constant conditions. Therefore this may be a cumulative damage hypothesis for combined changes of strains and frequencies. However, more test data is required to test its validity.

SUMMARY OF RESULTS

Low-cycle fatigue phenomenon in low carbon steel was studied in 1 to 2% total strain and 0.2 to 100 cpm frequency ranges. Conclusions reached apply for this strain-frequency field and are summarized below:

1. Bending moment and strain values and their ranges stabilize after approximately 5 cycles.
2. Stabilized range values of bending moment, elastic strain increase, and that of plastic strain decrease with increasing frequency; whereas total strain range is unaffected by frequency, hence better suited for the correlation of test data when frequency effects are studied.
3. There is need for closer study of the Coffin relationship in view of the frequency dependence of plastic strain range.
4. Elastic and plastic time ratio parameters were defined and evaluated quantitatively in order to explain the frequency dependence of endurance life.
5. Effect of frequency on endurance life was found to be of the same order of magnitude as that of strain in the strain-frequency field investigated.

6. Endurance life-frequency dependence obeys the Eckel relationship and correlation coefficient does not change with strain level.

7. Fatigue crack propagates slower at high frequencies, and faster at low frequencies.

8. A cumulative fatigue hypothesis incorporating strain and frequency parameters was formulated as

$$\sum_{ij} \frac{n_{ij}}{N_{ij}} = 1 , \qquad (i,j = 1,2,3,\ldots)$$

where i indicates frequencies and j strain levels. It was shown that this relationship holds under constant strain changing frequency, constant frequency changing strain conditions and under concurrent changes of frequency and strain.

REFERENCES

1. Van Leeuwen, H.P. — *"Predicting Material Behavior under Load, Time and Temperature Conditions"*, AGARD Report No. 513 (1965)

2. Forrest, P.G. — *"Fatigue of Metals"*, Pergamon Press (1962)

3. Stephenson, N. — *"A Review of the Literature on the Effect of Frequency on the Fatigue Properties of Metals and Alloys"*. N.G.T.E. Memo No. 320 (1958)

4. Bradshaw, F.J. — *"Frequency Effects in Fatigue Testing for Aircraft Structures"*. RAE Tech. Memo, Metal Physics 225 (1961).

5. Weller, J. — *"Die Bedebtung der Last-Spielfrequenz beim Dauerschwing-versuch metallischer Proben unter besonderer Berücksichtigung hochfester Leichtmetalle"*. Neue Hütte, 6 (1961), 7/91.

6. Coffin, L.F. Jr — *"Cyclic Straining-Fatigue"*. Symp. "Internal Stress and Fatigue in Metals", General Motors U.S.A. (1958). Elsevier, Amsterdam and London (1959) 363.

7. Manson, S.S. — *"Behavior of Metals under Conditions of Thermal Stress"*. Nat Adv. Co. Aero. Report 1170 (1954).

8. Gücer, D.E. — *"On the Role of Strain Hardening in the Plastic Range Fatigue"* Trans. AIME, 221 (1961) 415

9. Eckel, J.F. — *"Influence of Frequency on the Repeated Bending Life of Acid Lead."* Proc. A.S.T.M. 51 (1951) 745

10. Gohn, G.R. Ellis, W.C. — *"Fatigue of Lead Cable Sheath"*, Proc. A.S.T.M. 51 (1951) 721.

11. McKeown, — *"Fatigue Properties of some Non-Ferrous Metals Excluding Light Alloys"*. Int. Conf. on Fatigue. Instn. Mech. Engrs. (1956) 432.

12. Harris, J.W. — *"Cyclic Stressing Frequency Effect on Fatigue Strength"*. Aircraft Engineering, 31 (1959) 352.

13. Gücer, D.E. — *"Cumulative Fatigue at High Plastic Strains."* Trans. A.S.M. 54 (1961) 176.

14. Gross, J.H. et al. — *"The Plastic Fatigue Strength of Pressure Vessel Steels."* The Welding Journal, Research Supplement, 19 (1954) 31-S.

15. Miner, M.A. — *"Cumulative Damage in Fatigue"*. J. Appl. Mech. 12 (1945) A-159.

16. Mann, J.Y. — *"The Effect of Rate of Cycling on the Fatigue Properties of 24 S-T Aluminium Alloy"*. Aeronautical Research Laboratories (Australia). Report ARL/SM 188 (1954).

17. Wade, A.R. Grootenhuis, P. — *"Very High-Speed Fatigue Testing"*. IME-A.S.M.E. International Conference on Fatigue of Metals, Paper 4-5 (1956).

18. Schijve, J. et al. — *"The Effect of Frequency of an Alternating Load on the Crack Rate in a Light Alloy Sheet"*. N.L.R. The Netherlands, Report M. 2092 (1961)

19. Lachenaud, R. — *"Tenue en fatigue et Propagation des criques de l'A. U2GN en fonction de la temperature et de la fréquence."* Paper presented at the ICAF-AGARD Symposium, Rome (1963).

TABLE I

Chemical Composition and Mechanical Properties of the Steel

Chemical Composition	*C*	*Mn*	*P*	*S*	*Si*
	0.18	*0.38*	*0.030*	*0.020*	
Mechanical Properties	Yield pt. kp/mm^2	UTS kp/mm^2	Reduc. in area %	Elong. at fract. in 5 cms. %	
	19.1	36.5	60.2	40.0	

TABLE II

Stabilized Strain Range Values at the Critical Test Section

Excentric Angle	*Deflection mm*	l_0=	*Total Strain range* $\Delta\epsilon_t$ %		*Plastic strain range* $\Delta\epsilon_p$, %		*Elastic strain range* $\Delta\epsilon_e$, %	
			500 μ	*40 mm*	*500 μ*	*40 mm*	*500 μ*	*40 mm*
14^o	7.22		1.083	0.930	0.820	0.477	0.263	0.453
$16^o30'$	8.66		1.571	1.180	1.191	0.695	0.380	0.485
20^o	10.50		1.919	1.460	1.424	0.950	0.495	0.510

TABLE III

Elastic and Plastic Time Ratios

Tot. strain range $\Delta\epsilon_t$, %	*1.083*		*1.571*		*1.919*	
Frequency f, cpm	θ_e, %	θ_p, %	θ_e, %	θ_p, %	θ_e, %	θ_p, %
0.2	28.2	71.8	22.6	77.4	16.8	83.2
1	36.2	63.8	31.4	68.6	30.0	70.0
10	36.8	63.2	36.4	63.6	36.0	64.0
100	37.2	63.8	37.4	62.6	46.6	53.4

TABLE IV

Effect of Frequency and Total Strain Range on Endurance Life, N

Total strain range $\Delta\epsilon_t$ %	*1.083*		*1.571*		*1.919*	
Frequency f, cpm	*N*	*Perc. N_{ave} decr.*	*N*	*Perc. N_{ave} decr.*	*N*	*Perc. N_{ave} decr.*
100	3250 2900 2800	2983 0	1805 1950 1822	1859 0	1020 1150 1170	1113 0
10	2380 2500 2350	2410 19.2	1600 1665 1560	1608 13.5	900 850 910	887 20.3
1	2100 1950 2025	2025 32.1	1270 1181 1165	1205 35.2	728 780 690	733 34.2
0.2	1730 1560 1750	1680 43.8	1040 1120 1111	1091 41.3	578 534 586	566 51.0

TABLE V

Maximum Temperatures of Test Specimens

Total strain range %	*1.083*	*1.571*	*1.919*
Frequency f, cpm	*Maximum Temperatures at the Surface of the Critical Section, °C*		
1	20.6	20.9	21.7
10	21.3	22.1	23.1
100	32.4	38.4	41.3

TABLE VI

Cumulative Cycle Ratios at Constant Total Strain Ranges and Under Varying Frequencies

$\Delta\epsilon_t$ = 1.571 %							$\Delta\epsilon_t$ = 1.919 %						
f_1	f_2	n_1	r_1	n_2	r_2	r_1+r_2	f_1	f_2	n_1	r_1	n_2	r_2	r_1+r_2
1	100	603	0.50	916	0.49	0.99	1	100	365	0.50	459	0.43	0.93
1	100	301	0.25	1430	0.77	1.02	1	100	183	0.25	672	0.59	0.84
1	100	120	0.10	1682	0.92	1.02	1	100	73	0.10	831	0.77	0.87
1	10	603	0.50	898	0.51	1.04	1	10	365	0.50	443	0.49	0.99
1	10	301	0.25	1177	0.72	0.97	1	10	183	0.25	652	0.73	0.98
1	10	120	0.10	1332	0.82	0.92	1	10	73	0.10	744	0.77	0.87
1	0.2	603	0.50	837	0.68	1.18	1	0.2	365	0.50	393	0.68	1.18
1	0.2	301	0.25	846	0.77	1.02	1	0.2	183	0.25	530	0.93	1.18
1	0.2	120	0.10	1102	1.00	1.10	1	0.2	73	0.10	484	0.98	1.08
100	10	930	0.50	658	0.42	0.92	100	10	557	0.50	304	0.34	0.84
100	10	465	0.25	1296	0.79	1.04	100	10	278	0.25	587	0.59	0.84
100	10	186	0.10	1495	0.92	1.02	100	10	111	0.10	830	0.92	1.02
100	1	930	0.50	614	0.51	1.01	100	1	557	0.50	309	0.43	0.83
100	1	465	0.25	974	0.79	1.04	100	1	278	0.25	559	0.76	1.01
100	1	186	0.10	1145	0.94	1.04	100	1	111	0.10	638	0.88	0.98
100	0.2	930	0.50	560	0.51	1.01	100	0.2	557	0.50	289	0.51	1.01
100	0.2	465	0.25	841	0.77	1.02	100	0.2	278	0.25	453	0.80	1.05
100	0.2	186	0.10	1040	1.02	1.12	100	0.2	111	0.10	492	0.93	1.03

TABLE VII

Cumulative Cycle Ratios Under Varying Frequency and Strain Level Conditions

Frequency Levels f_i, cpm	*Strain Levels* $\Delta\epsilon_t$, %	*Cycles run,* n_{ij} *Test I*	*Test II*	*Cycles to Fractures* N_{ij}	*Cycle Ratios,* r_{ij} *Test I*	*Test II*
100	1.571	174	174	1859	0.0935	0.0935
10	1.571	96	96	1608	0.059	0.059
1	1.571	70	70	1205	0.0581	0.0581
100	1.083	200	200	2983	0.0985	0.0985
10	1.083	280	280	2410	0.116	0.116
1	1.083	435	435	2025	0.145	0.145
100	1.919	144	144	1113	0.129	0.129
1	1.919	95	95	733	0.130	0.130
10	1.919	146	276	887	0.161	0.305
Cumulative cycle ratio				Σr_{ij} =	0.990	1.134

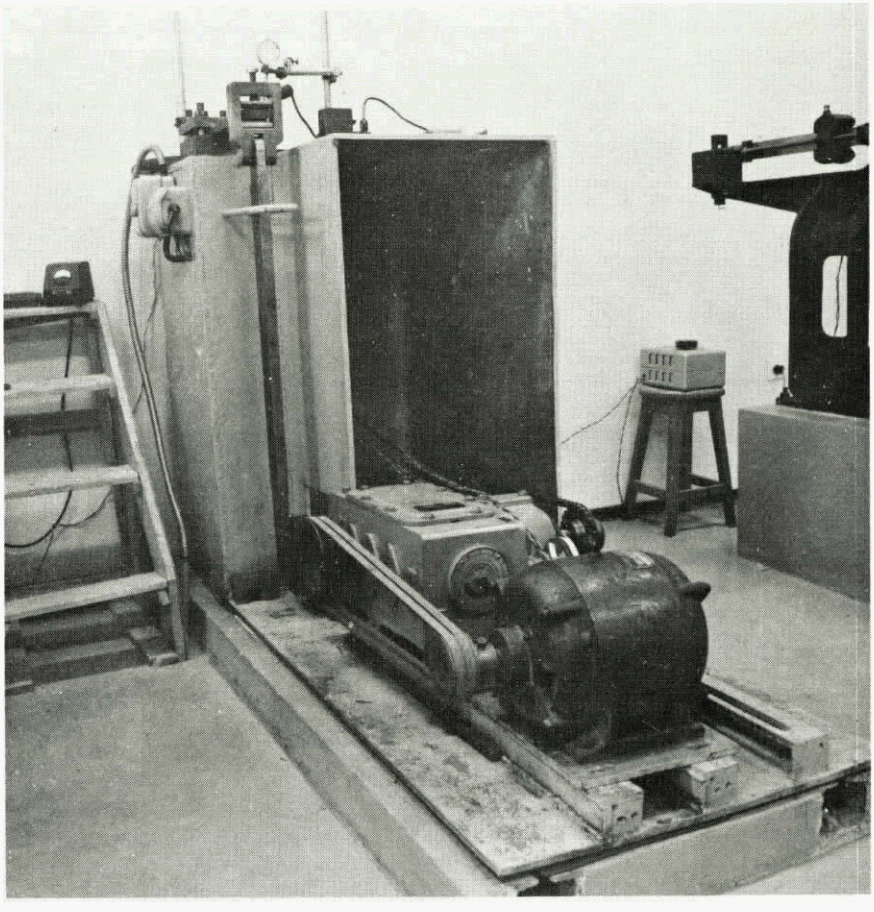

Fig.1 The testing machine

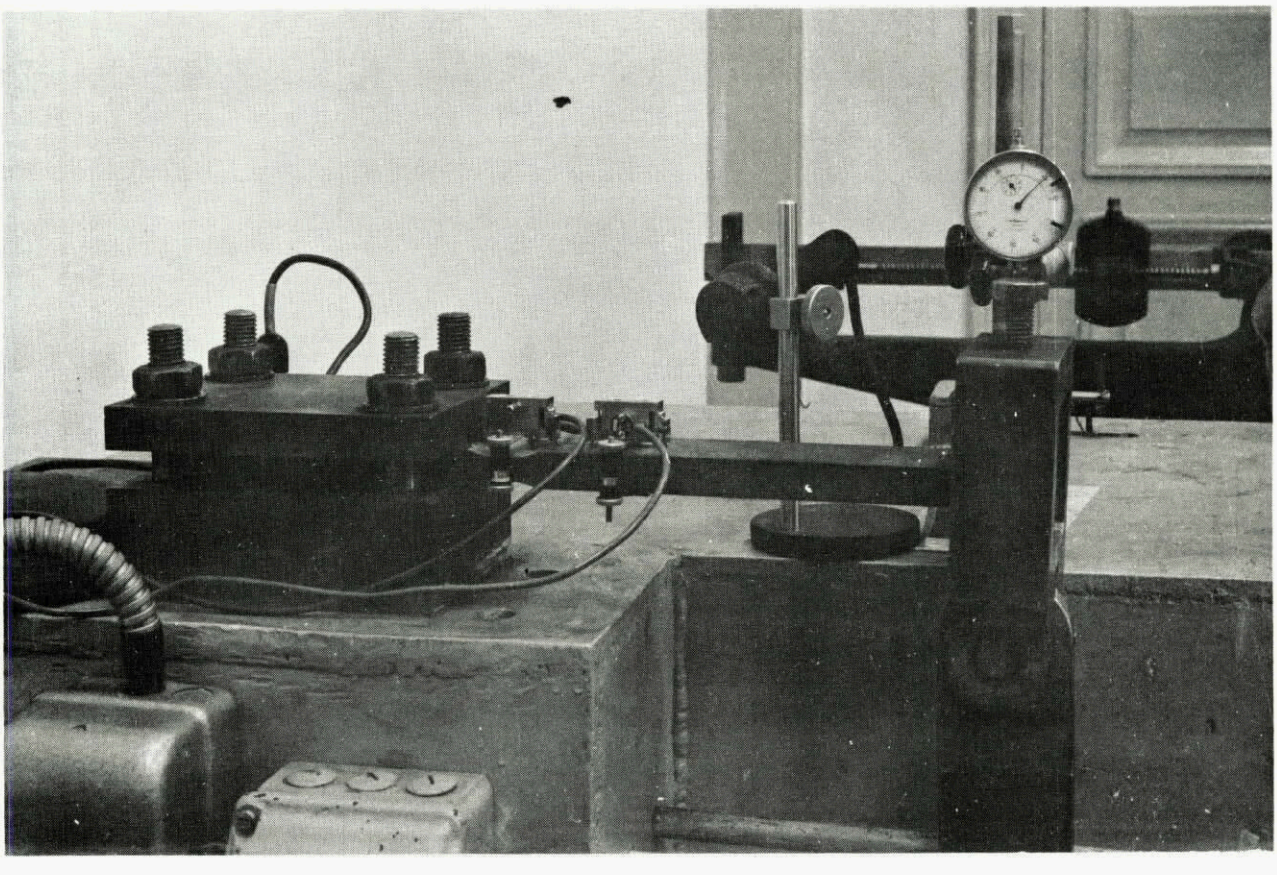

Fig.3 Arrangement for recording strains and hysteresis loops

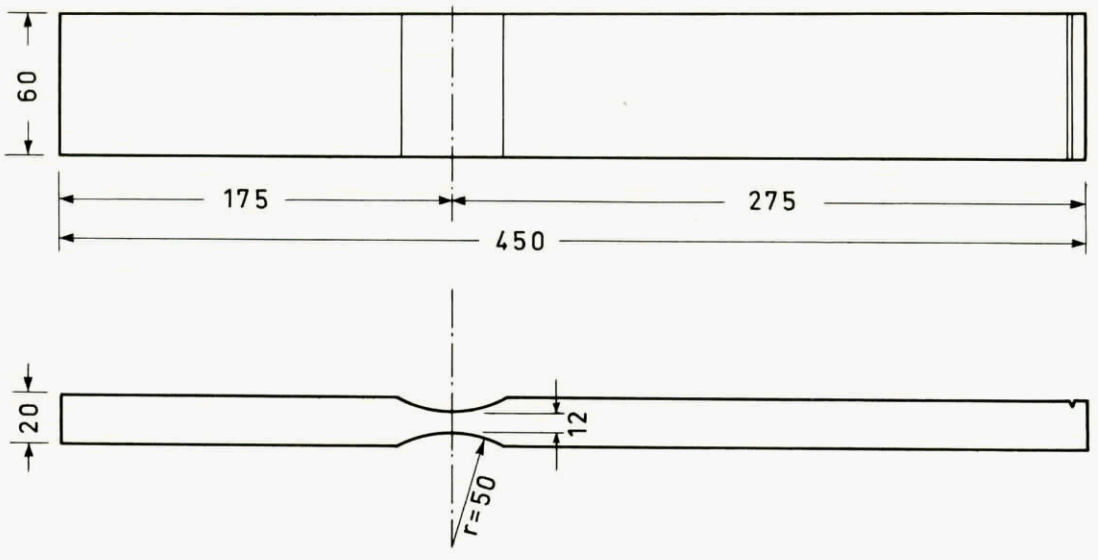

Fig. 2 The test specimen

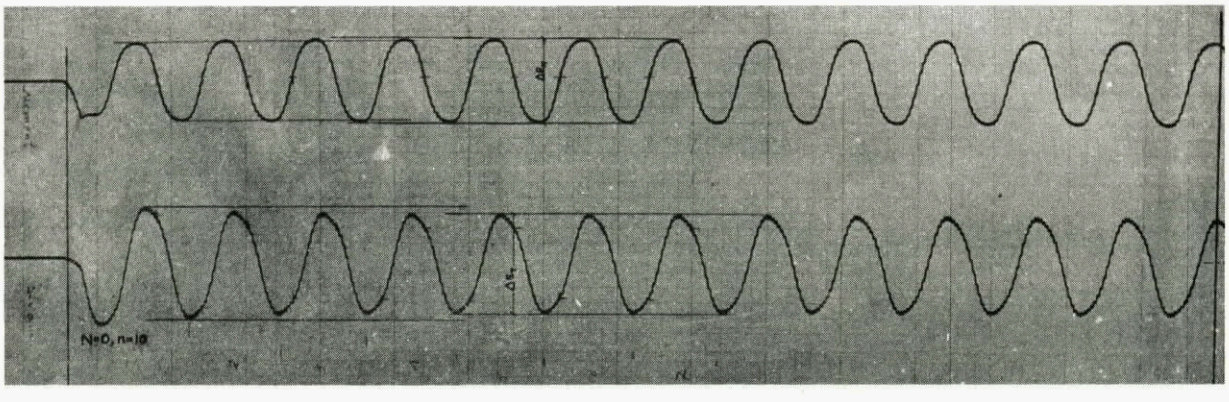

Fig. 4 Continuous and simultaneous records of the bending moments and strains during initial cycles ($\Delta\epsilon_t$ = 1.083%, f = 10 cpm.)

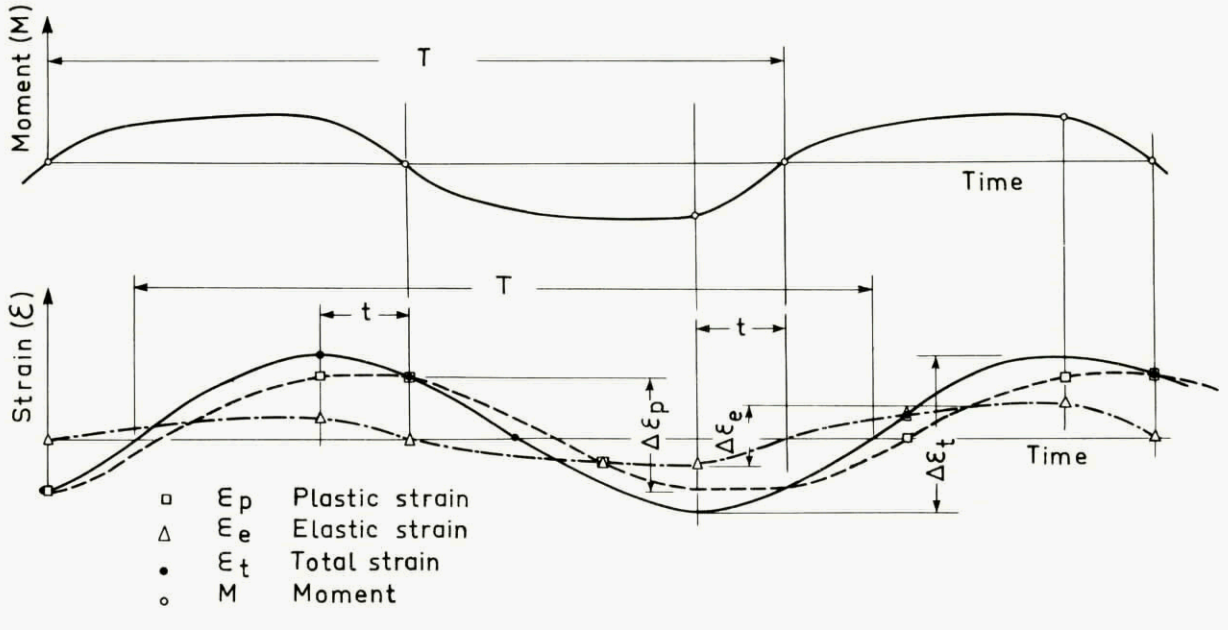

Fig. 5 Graphical representation of the simultaneous recordings of the stabilized cycles of bending moment and longitudinal strain.

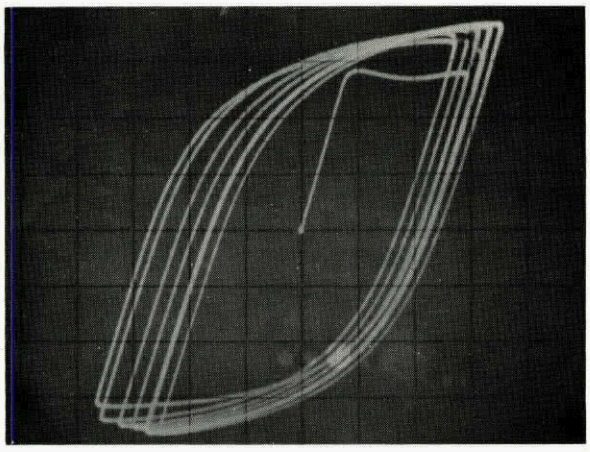

Fig. 6 Bending moment-longitudinal strain hysteresis loops (slightly shifted to show successive cycles)

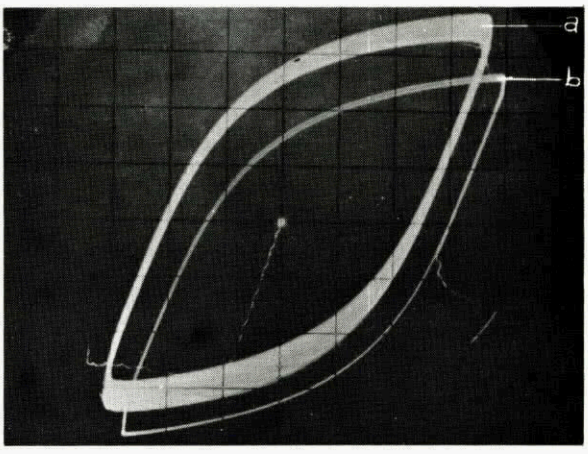

Fig. 8 Hysteresis loops allowed to overlap to show the changes in the bending moment and strain ranges.

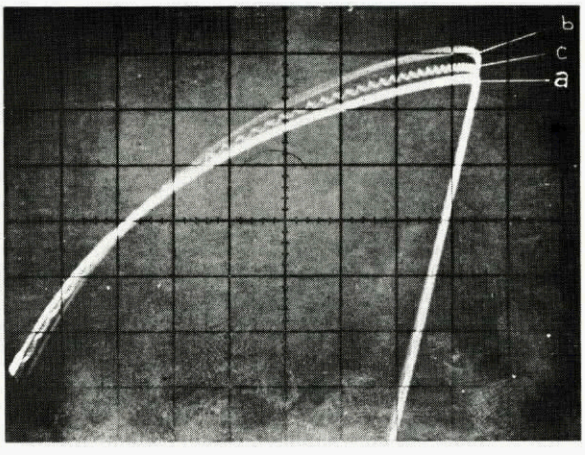

Fig. 10(a)

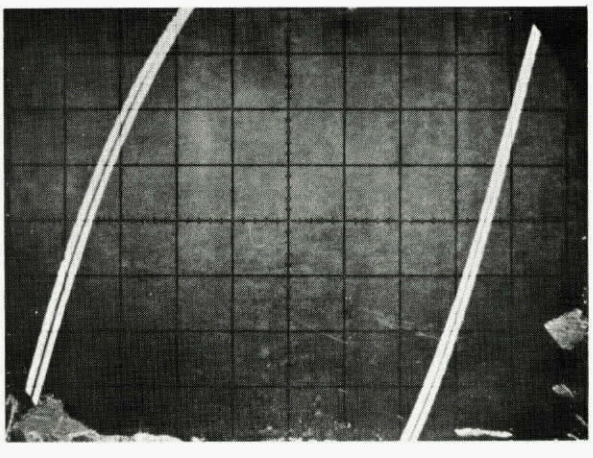

Fig. 10(b)

Fig. 10 Changes in the range values with frequency. (a) Changes in bending moment, (b) changes in plastic strain range

(Gage length 40 mm, $\Delta\epsilon_t$ = 1,460%)

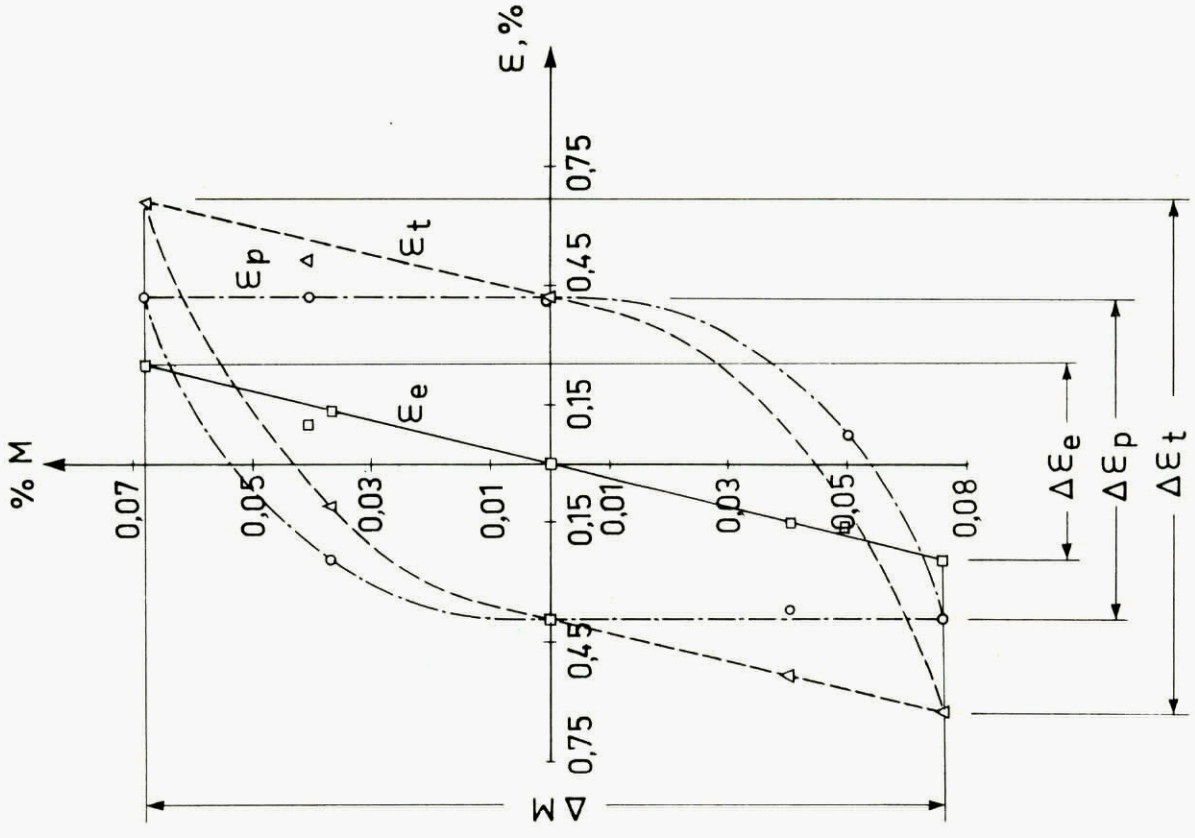

Fig.9 Analysis of bending moment-total strain hysteresis loop into elastic and plastic components

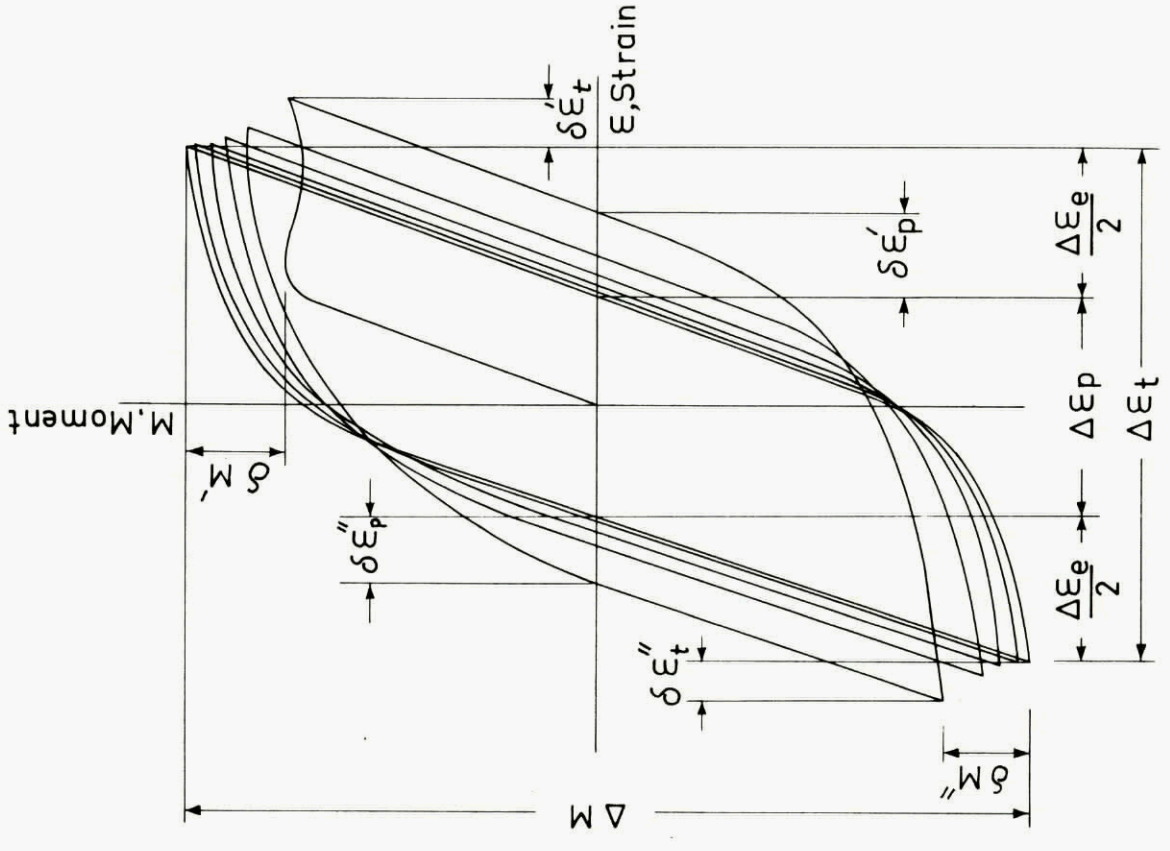

Fig.7 Graphical representation of hysteresis loops

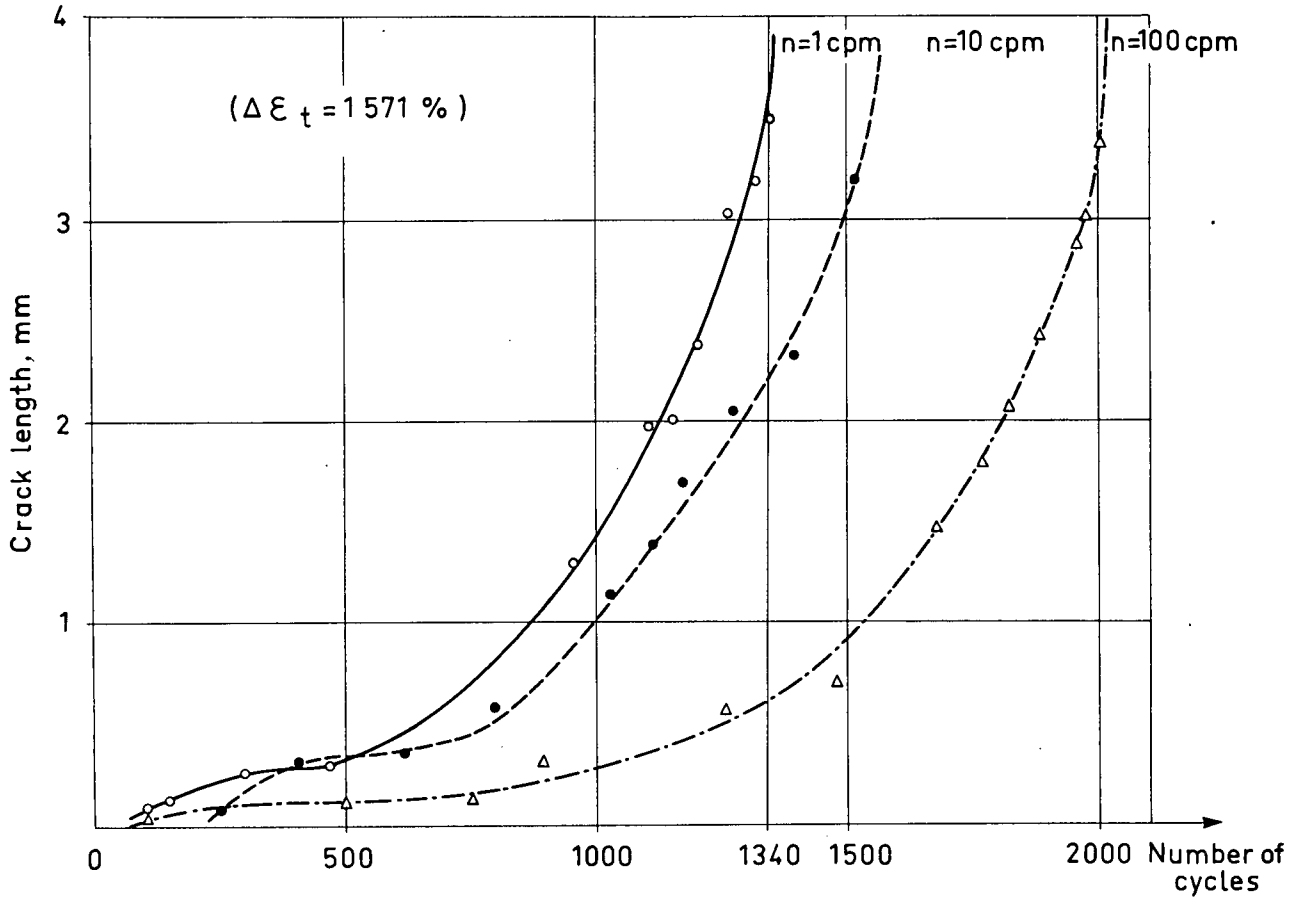

Fig. 11 Dependence of crack propagation rate on frequency.

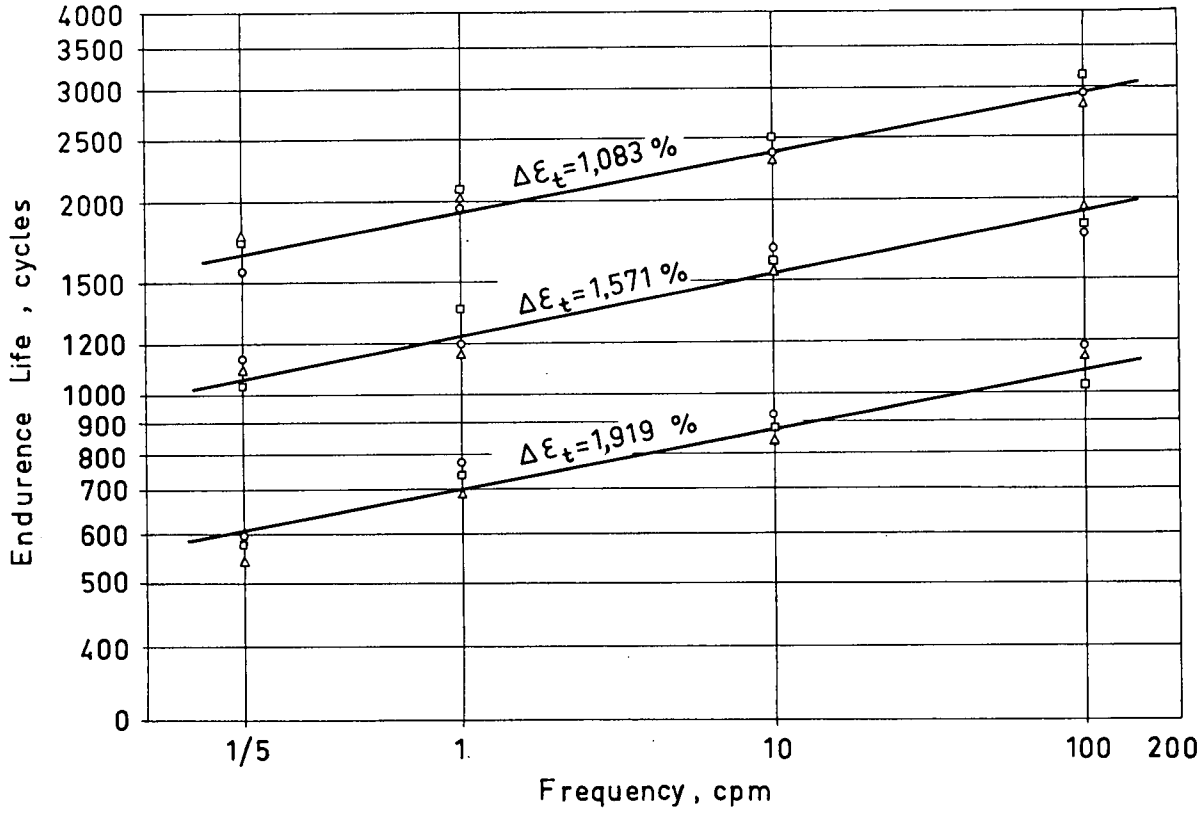

Fig. 12 Change of endurance life with frequency at three total strain range levels.

ERRATA SHEET

Since publication the author has amended the following passages in this report:

1. The paragraph, following the table on page 5, which should now read:

In these tests the following notations were used. In a test at f_i frequency and $\Delta\epsilon_{tj}$ strain level, total endurance life was denoted by N_{ij}, a partial number of cycles run at this level by n_{ij}, and by partial cycle ratio $r_{ij} = n_{ij}/N_{ij}$. For the program given above, $f_1 = 100$, $f_2 = 10$, $f_3 = 1$ cpm and $\Delta\epsilon_{t1} = 1.571$, $\Delta\epsilon_{t2} = 1.083$, $\Delta\epsilon_{t3} = 1.919\%$. N_{ij} are to be taken out of Table IV. The partial cycle ratios in both tests are shown in Table VII. It will be seen that in these two tests, where all the cycle ratios, except r_{32}, are kept the same, cumulative cycle ratios give the values 0.9949 and 1.1613 or an average of 1.078 which again is close to 1. Therefore we can hypothesize that damage accumulation is linear and partial damage $d_{ij} = r_{ij}$. With further assumptions stated in the previous section we can generalize the relation (7) to the following form:

2. Table VII should now read:

Cumulative Cycle Ratios Under Varying Frequency and Strain Level Conditions

Frequency Levels f_i, cpm	*Strain Levels* $\Delta\epsilon_t$, %	*Cycles run,* n_{ij} *Test I*	*Test II*	*Cycles to Fractures* N_{ij}	*Cycle Ratios,* r_{ij} *Test I*	*Test II*
100	1.571	174	174	1859	0.0935	0.0935
10	1.571	96	96	1608	0.0590	0.0590
1	1.571	70	70	1205	0.0587	0.1185
1	1.083	200	240	2045	0.0985	0.0985
10	1.083	280	280	2410	0.1161	0.1161
100	1.083	435	435	2983	0.1458	0.1458
100	1.919	144	144	1113	0.1290	0.1290
1	1.919	95	95	733	0.1296	0.1296
10	1.919	146	276	887	0.1645	0.3111
Cumulative cycle ratio					Σr_{ij} = 0.9949	1.1613

AGARD Report No.572 North Atlantic Treaty Organization, Advisory Group for Aerospace Research and Development EFFECT OF LOADING FREQUENCY ON THE STRAIN BEHAVIOR AND DAMAGE ACCUMULATION IN LOW-CYCLE FATIGUE D.E.Gücer and M.Çapa Published June 1970 15 pages incl. figs. In this report low cycle fatigue phenomenon is investigated in total strain ranges from 1 to 2 per cent, and frequencies from 0.2 to 100 cpm. Changes in endurance life under varying strain and frequency conditions were determined. During the endurance tests changes in the moment and strain values at the critical minimum section of the P.T.O.	539.451:539.382	AGARD Report No.572 North Atlantic Treaty Organization, Advisory Group for Aerospace Research and Development EFFECT OF LOADING FREQUENCY ON THE STRAIN BEHAVIOR AND DAMAGE ACCUMULATION IN LOW-CYCLE FATIGUE D.E.Gücer and M.Çapa Published June 1970 15 pages incl. figs. In this report low cycle fatigue phenomenon is investigated in total strain ranges from 1 to 2 per cent, and frequencies from 0.2 to 100 cpm. Changes in endurance life under varying strain and frequency conditions were determined. During the endurance tests changes in the moment and strain values at the critical minimum section of the P.T.O.	539.451:539.382
AGARD Report No.572 North Atlantic Treaty Organization, Advisory Group for Aerospace Research and Development EFFECT OF LOADING FREQUENCY ON THE STRAIN BEHAVIOR AND DAMAGE ACCUMULATION IN LOW-CYCLE FATIGUE D.E.Gücer and M.Çapa Published June 1970 15 pages incl. figs. In this report low cycle fatigue phenomenon is investigated in total strain ranges from 1 to 2 per cent, and frequencies from 0.2 to 100 cpm. Changes in endurance life under varying strain and frequency conditions were determined. During the endurance tests changes in the moment and strain values at the critical minimum section of the P.T.O.	539.451:539.382	AGARD Report No.572 North Atlantic Treaty Organization, Advisory Group for Aerospace Research and Development EFFECT OF LOADING FREQUENCY ON THE STRAIN BEHAVIOR AND DAMAGE ACCUMULATION IN LOW-CYCLE FATIGUE D.E.Gücer and M.Çapa Published June 1970 15 pages incl. figs. In this report low cycle fatigue phenomenon is investigated in total strain ranges from 1 to 2 per cent, and frequencies from 0.2 to 100 cpm. Changes in endurance life under varying strain and frequency conditions were determined. During the endurance tests changes in the moment and strain values at the critical minimum section of the P.T.O.	539.451:539.382

specimens were recorded. From the continuous time recordings of these parameters, elastic and plastic time ratios of specimen lives were defined and their dependence on strain and frequency levels found. Change of crack propagation rate with frequency was also studied. Finally a cumulative fatigue hypothesis, incorporating both frequency and strain parameters, was formulated and shown to be valid under varying strain and frequency conditions.

This Report was prepared at the request of the Structures and Materials Panel of AGARD

specimens were recorded. From the continuous time recordings of these parameters, elastic and plastic time ratios of specimen lives were defined and their dependence on strain and frequency levels found. Change of crack propagation rate with frequency was also studied. Finally a cumulative fatigue hypothesis, incorporating both frequency and strain parameters, was formulated and shown to be valid under varying strain and frequency conditions.

This Report was prepared at the request of the Structures and Materials Panel of AGARD

specimens were recorded. From the continuous time recordings of these parameters, elastic and plastic time ratios of specimen lives were defined and their dependence on strain and frequency levels found. Change of crack propagation rate with frequency was also studied. Finally a cumulative fatigue hypothesis, incorporating both frequency and strain parameters, was formulated and shown to be valid under varying strain and frequency conditions.

This Report was prepared at the request of the Structures and Materials Panel of AGARD

specimens were recorded. From the continuous time recordings of these parameters, elastic and plastic time ratios of specimen lives were defined and their dependence on strain and frequency levels found. Change of crack propagation rate with frequency was also studied. Finally a cumulative fatigue hypothesis, incorporating both frequency and strain parameters, was formulated and shown to be valid under varying strain and frequency conditions.

This Report was prepared at the request of the Structures and Materials Panel of AGARD

AGARD Report No.572 North Atlantic Treaty Organization, Advisory Group for Aerospace Research and Development EFFECT OF LOADING FREQUENCY ON THE STRAIN BEHAVIOR AND DAMAGE ACCUMULATION IN LOW-CYCLE FATIGUE D.E.Gücer and M.Çapa Published June 1970 15 pages incl. figs. In this report low cycle fatigue phenomenon is investigated in total strain ranges from 1 to 2 per cent, and frequencies from 0.2 to 100 cpm. Changes in endurance life under varying strain and frequency conditions were determined. During the endurance tests changes in the moment and strain values at the critical minimum section of the P.T.O.	539.451:539.382	AGARD Report No.572 North Atlantic Treaty Organization, Advisory Group for Aerospace Research and Development EFFECT OF LOADING FREQUENCY ON THE STRAIN BEHAVIOR AND DAMAGE ACCUMULATION IN LOW-CYCLE FATIGUE D.E.Gücer and M.Çapa Published June 1970 15 pages incl. figs. In this report low cycle fatigue phenomenon is investigated in total strain ranges from 1 to 2 per cent, and frequencies from 0.2 to 100 cpm. Changes in endurance life under varying strain and frequency conditions were determined. During the endurance tests changes in the moment and strain values at the critical minimum section of the P.T.O.	539.451:539.382
AGARD Report No.572 North Atlantic Treaty Organization, Advisory Group for Aerospace Research and Development EFFECT OF LOADING FREQUENCY ON THE STRAIN BEHAVIOR AND DAMAGE ACCUMULATION IN LOW-CYCLE FATIGUE D.E.Gücer and M.Çapa Published June 1970 15 pages incl. figs. In this report low cycle fatigue phenomenon is investigated in total strain ranges from 1 to 2 per cent, and frequencies from 0.2 to 100 cpm. Changes in endurance life under varying strain and frequency conditions were determined. During the endurance tests changes in the moment and strain values at the critical minimum section of the P.T.O.	539.451:539.382	AGARD Report No.572 North Atlantic Treaty Organization, Advisory Group for Aerospace Research and Development EFFECT OF LOADING FREQUENCY ON THE STRAIN BEHAVIOR AND DAMAGE ACCUMULATION IN LOW-CYCLE FATIGUE D.E.Gücer and M.Çapa Published June 1970 15 pages incl. figs. In this report low cycle fatigue phenomenon is investigated in total strain ranges from 1 to 2 per cent, and frequencies from 0.2 to 100 cpm. Changes in endurance life under varying strain and frequency conditions were determined. During the endurance tests changes in the moment and strain values at the critical minimum section of the P.T.O.	539.451:539.382

specimens were recorded. From the continuous time recordings of these parameters, elastic and plastic time ratios of specimen lives were defined and their dependence on strain and frequency levels found. Change of crack propagation rate with frequency was also studied. Finally a cumulative fatigue hypothesis, incorporating both frequency and strain parameters, was formulated and shown to be valid under varying strain and frequency conditions.

This Report was prepared at the request of the Structures and Materials Panel of AGARD

specimens were recorded. From the continuous time recordings of these parameters, elastic and plastic time ratios of specimen lives were defined and their dependence on strain and frequency levels found. Change of crack propagation rate with frequency was also studied. Finally a cumulative fatigue hypothesis, incorporating both frequency and strain parameters, was formulated and shown to be valid under varying strain and frequency conditions.

This Report was prepared at the request of the Structures and Materials Panel of AGARD

specimens were recorded. From the continuous time recordings of these parameters, elastic and plastic time ratios of specimen lives were defined and their dependence on strain and frequency levels found. Change of crack propagation rate with frequency was also studied. Finally a cumulative fatigue hypothesis, incorporating both frequency and strain parameters, was formulated and shown to be valid under varying strain and frequency conditions.

This Report was prepared at the request of the Structures and Materials Panel of AGARD

specimens were recorded. From the continuous time recordings of these parameters, elastic and plastic time ratios of specimen lives were defined and their dependence on strain and frequency levels found. Change of crack propagation rate with frequency was also studied. Finally a cumulative fatigue hypothesis, incorporating both frequency and strain parameters, was formulated and shown to be valid under varying strain and frequency conditions.

This Report was prepared at the request of the Structures and Materials Panel of AGARD

NATIONAL DISTRIBUTION CENTRES FOR AGARD PUBLICATIONS

AGARD publications are distributed to NATO Member Nations through the National Distribution Centres listed below.

BELGIUM
General J.DELHAYE
Coordinateur AGARD - V.S.L.
Etat Major Forces Aériennes
Caserne Prince Baudouin
Place Dailly, Bruxelles 3

CANADA
Director of Scientific Information Services
Defence Research Board
Department of National Defence - 'A' Building
Ottawa, Ontario

DENMARK
Danish Defence Research Board
Østerbrogades Kaserne
Copenhagen Ø

FRANCE
O.N.E.R.A. (Direction)
29, Avenue de la Division Leclerc
92. Châtillon-sous-Bagneux

GERMANY
Zentralstelle für Lüftfahrdokumentation
und Information
Maria-Theresia Str. 21
8 München 27
Attn: Dr Ing. H.J.RAUTENBERG

GREECE
Hellenic Armed Forces Command
D Branch, Athens

ICELAND
Director of Aviation
c/o Flugrad
Reykjavik

ITALY
Aeronautica Militare
Ufficio del Delegato Nazionale all' AGARD
3, P. le del Turismo
Roma/Eur

LUXEMBOURG
Obtainable through BELGIUM

NETHERLANDS
Netherlands Delegation to AGARD
National Aerospace Laboratory, NLR
Attn: Mr A.H.GEUDEKER
P.O. Box 126
Delft

NORWAY
Norwegian Defense Research Establishment
Main Library, c/o Mr P.L.EKERN
P.O. Box 25
N-2007 Kjeller

PORTUGAL
Direccao do Servico de Material
da Forca Aerea
Rua de Escola Politecnica 42
Lisboa
Attn: Brig. General Jose de Sousa OLIVEIRA

TURKEY
Turkish General Staff (ARGE)
Ankara

UNITED KINGDOM
Ministry of Technology Reports Centre
Station Square House
St. Mary Cray
Orpington, Kent BR5 3RE

UNITED STATES
National Aeronautics and Space Administration (NASA)
Langley Field, Virginia
Attn: Report Distribution and Storage Unit

★ ★ ★

If spare copies are not available at these centres, microfiche or hard copy (printed facsimile, or reproduction from microcopy) may be purchased from:

Clearinghouse for Federal
Scientific and Technical
Information (CFSTI)
Springfield
Virginia 22151, USA

ESRO/ELDO Space
Documentation Service
European Space Research Organization
114, Avenue de Neuilly
92, Neuilly-sur-Seine, France

The request for microfiche or hard copy of an AGARD document should include the AGARD serial number when available, title, author (or editor) and publication date; if known, the NASA Accession Number should also be quoted.

Full bibliographical references and abstracts of the newly issued AGARD publications are given in the following bi-monthly abstract journals with indexes:

Scientific and Technical Aerospace Reports (STAR) published by NASA,
Scientific and Technical Information Facility,
P.O. Box 33, College Park,
Maryland 20740, USA

United States Government Research and Development Report Index (USGDRI), published by the Clearinghouse for Federal Scientific and Technical Information, Springfield,
Virginia 22151, USA

Printed by Technical Editing and Reproduction Ltd
Harford House, 7-9 Charlotte St. London, W1P 1HD

Paper No.

27. Prof. M. D. van Dyke,
Stanford University,
California, U.S.A.

28. Dr. J. C. Adams, Jr.,
von Karman Gas Dynamics Facility,
ARO Inc.,
Arnold Air Force Station,
Tennessee, U.S.A.

29. M. G. Kretschmar,
O.N.E.R.A.,
29, Av. de la Div. Leclerc,
92-Châtillon/Bagneux,
France.

30. Mr. C. H. Lewis,
von Karman Gas Dynamics Facility,
ARO Inc.,
Arnold Air Force Station,
Tennessee, U.S.A.

Paper No.

31. Dr. R. S. Lee,
MacDonnell Douglas Corp.,
Santa Monica, Cal., U.S.A.

32. Dr. R. T. Davis,
College of Engineering,
Virginia Polytechnic Institute,
Blacksburg, Virginia, U.S.A.

33. Dr. F. G. Blottner,
Sandia Corp.,
P.O. Box 5800,
Albuquerque, New Mexico 87115,
U.S.A.

34. Prof. P. M. Chung,
Aerospace Corp.,
El Segundo, Cal., U.S.A.

LIST OF AUTHORS' ADDRESSES

Paper No.

1. Prof. R. Finn,
Dept. of Mathematics,
Stanford University,
Cal., U.S.A.

2. Dr. K. Kirchgässner,
Inst. fur Angewandte
Mathematik and Mechanik,
University of Freiburg,
Freiburg, Germany.

3. Prof. A. A. Szewczyk,
Dept. of Mech. Engineering,
University of Notre Dame,
Indiana, U.S.A.

4. Mr. P. Michael,
Brookhaven National Laboratory,
Upton, New York,
U.S.A.

5. Dr. Y. Rimon,
David Taylor Model Basin,
Carderock, Minnesota,
U.S.A.

6. M. L'Ing. Général,
R. Legendre,
O.N.E.R.A.,
Châtillon/Bagneux,
France

7. Prof. S. C. R. Dennis,
Dept. of Mathematics,
University of Western Ontario,
London, Canada.

8. Prof. D. B. Spalding,
Dept. of Engineering,
Imperial College,
London, U.K.

9. M. M. C. Francois,
O.N.E.R.A.,
29 Av. de la Div. Leclerc,
92-Châtillon/Bagneux,
France.

10. Dr. L. Gerking,
Inst. fur Angewandte Grenzschichttheory,
Techn. Hochschule Karlsruhe,
Karlsruhe, Germany.

11. Dr. H. U. Thommen,
Massachusetts Institute of
Technology,
Southeastern Institute,
Cambridge, Mass. 02139, U.S.A.

12. Dr. R. J. Magnus,
Space Science Laboratory,
Convair Division,
General Dynamics,
San Diego, Cal., U.S.A.

13. Dr. C. W. Hirt,
University of California,
Scientific Laboratory,
Los Alamos, New Mexico, U.S.A.

Paper No.

14. Prof. S. I. Cheng,
Dept. of Aerosp. & Mech. Sciences,
Princeton University,
Princeton, N.J., U.S.A.

15. Dr. S. M. Scala,
Space Sciences Laboratory,
General Electric Co.,
Valley Forge Space Center,
P.O. Box 8555,
Philadelphia, U.S.A.

16. Mr. P. Bradshaw,
Dept. of Aeronautics,
Imperial College,
London, U.K.

17. Prof. D. B. Spalding,
Dept. of Mech. Engineering,
Imperial College,
London, U.K.

18. Dr. K. W. Mangler,
R.A.E.,
Farnborough, Hants, U.K.

19. Prof. F. Schultz-Grunow,
Lehrstuhl und Inst.
für Mechanik,
51 Technische Hochschule Aachen,
Aachen, Templergraben 55,
Germany.

20. Dr. P. G. Williams,
Mathematics Dept.,
University College,
London, U.K.

21. Mr. A. M. O. Smith,
MacDonnell-Douglas Co.,
Long Beach,
Cal., U.S.A.

22. Dr. N. A. Jaffe,
Engineering Dept.,
Oxford University,
Parks Road, Oxford, U.K.

23. Prof. P. A. Libby,
Dept. of Aerosp. & Mech. Eng.
Sciences,
University of California -
San Diego, La Jolla -
California 92038, U.S.A.

24. Dr. W. Schönauer,
Inst. für Angewandte Grenzschichttheory,
Techn. Hochschule,
Karlsruhe,
Kaiserstrasse, Germany.

25. Dr. F. G. Blottner,
Sandia Corp.,
P.O. Box 5800,
Albuquerque, New Mexico 87115,
U.S.A.

26. Dr. R. M. Kendall,
Aerotherm Corp.,
Palo Alto, California, U.S.A.

34. MERGED STAGNATION SHOCK LAYER OF NON-EQUILIBRIUM DISSOCIATING GAS*

P. M. Chung,** J. F. Holt and S. W. Liu
Aerospace Corporation, El Segundo, California

This paper presents the formulation of the problem, the numerical method leading to solution, and the physical significance of the results obtained for the fluid flow of a viscous merged layer with non-equilibrium chemical reactions. The solution is limited to the stagnation region of a blunt body. The chemical reactions considered are the dissociation and the recombination of air.

It is first shown that the reduced Navier-Stokes equation and the corresponding energy and species conservation equations, wherein certain curvature effects have been neglected, are sufficiently accurate for the flow regime in which $Re_s \gtrsim 20$, where Re_s is the Reynolds number behind the bow shock. It is also shown that only in this regime are the non-equilibrium chemical reactions important.

The system of non-linear differential equations defining the flow and algebraic equations defining the gas properties is replaced by a set of finite-difference equations and solved with a digital computer by Newton's method between the free-stream and the surface.

Suppose, for example, that the equations are given by

$$f_i(\theta_1, \theta_2, \ldots \theta_n, \xi) = 0 \qquad (i = 1, 2, \ldots n)$$

If, at any stage, approximate solutions θ_s are known, then corrections η_s are given, by Newton's rule, from the equations

$$\sum_{s=1}^{n} \eta_s \frac{\partial f_i}{\partial \theta_s} = -f_i \qquad (i = 1, 2, \ldots n)$$

The above equations constitute a set of linear equations $(A\eta_s = -f_i)$ where A is a band matrix, from which the corrections η_s can be computed by Gaussian elimination. The new approximations $\theta_s + \eta_s$ are then used in place of the previous θ_s, and the process is repeated until convergence is achieved. A special sub-routine was used for the band matrix A, thus saving a large amount of machine time and storage.

The major difficulty in using Newton's method for this type of problem is that fairly accurate initial approximation is required for all variables across the entire range of integration. However, the advantage of the method is that once a particular solution has been obtained, it can be used as an initial approximation for other values of the parameters. For subsequent approximations, convergence is quadratic, requiring only five to ten iterations per solution.

From the solutions it was found, as was expected, that a strong coupling exists between the chemical reactions and the rarefaction of the shock layer. One of the unexpected results is that, for a given flight condition, increase of the surface catalycity causes the shock layer to become thinner. Since the increase in surface catalycity reduces the degree of dissociation within the merged shock layer, it had been expected that it would increase the shock layer thickness instead of decreasing it. The physical interpretation of the phenomenon and its possible implications are discussed in this paper.

Based on the solutions obtained, calculation of the ionization profile in the merged layer can be carried out in a relatively straightforward manner. Such calculations, reported elsewhere, have shown that there is a pronounced effect on the ionization level, which can be as much as two orders of magnitude lower than that predicted on the basis of a Hugoniot shock model.

Finally, the paper presents comparisons of the present results with results previously obtained from more approximate analyses.

---

* The research reported in this paper was supported by the United States Air Force under Contract No. F04695-67-C-0158.

** Consultant. Professor of Fluid Mechanics, University of Illinois at Chicago Circle.

33. VISCOUS SHOCK LAYER PROBLEM FOR THE STAGNATION POINT OF A BLUNT BODY*

F. G. Blottner**
Sandia Laboratories
P. O. Box 5800
Albuquerque, New Mexico 87115

There has been a significant amount of work devoted to the understanding of the fluid dynamics of the viscous hypersonic blunt body problem. The present investigation is intended to provide solutions to this problem with more realistic gas models than previously employed. Also, the purpose of this study is to investigate and develop techniques for solving the governing equations which are ordinary differential equations with two-point boundary conditions.

The governing equations for a thin hypersonic shock layer in the form used are presented. These equations have been developed by a number of authors but have not been considered for a complete reacting air model as presently employed.

A review is given of techniques developed for solving two-point boundary problems. The finite-difference and non-linear over-relaxation methods have been applied to the flow of a binary gas at a stagnation point. A comparison of the convergence of the two procedures is made and the results for the velocity, temperature and atom mass fraction are presented. The application of these methods to pure air shock layer and boundary flow is discussed.

Solutions for pure air flows at the stagnation point of a hyperboloid† at various altitudes and a velocity of 20,000 fps are presented. The properties of the flow such as velocity, temperature, and chemical species from the body to the shock wave are given. The electron density across the shock layer is also given. The heat transfer and skin friction parameters are obtained for the various altitudes and theories employed (shock layer or boundary layer).

---

*This paper has been accepted for publication in the AIAA Journal.

**Staff Member, Aerothermodynamics Research Department.
This work was supported by the U.S. Atomic Energy Commission.

†This problem and body geometry were requested to be employed by participators in the AGARD Seminar.

32. THE HYPERSONIC VISCOUS SHOCK-LAYER PROBLEM

R. T. Davis
Virginia Polytechnic Institute

Laminar flow past blunt bodies moving at hypersonic speeds is considered on the basis of a set of equations which govern the fully viscous shock-layer for moderate to high Reynolds numbers. The method of solution used is an implicit finite-difference method which is similar to the method developed by Blottner and Flugge-Lotz[1] for solving the compressible boundary-layer equations.

First the full Navier-Stokes equations are written in boundary-layer co-ordinates and an order of magnitude analysis is performed on the terms in the equations. Terms are kept up to second-order in the square root of the Reynolds number from both a viscous and an inviscid viewpoint, so that the simplified governing equations are uniformly valid to moderately low Reynolds numbers (see Davis and Flugge-Lotz [2]). To the order of the approximations involved the body surface conditions are given by slip and temperature jump conditions while the ordinary Rankine-Hugoniot relations are used to determine conditions behind the shock. This formulation is similar to that given by Cheng [3], the difference being that some second-order terms are retained which were not considered by him.

Next, the thin shock-layer approximation is applied to the simplified set of governing equations, and the resulting equations are found to be of parabolic type. This is an important simplification as far as numerical solution of the problem is concerned. The thin shock-layer equations can be solved by numerical methods similar to those developed for solving the boundary-layer equations. The numerical procedure consists of finding initial data at the stagnation-point and then integrating downstream using an implicit finite-difference method. The method is developed so that the equations yield the stagnation-point solutions directly.

Rather than work with the governing equations in boundary-layer co-ordinates, it is found that it is more convenient to work with the equations in a transformed form. New dependent variables are defined by dividing the old normal variable by the local distance from the body to the shock. The advantage of this transformed co-ordinate system is that the transformed distance to the shock is always one and the new dependent variables are always one at the shock. This means that in using the finite-difference method a constant number of steps can be taken between the body and the shock. This eliminates interpolation to find the shock position and makes it much easier to satisfy conservation of mass in order to determine the shock position.

Several example cases are presented in Davis[4] for flows over various bodies. The results are compared with the second-order boundary-layer results of Adams [5] and with the experimental results of Little [6].

References

[1] Blottner, F. G. and Flugge-Lotz, I. Computation of the compressible laminar boundary-layer flow including displacement-thickness interaction using finite-difference methods. J. Mechanique, 2, 397-423, (1963).

[2] Davis, R. T. and Flugge-Lotz, I. Second-order boundary-layer effects in hypersonic flow past axisymmetric blunt bodies. J. Fluid Mech., 20, 593-623. (1964).

[3] Cheng, H. K. The blunt-body problem in hypersonic flow at low Reynolds number. Cornell Aero. Lab. Rept., No. AF-1285-A-10. (1963).

[4] Davis, T. T. The hypersonic fully viscous shock-layer problem. Sandia Laboratories Report SC-RR-68-840, accepted for publication in the AIAA Journal. (1968).

[5] Adams, J. C. Higher order boundary-layer effects on analytic bodies of revolution. AEDC-TR-68-57. (1968).

[6] Little, H. R. An experimental investigation of surface conditions on hyperboloids and paraboloids at a Mach number of 10. University of Tennessee, M.S. Thesis. (1969).

$\omega < 1$, by either the behaviour (1) $T_b \sim K_1 \zeta_b^{-2(1-\omega)}$ as $\zeta_b \to \infty$, where K_1 is determined by all three terms in the energy equation, or the behaviour (2) $T_b \sim K_2 (\zeta_{be} - \zeta_b)^{1/\omega}$ as $\zeta_b \to \zeta_{be}$ (finite), which means the viscous term being dominant. Because of the larger mass flow in the transition layer, the second behaviour is ruled out. In the case of $\omega > 1$, there are again two types of possible satisfying behaviour: (1) $T_b \sim [(\omega-1)\zeta_{be}(\zeta_{be} - \zeta_b)/4]^{1/(\omega-1)}$, which is a balance between the viscous and convective terms, and (2) $T_b \sim K_3 (\zeta_{be} - \zeta_b)^{1/\omega}$, which is again given by the (dominant) viscous term. It is noted that while the first behaviour has a zero slope at $\zeta_b = \zeta_{be}$, the second behaviour has an infinite slope. The second behaviour is screened out by the transition layer. It is clear now that in any case the boundary-layer temperature behaviour can't match with the inviscid behaviour.

The temperature transition for the case of $\omega < 1$ was studied by Bush (1966) on a phase plane by which he showed also the matching of the temperature behaviour between the three regions. A more general study (Ref. 2) shows that the ordinary differential equation governing the temperature transition takes essentially the same form for a large class of flows with power-law shocks, and that it is even possible to match the transition-layer solution to an inviscid entropy-layer solution. The present work treats, in addition, $y = \delta[y_t(x) + \delta^n y_{tt} + \dots]$. The first term y_t only gives the shape of the sharp edge. The distribution of streamlines in the transition layer is given by the second term y_{tt}, the determination of which depends on the asymptotic value of y_{bb} as $\zeta_b \to \infty$. In this sense, the higher-order boundary-layer problem neglected by Bush (1966) is necessary. The temperature transition in the case of $\omega > 1$ is accomplished in two sublayers. Through the principal transition layer, the temperature is brought from its boundary-layer behaviour to a reference temperature based on the inviscid solution at the stream function corresponding to $\zeta_b = \zeta_{be}$. The transition to the inviscid behaviour is conducted in the exterior transition layer. Since the momentum equation is decoupled from the energy equation in the transition layer, the $(u - 1)$ transition can be studied separately in a similar manner.

In addition to the higher-order effect due to the transition-layer displacement which is treated in detail in the present work for the case of $\omega < 1$, there are other higher-order effects of comparable importance which can be treated separately. The slip and temperature-jump effects are of the order $\delta(T_{b,w})^{1/2}$, which can be lower or higher than the order δ^n depending on the wall temperature. However, in the self-similar flat-plate problem, their influence on surface heat transfer is of a higher order, as noted by Aroesty (1964). The strong and highly curved shock wave generates the heating and external vorticity effects which are of the order $\delta^{2n/(1+\omega)}$, higher than the order δ^n in the case of $\omega < 1$ but lower in the case of $\omega > 1$. In the case of $\omega < 1$, the present analysis also finds that, due to the singular behaviour of the transition-layer solution, there is another boundary-layer correction of the order between δ^n and $\delta^{2n/(1+\omega)}$. Finally, the effect of uncertainty about the leading edge is assumed to be of still higher order since no indeterminacy is encountered in our analysis up to the order δ^n.

The details of the present work, plus some numerical results, will be submitted for publication in an open journal.

References

[1] Lee, Richard S., and Cheng, H. K. On the outer-edge problem of a hypersonic boundary layer. Journal of Fluid Mechanics, Vol. 38, Pt. 1, p. 161. (1969).

[2] Cheng, H. K. Viscous and inviscid slender-body problems of hypersonic flow. University of Southern California Aerospace Engineering Department Report USCAE 108. (1969).

---

31. # THE HYPERSONIC BOUNDARY LAYER ON SLENDER BODIES, ITS OUTER-EDGE BEHAVIOUR AND HIGHER-ORDER APPROXIMATIONS*

Richard S. Lee
McDonnell Douglas Astronautics Company-Western Division
Santa Monica, California

H. K. Cheng
University of Southern California
Los Angeles, California

There are several characteristics which distinguish the hypersonic boundary layer on slender bodies from its supersonic or subsonic counterparts. Its comparatively large displacement effect has long been recognized to induce pressure interactions, strong or weak, with the accompanying inviscid flow. Another character is the low temperature at its outer edge as compared with the typical temperature level in its interior. Thus a commonly practised approximation is to solve the boundary-layer equations with the condition of a vanishing temperature at a sharp edge, regardless of the actual value and distribution of the edge temperature (and hence Mach number). However, the vanishing-temperature condition can be satisfied by more than one asymptotic (singular) behaviour of the boundary-layer equations; and, in any case, such a boundary-layer solution cannot be expected to match properly with the inviscid solution. In general, what is needed theoretically, is a transition layer in the neighbourhood of the sharp edge to screen the proper choice of the boundary-layer solution and to allow the transition from the boundary-layer-solution behaviour to the inviscid-solution behaviour. In fact, recently, Bush (1966), treating the problem of a flat plate in the hypersonic strong-interaction regime with the viscosity law $\mu \propto T^{\omega}$ $(\omega < 1)$, demonstrated such a three-region flow structure in von Mises' co-ordinates. However, we shall emphasize that the physical location of streamlines in the transition layer can not be uniquely determined without solving the boundary layer problem to the higher approximation treated in the present work.

The analysis of the transition layer can be circumvented by using von Mises' variables (or variables of a similar nature), in the exceptional case of a linear viscosity law $\mu \propto T$. The same authors have shown that in such a case, the boundary-layer solution combined with its higher-order approximation due to the transition-layer displacement is the composite asymptotic solution for both the boundary layer and the transition layer. In the transition layer, the boundary-layer solution becomes of the same order as its higher-order approximation and, near the inviscid region, the higher-order approximation furnishes the proper dominant behaviour to match with the inviscid solution. The details and some useful numerical results are published in Ref. 1.

In the present work, the flat plate in the hypersonic strong-interaction regime is used as an example to study the hypersonic boundary layer on slender bodies, its outer-edge behaviour and higher-order approximations in the case of a non-linear viscosity law $\mu = CT^{\omega}$ $(\omega \neq 1)$. A comprehensive presentation for more general power-law bodies is included in Ref. 2, where a detailed review of past relevant works can also be found. Since the mass flow in the transition layer is greater than that in the boundary layer in the case of $\omega < 1$ and vice versa in the case of $\omega > 1$, the outer-edge behaviour for these two cases differ significantly and have to be separately studied. In the present analysis, matched asymptotic expansions in terms of the small parameter $\delta = (C(\gamma M_\infty^2)^{\omega}/R_\infty)^{1/4}$ are made from the non-dimensional Navier-Stokes equations in von Mises' variables in the inviscid region, the transition layer and the boundary layer.

In the inviscid region, we assume a strong $(1/M_\infty^2 \, \delta^2 = O(\delta^2)$ or smaller) Rankine-Hugoniot shock of the shape $y_s = \delta A x^{3/4}(1 + a\delta^n x^{-n/4} \ldots)$, where $n = (1 + \omega)(3\gamma - 2)/(3\gamma - 1 + \omega)$ and the higher-order term is determined by the transition-layer displacement. The expansions for the flow quantities and the governing equations are those of the hypersonic small-disturbance theory. These equations can be reduced to the self-similar form, in terms of the independent variable $\zeta_h = \psi/\delta A x^{3/4}$, and can be integrated numerically with the constants "A" and "a" scaled out. Near the viscous regions, i.e., as $\zeta_h \to 0$, we have the asymptotic behaviour $p = \gamma M_\infty^2 \delta^2 A^2 x^{-1/2}(P_o + a\delta^n x^{-n/4} P_{oo} + \ldots)$, $T = \gamma M_\infty^2 \delta^2 A^2 x^{-1/2} \theta_o \zeta_h^{-2/3\gamma} + \ldots$ and $y = \delta A x^{3/4}(Y_o + Y_1 \zeta_h^{1-2/3\gamma} + a\delta^n x^{n/4} Y_{oo} + \ldots)$, where the constants P_o, P_{oo}, θ_o, Y_o, Y_1 and Y_{oo} are known from the integration.

In the boundary layer, the temperature is at the level of stagnation temperature, hence we assume $T = \gamma M_\infty^2 [T_b + \delta^n T_{bb} + \ldots]$. Other expansions are $u = u_b + \delta^n u_{bb} + \ldots$ and $y = \delta[y_b + \delta^n y_{bb} + \ldots]$. The second term in the expansions is again due to the transition-layer displacement. The pressure does not change across the viscous layers and is thus given by the inviscid behaviour near $\zeta_h = 0$. The sub-b quantities in the expansions are governed by the classical boundary-layer equations which can be reduced to the self-similar form, in terms of the independent variable $\zeta_b = \psi/\delta^3 A P_o^{1/2} x^{1/4}$. Near the outer edge, u_b approaches unity and the energy equation (with the dissipation term being of higher order) takes the form $(T_b^{\omega-1} T_b')'/\sigma + \zeta_b T_b'/4 - (\gamma - 1)T_b/2\gamma = 0$, where the prime denotes differentiation with respect to ζ_b. The vanishing temperature condition can be satisfied, in the case of

---

*This work was supported by the Douglas Independent Research and Development (IRAD) Program, to which one of the authors (H. K. Cheng) is a consultant, and by the Aerospace Engineering Department of the University of Southern California. The authors wish to thank Prof. W. B. Bush for his discussions.

References (contd)

[11] Lewis, C. H. Pressure distribution and shock shape over blunted slender cones at Mach numbers from 16 to 19.
AEDC-TN-61-81 (AD 261846). (1961).

[12] Griffith, B. J. and Lewis, C. H. Laminar heat transfer to spherically blunted cones at hypersonic conditions.
AIAA J., 2, 438-444. (1964).

[13] Whitfield, J. D. and Griffith, B. J. Hypersonic viscous drag effects on blunt slender cones.
AIAA J., 2, 1714-1711. (1964); see also AIAA J., 2, 1165-1166. (1965).

[14] Davis, R. T. The hypersonic fully viscous shock layer problem.
Paper to be presented in AGARD Seminar on Solution of the Higher-Order Boundary-Layer Problem, Teddington, England, September 18-21, 1967.

30.

FIRST- AND SECOND-ORDER BOUNDARY LAYER EFFECTS AT HYPERSONIC CONDITIONS*

Clark H. Lewis†
ARO, Inc.
Arnold Air Force Station, Tennessee

First- and second-order boundary-layer solutions are presented for a 9-deg half-angle, spherically blunted cone at $M_\infty = 9$ and 18. The effects of transverse curvature, vorticity, displacement and slip and temperature jump are considered both as first-order and second-order effects. The first-order results were obtained by modifying the classical boundary-layer equations and method of Clutter and Smith. The second-order results were obtained from the theory of Van Dyke using the implicit finite difference method of Davis and Flügge-Lotz. Primary interest is given to the higher-order effects on zero-lift drag including comparisons with the experimental data. Comparisons of displacement thickness, wall shear stress, heat transfer, and pressure distributions are presented. Limitations in the theories are indicated based upon comparisons between the numerical results and comparison with previously published experimental data.

References

[1] Lewis, C. H. and Whitfield, J. D. Theoretical and experimental studies of hypersonic viscous effects.
Recent Developments in Boundary Layer Research (AGARD Specialists' Meeting, Naples, Italy, May 1965) AGARDograph 97, Part III; also AEDC-TR-65-100 (AD 462717). (1965).

[2] Inouye, M., Rakich, J. V. and Lomax, H. A description of numerical methods and computer programs for two-dimensional and axisymmetric supersonic flow over blunt-nosed and flared bodies.
NASA TN D-2970. (1965).

[3] Clutter, D. W. and Smith, A. M. O. Solution of the general boundary-layer equations for compressible laminar flow, including transverse curvature.
Douglas Aircraft Company Report LB 31088 (1963) and revised October, 1964.

[4] Davis, R. T. and Flügge-Lotz, I. Laminar compressible flow past axisymmetric blunt bodies (results of a second-order theory).
Stanford University Report 143. (1963).

[5] Van Dyke, M. Second-order compressible boundary-layer theory with application to blunt bodies in hypersonic flow.
Hypersonic Flow Research (ed. F. R. Riddell), (Academic Press, New York, 1962), pp.37-76.

[6] Flügge-Lotz, I. and Blottner, F. G. Computation of the compressible laminar boundary-layer flow including displacement-thickness interaction using finite-difference methods.
Stanford University Report No. 131. (1962).

[7] Hayes, W. D. and Probstein, R. F. Hypersonic Flow Theory (Academic Press, New York, 1959), Chapt 9, Section 6, pp. 370f.

[8] Van Dyke, M. Higher approximations in boundary-layer theory, Part 1.
J. Fluid Mechanics, 14, 161-177. (1962).

[9] Jaffe, N. A., Lind, R. C. and Smith, A. M. O. Solution to the binary diffusion laminar boundary layer equations including the effect of second-order transverse curvature.
Douglas Aircraft Company Report LB 32613. (1966); also AEDC-TR-66-183 (AD 647285). (1967).

[10] Adams, J. C., Jr. Higher-order boundary-layer effects on analytic bodies of revolution.
Paper to be presented in AGARD Seminar on Solution of the Higher-Order Boundary-Layer Problem, Teddington, England, September 18-21, 1967.

---

*This work was sponsored by the Arnold Engineering Development Center (AEDC), Air Force Systems Command, U.S. Air Force under contract AF40(600)-1200 with ARO, Inc., Contract Operator AEDC. Some of this research will later be included in a doctoral dissertation to be submitted to the University of Tennessee in partial fulfilment of requirements for the Ph.D degree.

†Supervisor, Theoretical Gas Dynamics Section, Hypervelocity Branch, von Karman Gas Dynamics Facility.

The final results of the calculations are the coefficients α, β defined by:

$$\frac{\tau_\omega}{\tau_{\omega_{\Sigma=0}}} = 1 + \alpha \Sigma$$

$$\frac{q_\omega}{q_{\omega_{\Sigma=0}}} = 1 + \beta \Sigma$$

shown in Fig. 1. The parameter Σ is a measure for the vorticity intensity:

$$\sum = \frac{(\partial u/\partial y)_\delta}{\chi} \sqrt{\frac{\mu_\delta}{2\rho_\delta K_1^3}} \quad .$$

References

[1] Van Dyke, M. JFM 14, 161-177 and 481-495. (1963).

[2] Kretzschmar, G. ONERA T.P. 507. (1967).

[3] Kretzschmar, G. Thesis, RWTH Aix-la-Chapelle. (1969).

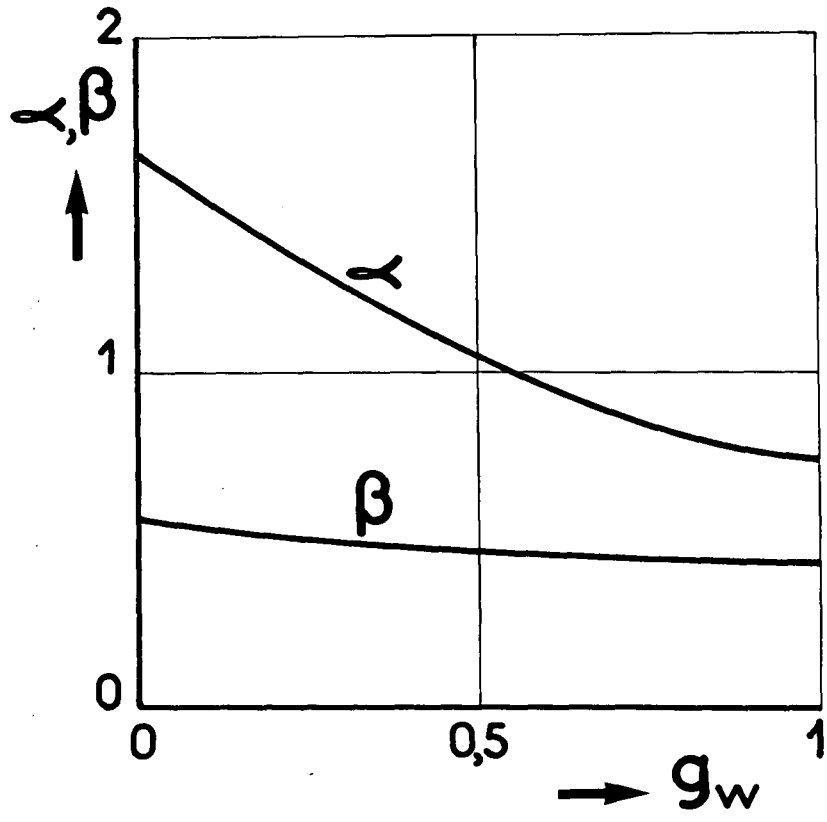

figure 1

29.

EFFECTS OF AN EXTERNAL VORTEX ON THE BOUNDARY LAYER AT AN AXISYMMETRIC STAGNATION POINT

Gunter Kretzschmar
O.N.E.R.A., Paris

Several second-order effects may be important in modern boundary-layer problems [1]. In the case of hypersonic flight of a blunt body in a not too rarefied atmosphere two of these second-order effects will be of particular importance, namely the combined effects of boundary-layer displacement and vorticity in the outer flow.

Recently an integral method of calculation which takes into account these effects has been elaborated in order to predict the development of laminar boundary layers [2], [3]. As a part of this investigation an exact solution of the boundary-layer equations at an axisymmetric stagnation point has been evolved. A large number of boundary-layer profiles (velocity, temperature, shear stress and heat flux) as well as some characteristic quantities (thicknesses, wall heat flux coefficient) have been obtained on an analogue computer as functions of the wall to free-stream temperature ratio and the vorticity intensity.

The boundary-layer equations in the usual form include the second-order effects of displacement and vorticity. The Levy-Lees transformation, when applied to the stagnation point flow, yields:

$$\left(\frac{\rho\mu}{\rho_\delta\,\mu_\delta}\,f''\right)' + ff'' - 2f'^2\,\frac{\xi}{\mu_\delta}\,\frac{du_\delta}{d\xi} - 2\,\frac{\rho_\delta}{\rho}\,\frac{\xi}{\rho_\delta\,u_\delta^2}\,\frac{dp_\delta}{d\xi} = 0$$

$$\left(\frac{\rho\mu}{\rho_\delta\,\mu_\delta}\,g'\right)' + Pfg' = 0\ .$$

Here the subscript δ refers to the conditions at the outer edge of the boundary layer. The velocity and pressure gradient parameters

$$\frac{\xi}{u_\delta}\,\frac{du_\delta}{d\xi} \quad \text{and} \quad \frac{\xi}{\rho_\delta\,u_\delta^2}\,\frac{dp_\delta}{d\xi}$$

may be expressed with the aid of the outer velocity distribution

$$u_e(x,y) = K_1 \times [1 + K_2\,(y - \delta^*)]$$

where the constant K_2 measures the vorticity intensity. One finds:

$$\frac{\xi}{u_\delta}\,\frac{du_\delta}{d\xi} = \frac{1}{4}$$

$$\frac{\xi}{\rho_\delta\,u_\delta^2}\,\frac{dp_\delta}{d\xi} = -\frac{1}{4}\cdot\frac{1}{[1 + K_2(\delta - \delta^*)]^2}\ .$$

Thus, the solution of the boundary-layer equations depends on the parameter $\pi = [1 + K_2(\delta - \delta^*)]^2$ which may be expressed in terms of the dimensionless stream-function and its second derivative at the outer edge:

$$\frac{1}{[1 + K_2\,(\delta - \delta^*)]^2} = 1 - 2\,(ff'')_{\eta=\eta_\delta}\ .$$

The parameter π represents the combined effects of displacement (factor $\delta - \delta^*$) and of outer vorticity (factor K_2).

For a fixed value of π the solution has been obtained by starting the integration at the wall with different assumed values of f'' and g' until the preceding relationship was met when $f'_{\eta\delta} = 1$. The corresponding value of the dimensionless co-ordinate η_δ indicates the position of the outer edge of the boundary layer which is at a finite distance from the wall.

28. HIGHER ORDER BOUNDARY-LAYER EFFECTS ON ANALYTIC BODIES OF REVOLUTION*

John C. Adams, Jr.†
ARO, Inc.
Arnold Air Force Station, Tennessee

Results are presented from an investigation into second-order compressible boundary-layer theory applicable to blunt bodies formulated for numerical solution in the transformed plane using an implicit finite-difference scheme. Various combinations of second-order effects (external vorticity, displacement, transverse curvature, longitudinal curvature, slip, and temperature jump) are considered for two different bodies, a paraboloid and a hyperboloid of 22.5° asymptotic half-angle, in a Mach 10 flow under low Reynolds number conditions. Two different wall-to-stagnation temperature ratios are used, namely 0.20 and 0.60, in order to simulate both cold and hot wall conditions, respectively. For comparison purposes, solutions are obtained using three different viscosity laws - Sutherland, linear, and square-root - as well as two different Prandtl numbers 0.70 and 1.0. A locally similar first-order solution using the finite-difference scheme is also presented in order to permit a critical assessment of the locally similar approximation.

Particular attention is devoted to the treatment of the separate second-order vorticity and displacement effects. It is shown that the only correct manner to treat these separate effects is in a displacement speed sense - a displacement pressure approach is not consistent with the mathematics of second-order boundary-layer theory. However, a displacement speed treatment is unreasonable with respect to the magnitude of the separate effects and certainly not representative of the actual physical effects. Hence it is proposed that one should properly interpret second-order vorticity and displacement in a combined sense as a vorticity-displacement interaction. Furthermore, a new and powerful technique for considering the second-order displacement effect using first-order inviscid theory is presented; this approach is not limited to the nose region and may be applied equally well over the entire body.

Numerical results indicate that the vorticity-displacement interaction is the dominant second-order effect on the bodies under consideration, especially for the hyperboloid where it becomes a first-order effect. Considerable attention is devoted to the effects of viscosity law on both first- and second-order solutions; Prandtl number and wall temperature effects are also considered. It is shown that a severe underprediction in skin friction and heat transfer results from use of the linear viscosity law. An interesting wall temperature effect on the hyperboloid is observed in that the cool wall case has a higher skin-friction drag than does the hot wall case; this is explained in terms of a "transition" to flat plate behaviour on the aft portion of the hyperboloid due to the surface pressure distribution.

References

Adams, J. C., Jr. Higher-order boundary-layer effects on analytic bodies or revolution. AEDC-TR-68-57. (April 1968).

Marchand, E. O., Lewis, C. H. and Davis, R. T. Second-order boundary-layer effects on a slender blunt cone at hypersonic conditions. Paper 68-54 presented at the Sixth AIAA Aerospace Sciences Meeting, New York, January 1968.

Lewis, C. H. Comparison of a first-order treatment of higher-order boundary-layer effects with second-order theory and experimental data. AEDC-TR-68-148. (October 1968).

Little, H. R. An experimental investigation of surface conditions on hyperboloids and paraboloids at a Mach number of 10. Master of Science Thesis, University of Tennessee Space Institute, Tullahoma, Tennessee. (June 1969).

---

*The research reported in this paper was supported by the Arnold Engineering Development Center (AEDC), Air Force Systems Command (AFSC), U.S. Air Force, under Contract No. AF40(600)-1200 with ARO, Inc., Contractor Operator, AEDC.

†Supervisor, Theoretical Gas Dynamics Section, Hypervelocity Branch, Aerophysics Division, von Karman Facility.

27. A SURVEY OF HIGHER-ORDER BOUNDARY-LAYER THEORY

Milton Van Dyke
Stanford University

At present one can discuss higher approximations to Prandtl's boundary-layer theory in any detail only for steady, plane or axisymmetric, laminar, and unseparated flows. Under these restrictions, higher-order boundary-layer theory appears to yield an asymptotic expansion in inverse half-powers of a characteristic Reynolds number. Only the second approximation has been examined in detail. Thanks to linearity, the second-order correction can be subdivided into a number of physically identifiable effects. The theory is developed most safely and systematically using the method of matched asymptotic expansions, but the intuitive approach yields greater physical insight.

For incompressible flow, the second-order effects are four in number. First, the easiest to understand but hardest to calculate, is the displacement effect, which modifies the outer inviscid flow and so alters the conditions at the outer edge of the boundary layer. Second, longitudinal curvature adds centrifugal forces to the momentum equation; attempts to calculate this effect have resulted in a protracted comedy of errors. Third, for axisymmetric shapes, transverse curvature adds further effects of the same sort. Fourth, vorticity in the oncoming stream also changes the outer boundary condition; and a second controversy over just how it is changed has only recently been resolved. In compressible flow, additional second-order effects result from slip and temperature jump at the wall, and external vorticity can be divided into gradients of entropy and of stagnation enthalpy. Each of these effects is discussed, and illustrated with the simplest possible example.

Aside from the complicated phenomenon of separation, non-uniformities are introduced into this scheme by sudden curvature, as at corners and edges, by indefinite length of the body, and by non-analyticity of the outer flow at the surface. The consequent modifications are outlined. Brief comparison is made with the limited available experimental measurements.

This paper appeared as a report of limited circulation: Air Force Office of Scientific Research Report No. AFOSR-67-2291, Sept. 1967. It has been published in an extensively revised and amplified form as

Van Dyke, Milton D. 1969 Higher-order boundary-layer theory. Annual Review of Fluid Mechanics 1, 265-292. Annual Reviews, Inc., Palo Alto, Calif.

Further discussion of the modifications introduced by non-analyticity of the external stream will appear shortly as

Conti, R. J. and Van Dyke, M. D. 1969 Reacting flow as an example of a boundary layer under singular external conditions. J. Fluid Mech. (to appear).

conservation equations. The quasi-linearization techniques typically employ conventional numerical integrating routines, the matrix method mentioned above uses conventional finite-difference relations to achieve the same goal, and the integral-matrix method presented here effects the integration with the connected cubics. Regardless of the form adopted for the conservation equations, the methods demand the introduction of these equations at each point in the integration routine, each point in the differential formulation, or each spline point, respectively. For most of the classical problems and the simpler solutions usually reported, this fact is of little consequence. It is of major consequence, however, when a general chemical environment is to be treated. The time required to evaluate the chemical state often dominates all other time considerations, and this state must be evaluated each time the conservation equations are introduced.

The matrix formalization introduced with the Newton-Raphson procedure is of particular value in the present application. Two major reductions are performed at each iteration in the solution process. The first is based on the a priori solution of all the originally linear equations, in particular the spline fit relations, and results in a major reduction in the order of the resultant matrix equation. A subsequent matrix reduction permits the inclusion of general and varied wall boundary conditions. In this reduction the entire boundary-layer solution (including wall fluxes) is expressed at each iteration, in terms of wall values of f, H_T and $\tilde{K}_k$. Thus special energy and mass balances can be simply performed in terms of this very reduced set of variables.

Because of the fully coupled nature of this approach, rapid convergence is usually achieved (typically 5 iterations for stagnation points and 3 for downstream stations). The use of the spline interpolation functions yields accurate solutions with relatively few spline segments (3 to 4 place accuracy with 6 to 10 segments). The technique has been programmed in Fortran IV and applied to a broad range of problems with excellent results. Non-similar solutions have been obtained with coupled mass and energy balances for laminar and turbulent boundary layers over graphite, silica reinforced charring ablation materials, and porous surfaces with water transpiration, as well as problems of more classical interest.

References

Kendall, Robert M. and Bartlett, Eugene P. Non-similar solution of the multi c omponent laminar boundary layer by an integral-matrix method. AIAA Journal, Vol. 6, No. 6, pp. 1089-1097. (1968).

Bartlett, Eugene P. and Kendall, Robert M. Non-similar solution of the multi c omponent laminar boundary layer by an integral matrix method. Aerotherm Corp., Rept. 66-7, Part III. (1967) (NASA CR-1062 - June, 1968).

Bartlett, Eugene P., Nicolet, William, E., Anderson, Larry W., and Kendall, Robert M. Further studies of the coupled chemically reacting boundary layer and charring ablator, Part I, Summary Report. Aerotherm Corp., Rept. 68-38, Part I (NASA CR-92471) (October, 1968).

Anderson, Larry W. and Kendall, Robert M. A non-similar solution for multi c omponent reacting laminar and turbulent boundary layer flows including transverse curvature. Aerotherm Corp., Rept. 69-54. (October, 1969). (Air Force Weapons Laboratory, Rept. AFWL-TR-69-106).

26.

THE INTEGRAL MATRIX APPROACH TO THE SOLUTION OF THE GENERAL MULTICOMPONENT BOUNDARY LAYER

Robert M. Kendall and Eugene P. Bartlett**

The integral matrix procedure is introduced for the accurate prediction of the behaviour of laminar and turbulent boundary layers within a general equilibrium chemical environment. The current procedure utilizes an integral approach with square-wave weighting (or moment) functions and with spline (or connected cubic) interpolation functions for the primary dependent variables, that is, velocity, total enthalpy, and elemental mass fractions. Implicit quadratic finite-difference relations are applied to streamwise derivatives for non-similar solutions. All other terms in the conservation equations are expressed analytically in terms of the primary variables. The resultant set of linear and non-linear algebraic relations is solved using general Newton-Raphson iteration, with significant matrix reductions being employed.

The selection of the spline interpolation functions is based on their ability to accurately conform to complex curves without the often erratic character of high order polynomials. These functions are introduced into the equations by using a set of linear algebraic relations obtained by truncating Taylor series expansions. Thus, considering the velocity, f', to be described by a cubic in the range of a spline segment, the stream functions and its derivatives are related by

$$\left.\begin{aligned} f_{n+1} &= f_n + f'_n\delta\eta + f''_n \frac{(\delta\eta)^2}{2} + f'''_n \frac{(\delta\eta)^3}{8} + f'''_{n+1} \frac{(\delta\eta)^3}{24} \\ f'_{n+1} &= f'_n + f''_n \delta\eta + f'''_n \frac{(\delta\eta)^2}{3} + f'''_{n+1} \frac{(\delta\eta)^2}{6} \\ f''_{n+1} &= f''_n + f'''_n \frac{\delta\eta}{2} + f'''_{n+1} \frac{\delta\eta}{2} \end{aligned}\right\} \qquad (1)$$

Similar sets of relations apply for the enthalpy function and the elemental mass fractions. In the streamwise direction the implicitly defined quadratic representation of the primary variables is reasonably standard. A scaling parameter, α_H, which is an implicit function of the streamwise co-ordinate, is introduced into the definition of the stream-normal co-ordinate in order to assure efficient use of a fixed stream-normal grid. The criterion currently employed for this parameter assures a pre-selected velocity at a prescribed grid point.

When considering either the energy or species conservation equations in boundary-layer form, a significant simplification results as a consequence of stream-normal integration with a constant weighting function. This is due to the complexity of the divergence term in these equations when a general chemical environment is involved and particularly when unequal diffusion and thermal diffusion effects are included, as in the current example. For this reason, square-wave weighting functions were employed in the integration of the conservation equations, each square wave being aligned with an individual spline segment.

With but one exception (the density integration in the momentum equation) it is possible to express analytically all terms appearing in the integrated conservation equations as functions of the primary set of variables. A major factor in achieving this goal is the availability of means of evaluating the state and certain state derivatives in terms of this primary set of variables. Thus, for example, the density derivative at spline point n is defined by

$$\rho'_n = \left(\frac{\partial\rho}{\partial h}\right)_n \left(H'_{T_n} - \frac{u_e^2}{\alpha_H^2} f'_n f''_n\right) + \sum_k \left(\frac{\partial\rho}{\partial \tilde{K}_k}\right)_n \tilde{K}'_{k_n} \qquad (2)$$

where the partial derivatives are state properties obtained from the state solution at point n. In this equation H_T and $\tilde{K}_k$ are the total enthalpy and the elemental mass fraction of element k, respectively. With the density gradients provided as above, it is convenient to formulate the density integration in terms of a special set of connected cubics. At this juncture, the original partial differential equations have been reduced to a set of algebraic equations. Because of the analytical character of the formulation of these equations, the accuracy of any solutions of these algebraic relations can be assessed solely in terms of the accuracy of the distribution of the primary variables. Also the integral form selected assures overall conservation of mass and energy.

In order to achieve solution of this set of linear and non-linear algebraic equations, the general Newton-Raphson iterative solution procedure has been adopted. In this application all coefficients are considered variable and an effort is made to avoid successive approximation assumptions with regard to any coefficient or variable. In this respect, the present method differs from the matrix procedure of D. C. F. Leigh and most of the current quasi-linearization techniques. The other basic differences between this method and those just mentioned, with respect to their treatment of similar solutions, relate to the formulation of the numerical integration procedure and the means of introducing the

25. FINITE DIFFERENCE SOLUTION OF THE FIRST ORDER BOUNDARY LAYER EQUATIONS

F. G. Blottner**
Sandia Laboratories
P. O. Box 5800
Albuquerque, New Mexico 87115

A review of various methods for solving the first order boundary layer equations by numerical techniques is given. The emphasis is on the finite-difference schemes that have been employed recently and how the presently employed techniques have evolved. Procedures developed by authors in various countries such as Russia, Germany, France and the United States are considered.

The governing equations and boundary conditions for a multi-component non-equilibrium gas are presented in the similarity co-ordinate system. The boundary conditions at the surface require the mass flux of the chemical species to be specified. How these conditions can be determined for a catalytic type of interaction between the gas and the surface material are presented. The edge conditions are obtained from the inviscid flow. For a blunt body flow with chemical reactions taken into account, the classical boundary layer approach is not valid and swallowing of the inviscid flow should be included in the analysis. However, in the present case the edge conditions are obtained from the inviscid streamline along the surface of the body with finite rate chemistry. These conditions were provided to participants in the Seminar.

The solution of the boundary layer equations are next presented. An implicit finite-difference technique is presented which is appropriate for solving flows with a large number of chemical species, as occurs with ablation contaminants. This method does not require iterations at each step, and solutions can be obtained when the gas is near chemical equilibrium. With the equations uncoupled and the technique not requiring iterations at each step, the overall computing time for flows with many chemical species is reasonable.

The procedure has been employed to obtain the boundary layer flow on a sharp cone at 150 kft altitude, a velocity of 22 kfps and a wall temperature of 1000°K with the gas undissociated at the surface. The peak electron density along the body is compared to the results of several authors. The difference between the various results is mainly due to the gas models employed. The flow on a hyperboloid[ϕ] at an altitude of 100 kft and a velocity of 20 kfps is also obtained. The results presented are displacement thickness, heat transfer and skin friction along the body. The profiles of the boundary layer properties (velocity, temperature and chemical species) are given for both a catalytic and non-catalytic wall at 50 nose radii downstream from the stagnation point.

** Staff Member, Aerothermodynamics Research Department
This work was supported by the U.S. Atomic Energy Commission.

ϕ This problem and body geometry were requested to be employed by participators in the AGARD Seminar.

References

Blottner, F. G. Non-equilibrium laminar boundary layer flow of ionized air.
General Electric Space Sciences Laboratory, Technical information series, R 64SD56. (1964).

Rittmann, K. Die Berechnung der laminaren, stationären, inkompressiblen Grenzschicht eines angeströmten rotierenden Drehkörpers,
Ing. Arch. 37, 304-314. (1969).

Schönauer, W. Ein Differenzenverfahren zur Lösung der Grenzschichtgleichung für stationäre, laminare, inkompressible Strömung.
Ing. Arch. 33, 173-189. (1964).

Schönauer, W. Die Berechnung der laminaren Absaugegrenzschicht mit dem Differenzenverfahren.
Ing. Arch. 36, 8-18. (1967).

Wippermann, H. W. Ein Differenzenverfahren zur Lösung der Stewartson-Crocco-Gleichungen für kompressible, laminare Grenzschichten.
Acta Mechanica 3, 123-153. (1967).

Schönauer, W., Spreuer, H., Straub, D., Adams, E., Sui Lin Comments on the numerical results of hypersonic boundary layer calculation.
Will be published in a report edited by C. H. Lewis.

Schönauer, W., Spreuer, H., Adams, E., Sui Lin Erfahrungen bei der numerischen Lösung der Hyperschallgrenzschichtgleichungen.
DLR Mitt. 68-33, p. 157-171.

Schönauer, Straub, D., Wassner, L., Adams, E. Diskussion der Energie-gleichung für die Hyperschallgrenzschicht bei chemischem Gleichgewicht.
To be published in ZAMM 49, Sonderheft GAMM-Tagung. (1969).

ENERGY

$$\rho c_p (uT_x + vT_y) - \frac{K_\infty - 1}{K_\infty} up_x + \sum_{r=1}^{m} w_r H_r - \frac{1}{p_r} (\lambda T_y)_y - \frac{1}{Sc_\infty} \frac{K_\infty - 1}{K_\infty} \cdot$$

$$\cdot \left(\frac{k_A^T}{x_A - x_A^2} D_{AM} px_{Ay} \right)_y = M_\infty^2 (K_\infty - 1) \eta u_y^2 - \frac{1}{Sc_\infty} \frac{D_A^T}{T} (c_{pM} - c_{pA}) T_y^2 -$$

$$- \frac{1}{Sc_\infty} \sum_{i=1}^{n} \rho c_{pi} \frac{M_i}{\bar{M}} \sum_{\substack{j=1 \\ j \neq i}} D^{ij} x_{jy} T_y$$

COMPONENT CONTINUITY

$$u\rho_{ix} + u_x \rho_i + \frac{u}{r} \rho_i r_x + v\rho_{iy} + v_y \rho_i - \frac{M_i}{\bar{M}} \sum_{r=1}^{m} \nu_{ir} w_r - \frac{1}{Sc_\infty} \cdot$$

$$\cdot \left(D_i^T \frac{T_y}{T} \right)_y + \frac{1}{Sc_\infty} \sum_{\substack{j=1 \\ j \neq i}}^{n} \left(\rho \frac{M_i}{\bar{M}} D^{ij} x_{jy} \right)_y = 0 \cdot$$

In the momentum equation chemical forces appear. But the related coefficient λ_r is not known, so that these terms cannot be used for practical calculations. This leads to an unknown error. A further term from irreversible thermodynamics appears in the energy equation, the coefficient k_A^T can be evaluated from kinetic theory.

After a similarity transformation, the transformed variables u, v, T, x_i explicitly appearing in the equations are considered as dependent variables. All coefficients are estimated for the last profile. The equations are uncoupled by linearization; momentum $\rightarrow u$, continuity $\rightarrow v$, energy $\rightarrow T$, component continuity simultaneously $\rightarrow x_i$. This method diverges, unless the component continuities are replaced by the condition of chemical equilibrium. During the calculations all coefficients have been printed out.

Thus we could see, that for small deviations from chemical equilibrium the chemical terms became about 1000 times larger than the mechanical terms near the wall. So, small deviations from equilibrium lead to large deviations of temperature (and therefore of the equilibrium concentrations). But as the mechanical and chemical terms must have the same order of magnitude, the deviations from equilibrium for the new temperature must again be small, because the chemical terms have enormous gradients. Blottner has shown, that by expanding the chemical terms in x-direction these terms can be incorporated implicitly into the equations and thus the method becomes stable. Our aim is to preserve by a suitable expansion the uncoupling of the equations, which saves half the computing time and machine storage compared with the coupled solution of the equations. Further the uncoupling allows a separate iteration of the concentrations. This iteration is necessary for the boundary condition of chemical equilibrium at the wall. This is the only chemical boundary condition that does not lead to a singularity. The often used condition "no chemical reaction at the wall" leads to a contradiction to the compatibility condition at the wall and therefore to a singularity.

Numerical results for chemical equilibrium bdls. will be published in the report on the hyperboloid calculations of the AGARD Seminar, edited by C. H. Lewis.

24. NUMERICAL EXPERIMENTS IN IDEAL AND REAL GAS LAMINAR BOUNDARY LAYER FLOW

W. Schönauer
Inst. fur Angewandte Grenzschicht theory,
Techn. Hochschule, Karlsruhe

About the Crocco Transformation: In the last years many numerical experiments at the University of Karlsruhe have been made with implicit finite difference methods for the bdl. equs. in the Prandtl-, the v. Mises- and the Crocco-form. A modification of the Crocco-form, with $H \sim u_y^2$ as dependent variable has proved superior to all other forms. The Crocco-form has a rectangular domain of integration. But the Crocco profiles have infinite curvature at the outer edge of the bdl.

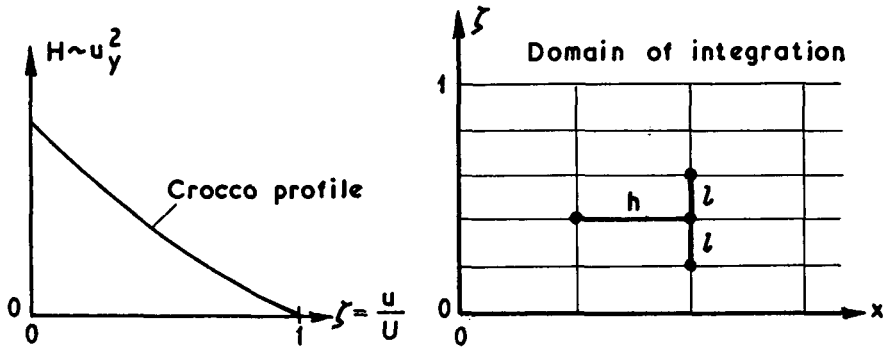

The consequence of the singularity (for $\zeta \to 1$: $H \to (1-\zeta)^2\,[a+b\,\ln(1-\zeta)]$) is, that 3- or 5-point equidistant net formulae for the ζ-derivatives and 3-point unequally spaced net-formulae all have an error $O(1)$. Therefore the best net is an unequally spaced net with a concentration of points near the outer edge (for the singularity) and near the wall (for the separation profiles). In the Prandtl form instead of the singularity we have an infinite domain. Here unequally spaced nets with a wider mesh at the outer edge give optimal accuracy for a given number of mesh points. Rittmann extended the Crocco-method for rotating bodies of revolution.

Wippermann studied the ideal gas compressible bdl. He applied first a Stewartson transformation and then the modified Crocco transformation on the momentum and energy equations. The equations are uncoupled by linearization. First is solved the energy equation for the enthalpy function, then the momentum equation for the Crocco variable H.

Initial Profile Calculation (arbitrary form of bdl. equs., but after a similarity transformation to avoid singularity at $x = 0$): The ordinary eqs. for the initial profile result from the partial differential eqs. by taking the x-dependent coefficients at $x = 0$. Therefore in the bdl. program one has only to fix $x = 0$, to begin with an arbitrary initial profile, to compute the "downstream" profile, to take this as new initial profile and so on, until the profile stands. Then the usual downstream calculation begins with the iterated profile.

Real Gas Boundary Layer (Prandtl form): A team has been formed at Karlsruhe to study the real gas effects with the concept of irreversible thermodynamics. With the mol concentrations x_i for the component i the equations are:

MOMENTUM

$$\rho u u_x + \rho v u_y = -\frac{p_x}{K M_\infty^2} + (\eta u_y)_y \left\{ - \sum_{r=1}^{m} \left(\frac{\lambda_r A_r}{T} \right)_x \right\}$$

$$p_y = 0$$

CONTINUITY

$$u\rho_x + u_x\rho + \frac{u}{r}\rho r_x + v\rho_y + v_y\rho = 0$$

23. SOME SIMILAR LAMINAR FLOWS OBTAINED BY QUASI-LINEARIZATION †

Paul A. Libby* and T. M. Liu**
Department of the Aerospace and Mechanical Engineering Sciences
University of California, San Diego
La Jolla, California

Laminar boundary layers exhibiting similarity have long played an important role in exposing the principal physical features of boundary layer phenomena and in providing bases for approximate methods of calculating more complex, non-similar cases. Despite the large number of similar solutions presently available, new ones continually appear in the literature since the number of combinations of distributions in the external stream, of mass and heat transfer and of three-dimensionality satisfying similarity requirements is apparently limitless.

Our purpose in the present work is to show that two relatively well-known sets of similarity equations have a multiplicity of solutions not previously obtained. The two sets correspond to the laminar compressible boundary layer with arbitrary pressure gradient and heat transfer, usually associated with Cohen and Reshotko, and to the laminar hypersonic boundary layer near a plane of symmetry studied by Trella and Libby.

In order to obtain the new solutions the method of quasi-linearization is applied to the treatment of the two-point boundary value problem. There are employed both a straightforward application of the technique and a modified application in which a wall value, usually considered unknown, is fixed a priori and a parameter, usually selected a priori, is determined as the iterations leading to a solution are carried out. It is indicated that the new solutions involving as they do complex profiles would be difficult if not impossible to obtain without numerical techniques of this sort.

The results of the numerical analysis indicate that these similarity equations contain for adverse pressure gradients a variety of solutions. Most dramatic is the result that for a given set of parameters defining a particular hypersonic flow near a plane of symmetry there are six solutions, each with exponential decay to free stream values, an extreme case of non-uniqueness. How many of these six and, indeed, how many of the new solutions obtained in this work are physically observable is not known but we do know that they satisfy the usual conservation equations and that obtaining them requires a sophisticated numerical technique.

† This study was carried out as part of a research program being performed under National Aeronautics and Space Administration Grant NGR-05-009-025. AIAA Journal 6, 1541 (1968).

• Professor of Aerospace Engineering.

**Research Assistant.

References (contd)

[7] Smith, A. M. O. and Jaffe, N. A. General method for solving the laminar non-equilibrium boundary-layer equations of a dissociating gas.
AIAA J., Vol. 4, No. 4, pp. 611-620. (April, 1966).

[8] Jaffe, N. A. and Thomas, J. The application of quasi-linearization and Chebyshev Series to the numerical analysis of viscous shear layers.
Department of Engineering Science, Oxford University Report 1,035.67. (September, 1967).

[9] Bellman, R. E. and Kalaba, R. E. Quasi-linearization and non-linear boundary-value problems.
American Elsevier Publishing Company, Inc., New York. (1965).

[10] Fox, L. Chebyshev Methods for ordinary differential equations.
Computer Journal, Vol. 4, pp. 318-331. (1962).

[11] Schubauer, G. B. Airflow in a separation laminar boundary layer.
NACA Report No. 527. (1935).

The approximate solution is chosen so as to satisfy equations (2a), (2b), and (2c); thus boundary conditions on (5) are given by

$$\varepsilon(0) = \varepsilon'(0) = \varepsilon'(\eta_\infty) = 0 \tag{7}$$

The interval $(0,\eta_\infty)$ is transformed to the interval $(-1,1)$ and the quantity ε and its higher derivatives are approximated by the Chebyshev series [10]

$$\varepsilon^{(n)}(z) = a_o^{(n)}/2 + \sum_{r=1}^{N-n} a_r^{(n)} T_r(z) \tag{8}$$

where

$$T_r(z) = \cos(r \arccos z) \qquad -1 \leq z \leq 1$$

The set of Chebyshev coefficients of the series for ε, ε', ε'', and ε''' constitute $4N - 2$ unknowns. The polynomials T_r are linearly independent; thus after substitution of the series given by equation (8) into equation (5) a solution is obtained by equating resulting coefficients of T_r to zero. This leads to a set of $N + 1$ linear equations for the coefficients of $T_1, T_2, \ldots, T_N$ and a constant term. The boundary conditions yield three more equations and in addition there are $3N - 6$ equations of the form

$$a_{r-1}^{(n-1)} = a_{r+1}^{(n-1)} + 2r a_r^{(n)} \tag{9}$$

relating coefficients of ε to ε', ε' to ε'', and ε'' to ε'''. The solution to equation (5) is used to generate a new approximation and the non-linear equation is satisfied upon convergence of successive approximations f_i given by

$$f_i^{(n)} = \varepsilon_{i-1}^{(n)} + f_{i-1}^{(n)} \tag{10}$$

The method has been applied to obtain solutions to the Falkner-Skan equation, a solution to the Howarth retarded flow problem and to the flow over an elliptic cylinder studied experimentally by Schubauer[11]. In addition, the solution for the wake behind a flat plate was obtained using the present method with modified boundary conditions. For most flows a series of 12 terms ensures 4-place accuracy; in the immediate vicinity of separation approximately twice as many terms are necessary for the same accuracy. Convergence of the solution to the non-linear equation to as many places as the Chebyshev series is accurate is usually guaranteed after four iterations (successive approximations) on the linearized equation. Comparisons with existing solutions and experiment have verified the accuracy and generality of the method. To date only a limited number of comparisons between the present method and implicit finite-difference techniques have been made; for those flows studied the present method is competitive with finite difference techniques. In addition, it has the advantage of providing the solution in an analytic form that is easily integrable or differentiable.

References

[1] Hartree, D. R. and Womersley, J. R. A method for the numerical or mechanical solution of partial differential equations.
Proc. Roy. Soc., Series A, Vol. 161, No. 902, p. 353. (August, 1937).

[2] Smith, A. M. O. and Clutter, D. W. Solution of the incompressible laminar boundary-layer equations.
Douglas Aircraft Company Report ES 40446. (29th July, 1961).

[3] Smith, A. M. O. and Clutter, D. W. Solution of the incompressible laminar boundary-layer equations.
AIAA J., Vol. 1, pp. 2062-2071. (September, 1963).

[4] Smith, A. M. O. and Clutter, D. W. A general method for solving the compressible laminar boundary-layer equations.
Douglas Aircraft Company Paper 1699. Presented at the International Symposium on Analogue and Digital Techniques Applied to Aeronautics, Liege, Belgium. (9th-12th September, 1963).

[5] Smith, A. M. O., and Clutter, D. W. Machine calculation of compressible laminar boundary layers.
AIAA J., Vol. 3, No. 4, pp. 639-647. (April, 1965).

[6] Jaffe, N. A., Lind, R.C. and Smith, A. M. O. Solution of the binary diffusion laminar boundary-layer equations with second-order transverse curvature.
AIAA J., Vol. 5, No. 9, pp. 1563-1569. (September, 1967).

22. THE APPLICATION OF QUASI-LINEARIZATION AND CHEBYSHEV SERIES TO THE NUMERICAL ANALYSIS OF VISCOUS SHEAR LAYERS

N. A. Jaffe* and J. Thomas**

A method for solving the incompressible laminar boundary-layer equations for arbitrarily-shaped axisymmetric or two-dimensional bodies is given. With little modification, the techniques described can be applied to wake flows. The method is capable of computing the flow field for similar and non-similar flows with arbitrarily specified surface mass transfer distributions.

The equations of momentum and continuity are combined leading to the following third-order, non-linear, parabolic, partial-differential equation for the dimensionless stream function f in transformed co-ordinates

$$f''' + M(1 - f'^2) + Nff'' = x\left(f'\frac{\partial f'}{\partial x} - f''\frac{\partial f}{\partial x}\right) \tag{1}$$

having the following boundary conditions:

$$f(0) = f_w(x) \text{ specified} \tag{2a}$$

$$f'(0) = 0 \tag{2b}$$

$$f'(\eta_\infty) = 1 \tag{2c}$$

The primes denote derivatives with respect to the transformed co-ordinate normal to the surface, x is the curvi-linear co-ordinate measured parallel to the surface, and the quantities M and N, which depend on body geometry are specified functions of x.

The problem of solving the above partial-differential equation is reduced to that of solving consecutively a sequence of ordinary-differential equations by replacing the streamwise derivatives $(\partial f'/\partial x)$ and $(\partial f/\partial x)$ with forward difference approximations in accordance with ideas originated by Hartree and Womersley [1]. That is, using a three-point Lagrange forward difference approximation at a given x, the streamwise derivative of a quantity $(\ )$ is approximated by

$$\frac{\partial(\ )}{\partial x} = a(\ ) + b(\ )_{-1} + c(\ )_{-2} \tag{3}$$

where a, b, and c are the appropriate Lagrange coefficients and the subscripts -1 -2 designate two stations previous to x. If solutions are known at x_{-1} and x_{-2} the equation is ordinary at x. At the initial station $(x = 0)$ the streamwise derivatives which are a multiple of x need not be evaluated; at the second station the above three-point approximation is replaced by a two-point approximation. Thus the flow field can be obtained by solving a sequence of ordinary equations marching downstream. This technique has been successfully employed by Smith and coworkers for incompressible flow [2,3], compressible flow [4,5] flow of a non-reacting binary gas [6], and non-equilibrium flow on a binary gas [7].

In Refs. [2] through [7] the ordinary differential equations resulting from the approximation given by equation (3) are solved by an initial value (shooting method) technique. Equation (1) is repeatedly integrated with boundary conditions (2a), (2b) and trial values of $f''(0)$ until it is possible to construct a solution satisfying equation (2c). In certain cases solutions at the outer boundary, η_∞, are extremely sensitive to trial values of $f''(0)$ and it is impossible or extremely time consuming to satisfy the boundary condition at η_∞. Moreover, there are flows in which the programmed logic that determines whether a given trial value of $f''(0)$ is high or low, after a trial solution has been obtained, fails and thus it is not possible to converge on the desired solution. An alternative method for solving the ordinary equations was therefore investigated [8]. The ordinary non-linear equation upon substitution of the approximation given by equation (3) is of the form

$$\varphi\,(f''',f'',f',f) = 0 \tag{4}$$

Expanding in a Taylor's series about an approximate solution f_o and neglecting non-linear terms in the dependent variable gives [9]:

$$\varphi_o + \left(\frac{\partial\varphi}{\partial f'''}\right)_o \varepsilon''' + \left(\frac{\partial\varphi}{\partial f''}\right)_o \varepsilon'' + \left(\frac{\partial\varphi}{\partial f'}\right)\varepsilon' + \left(\frac{\partial\varphi}{\partial f}\right)_o \varepsilon = 0 \tag{5}$$

where

$$\varepsilon^{(n)} = f^{(n)} - f_o^{(n)} \tag{6}$$

---

* Investigation conducted while visiting Oxford University; currently Senior Engineer/Scientist, Douglas Aircraft Company, McDonnell Douglas Corporation, Long Beach, Calif.
** Graduate research student, Oxford University, England

Reports and Internal Papers (continued)

Kaups, K. and Keltner, G. Laminar compressible boundary layer on a yawed infinite wing. Douglas Report No. LB 32706. (15th March, 1967).

Keltner, G. L. Laminar boundary layer calculations on bodies of revolution in hypersonic flow. Douglas Report No. DAC 66719. (1st March, 1968).

Kaups, K. and Smith, A. M. O. The laminar boundary layer in water with variable properties. Douglas Engineering Paper No. 3780. (30th March, 1967).

Jaffe, N. A. The numerical solution of the nonsimilar laminar boundary-layer equations including the effects of non-equilibrium dissociation. Douglas Engineering Paper No. 5550. (February, 1969). Presented to the Von Karman Institute for Fluid Mechanics as part of an AGARD-sponsored course on Hypersonic Boundary Layers, Rhode-Saint-Genese, Belgium.

Since the time of the meeting the author's main attention has been given to a rather conventional implicit finite-difference procedure used in connection with the turbulent boundary-layer equations. In turbulent boundary layers the eddy viscosity is an unknown function of the boundary layer thickness and another iteration cycle is required to find it. While the shooting method has been successfully applied to this problem it was slow because of the extra iteration. The finite-difference method is so constituted that no additional iteration is required for an eddy viscosity, making the method faster for turbulent flows. Based on this considerable experience with both methods it is the author's opinion that the shooting method can more easily give high accuracy - say five figures - if that is wanted. For equal accuracy the shooting method is somewhat slower, but not importantly. It is perhaps half as fast as the finite difference when applied to the same laminar flow problem. Because of the sophisticated integration procedure used in the shooting technique much larger y-steps can be used for the same accuracy. Often the two methods are compared timewise with equal steps. Then the finite-difference technique turns out to be much faster. But for the condition of equal accuracy in laminar flows the shooting method does not have an important time disadvantage. Below are listed the principal reports and publications based on the shooting method as developed by the author and his coworkers.

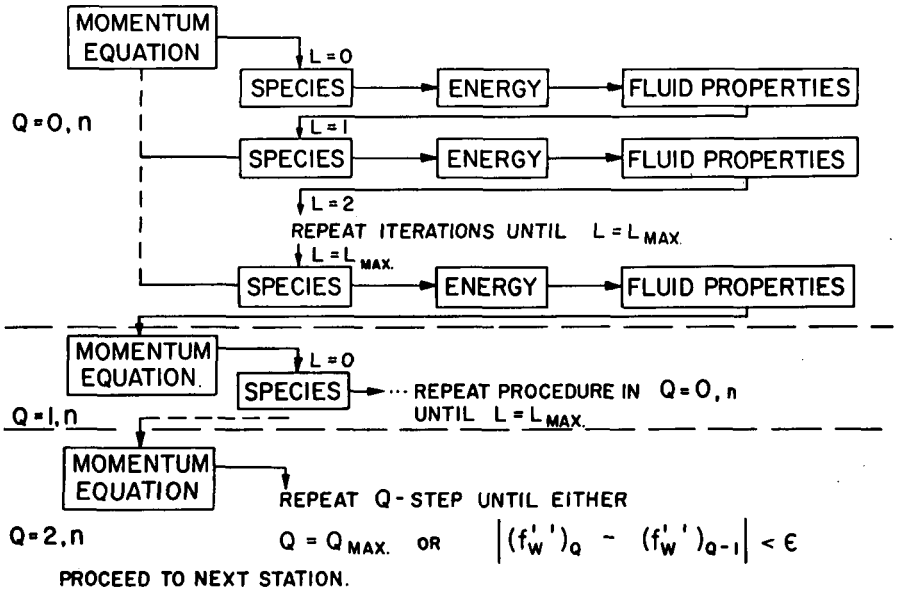

Fig. 1. Flow diagram for solution at station x_n

References

Smith, A. M. O., Clutter, D. W. Solution of the incompressible laminar boundary-layer equations. AIAA J., Vol. 1, No. 9. (September, 1963).

Smith, A. M. O., Clutter, D. W. Machine calculation of compressible boundary layers. AIAA J., Vol. 3, No. 4. (April, 1965).

Smith, A. M. O., Jaffe, N. A. General method for solving the laminar boundary layer equations of a non-equilibrium dissociating gas. AIAA J., Vol. 4, No. 4. (April, 1966).

Jaffe, N. A. Effects of a transverse magnetic field and spanwise electric field on the boundary layer of a conducting fluid. AIAA J., Vol. 4, No. 10. (October, 1966).

Jaffe, N. A., Lind, R. C., Smith, A. M. O. Solution of the binary diffusion laminar boundary-layer equations with second-order transverse curvature. AIAA J., Vol. 5, No. 9. (September, 1967).

Jaffe, N. A. and Okamura, T. T. The transverse curvature effect on the incompressible laminar boundary layer for longitudinal flow over a cylinder. ZAMP, Vol. 19, Fasc. 4. (1968).

Cebeci, T., Smith, A. M. O. and Mosinskis, G. Calculation of compressible adiabatic turbulent boundary layers. AIAA Preprint No. 69-787. (June, 1969). (This is a key to the finite-difference method).

Reports and Internal Papers

Smith, A. M. O. and Clutter, D. W. Solution of the incompressible laminar boundary-layer equations. Douglas Report No. ES 40446. (29th July, 1961).

Lind, R. C. and Cebeci, T. Solution of the equations of the compressible laminar boundary layer with surface radiation. Douglas Report No. DAC 33482. (15th December, 1966).

Treatment of the x-Derivative

All the transformed equations involve first, and only first, derivatives in x, as in equation (1). These derivatives are replaced by Lagrangian derivative formulae; two-, three-, and four-point formulae have been investigated. The substitution reduces the various equations to ordinary differential equations, for which there are many good numerical-solution techniques. Since the equations are parabolic, we have reduced the problem of solving the partial differential equations to one of solving an ordinary differential equation repeatedly at each x-station as we proceed downstream. It is emphasized that the equations applying to the individual x-stations are solved consecutively, not simultaneously. This basic approach was used much earlier by Hartree and Womersley, to adapt partial differential equations to the old Bush Differential Analyzer.

Integration

Integration is performed on the resulting transformed ordinary equations as they stand. The momentum equation is non-linear. The other equations are non-linear too, if variable gas properties are involved, because they are not known until the correct solution is found. However, in practice iteration is used, and gas properties are supplied by the last previous iteration. This process reduces the energy and species equations to linear forms.

In the development of the method of solution, both the Runge-Kutta and the Adams-Falkner integration methods have been used with success, but the latter has been used more often. In any one solution, the step size in the y-direction is taken to be constant, primarily because the computation of the x-derivatives would otherwise be greatly complicated.

Meeting Boundary Conditions

In the x-momentum equation two boundary conditions occur at the wall and the third at $\eta = \infty$. Since the momentum equation is non-linear the common "shooting" method is used to satisfy this third condition, with two refinements. The first refinement has to do with interpolation for f''_w, the derivative of f' at the wall. In practice the outer boundary condition must be satisfied at some finite η-value, called η_∞. Study showed that, within a limited range or corridor, $f'(\eta_\infty)$ was a very regular, slightly quadratic function of f''_w, the second derivative at the wall, which is the unknown being sought. Therefore it became possible to set up a simple three-point interpolation scheme that required only the construction of three trial solutions corresponding to three values of f''_w. The correct outer boundary condition is $f'(\eta_\infty) = 1$. Trial solutions meeting the requirement $0.5 \leq f'(\eta_\infty) \leq 1.5$ generally afforded an accurate base for three-point interpolation. By contrast, simple "shooting" would require systematic variation of f''_w until a solution was found such that, for usual accuracy, $0.999 \leq f'(\eta_\infty) \leq 1.001$. In favourable cases, the three-solution interpolation procedure reduces computation by 75 to 80 percent, compared with simple "shooting". Of course, for linear equations any two suitable trial solutions suffice as a base for interpolation. The energy equation is effectively linear.

The second refinement of the "shooting" method has to do with continuing the solution when excessively large numbers arise. Often, because of the exponential character of trial solutions, values of f' at η_∞ become too large to handle. Yet, two partial solutions may be found, one of which is clearly high with respect to the boundary condition $f'(\eta_\infty) = 1$ and the other clearly low. If these two solutions are compared, it will be found that they agree, to a certain degree of accuracy, up to some value of η_1 greater than zero, for example, $\eta_1 = 1$. The desired solution lies between this pair of high and low solutions. Hence, depending on the accuracy demanded, the correct solution has been established up to some point η_1. This point can then be treated as a new origin, and search can be continued by means of several trial values of f'_1. The process can be repeated several times, if necessary, to construct solutions running all the way to η_∞. This trick has been dubbed ETI (Extended Trajectory Integration).

If gas properties are temporarily assumed - as they are - the energy, species, and x-momentum equations all become linear. Meeting boundary conditions for these then becomes easy, because the desired solution is just a linear combination of two trial solutions, which have no special restrictions on their magnitude at η_∞. However, exponential growth still exists, and the ETI treatment must often be used, for solutions having values at η_∞ as high as 10^6 may often occur. They are legitimate, but accuracy is lost in the process of linear combination of two such solutions, and again ETI provides improvement.

In the more general flows, the gas properties themselves must be found as part of the solution. The process involves iterative or cyclic solution of several equations. First, gas properties are assumed and then the x-momentum equation is solved. When properties are assumed the process of solving the x-momentum equation, even for reacting flows, is just the same as for incompressible flow. When a solution with the assumed properties that meets the boundary conditions is found, the new velocity information is fed to the energy equation, which in turn is solved. The results are then used to compute improved fluid properties. The energy equation is solved again with these new fluid properties, and the process continues until convergence is obtained. But this convergence is obtained with only approximate values of velocity supplied by the momentum equation. Therefore, the final converged fluid properties are in turn supplied to the momentum equation, and the procedure is repeated. In an overall sense, when the momentum equation and energy equation are involved, the method of solution may be characterized as a combination of an inner iteration and an outer iteration. When a third equation, for example, a species, is used, it too is involved in the inner-iteration cycle. Fig. 1 shows the flow diagram for the most general case.

21. NUMERICAL SOLUTION OF LAMINAR BOUNDARY LAYERS

A. M. O. Smith*

General

This paper constitutes an abridged version of the complete paper of the same title presented at the NPL AGARD Seminar on "Numerical Methods for Viscous Flows". The basic purpose of the complete paper is to present a comprehensive description of one particular method of solution and its capabilities. Often, in a complete presentation, so many details are included that the fundamental underlying concepts are hidden. Therefore this summary is meant to be a kind of supplement that in a brief and non-mathematical fashion gives the essentials of the method.

Before proceeding to details, some general information will be presented. The author and several able collaborators have worked since 1960 on this numerical method for solving the laminar boundary layers. Because of the author's involvement with aircraft rather than with missiles, the emphasis has been more on development of the method of solution than on the chemistry and physics of the gases involved. The first problem attacked was incompressible laminar two-dimensional or axisymmetric flow subject to quite general boundary conditions. This problem involved solution of the continuity and x-momentum equations. The most advanced problems so far solved - with similar very general boundary conditions - involve the equations of (1) global continuity, (2) x-momentum, (3) energy, and (4) either continuity of species or z-momentum. The z-momentum equation is needed in describing three-dimensional flow past an infinite yawed cylinder. With these four equations non-equilibrium flow of a binary gas can be correctly treated, but non-equilibrium flow of air can be only approximated.

For three- to four-place accuracy, the flow is typically divided into about 24 x-stations. The y-direction is divided into about 100 stations. For incompressible flow, a solution at one station requires about 20 seconds on an IBM 7094. Four-equation flows require about 90 seconds per station. The total time is approximately equal to the time per station multiplied by the number of stations. We now turn to a general description of the method.

Equations

The basic equations are the complete first-order boundary-layer equations, except that in some of the most recent work second-order transverse-curvature effects have been included in treating axisymmetric flow. The important fact about the equations is the form actually used in the solution. It is some kind of f-transformation such as Levy-Lees. For example, one form used in solving incompressible flows is

$$f''' + ff'' + \beta(1 - f'^2) = 2x\left(f'\frac{\partial f'}{\partial x} - f''\frac{\partial f}{\partial x}\right) \qquad (1)$$

where x is a measure of distance from the stagnation point and primes denote derivatives with respect to η, the transformed y-variable.

This basic form for the system of equations has the following important advantages:

1. Starting the solution is remarkably easy. Note that at $x = 0$ in the above equation we are left with an ordinary differential equation, the Falkner-Skan equation.

2. Most of the variation in boundary-layer thickness is eliminated, making for easier handling of the outer boundary conditions.

3. Solutions are supplied in a well-known form.

4. "Overshoot" causes no problem. In certain other transformations, "overshoot" causes the solution to fail.

Gas Properties

Gas properties have always been defined by some algebraic relation or combinations of algebraic relations. Perfect-gas relations, Sutherland's law, piecewise polynomial descriptions of enthalpy and the density-viscosity product are a few examples. Others are the binary diffusion coefficient and the chemical source term arising in non-equilibrium flows. Different representations of gas properties involve new formulae and reprogramming only of the gas-property part of the entire computing program.

*Chief Aerodynamics Engineer, Research, Douglas Aircraft Company, McDonnell Douglas Corporation, Long Beach, California.

20.

DIFFERENCE APPROXIMATION OF THE BOUNDARY-LAYER EQUATIONS NEAR SEPARATION

P. G. Williams
University College, London

In this paper the behaviour near separation of a standard difference approximation to the boundary-layer equations is considered. Attention is first restricted to simple two-dimensional incompressible flow, then the extension to a quasi-three-dimensional flow and compressible flow are touched upon.

The singular behaviour of the solutions of the laminar boundary-layer equations at the separation point $x = x_s$, where the skin friction coefficient $\tau_x = \left(\frac{\partial u}{\partial z}\right)_{z=0}$ vanishes, has been the subject of a number of investigations (Refs. [1], [2], [3], [4], [5]). It has been established that a logically consistent expansion can be obtained in terms of the variables $\xi = (x_s - x)^{1/4}$, $\eta = z(x_s - x)^{-1/4}$; this leads to an expression for the skin friction coefficient of the form

$$\tau_x = 2\sqrt{2}\,\xi^2 \left[\alpha_1 + \alpha_2 \xi + \alpha_3 \xi^2 + \alpha_4 \xi^3 + (\beta_5 \ell n\, \xi + \alpha_5)\,\xi^4 + (\beta_6 \ell n\, \xi + \alpha_6)\,\xi^5 + O(\xi^6 \ell n\, \xi)\right]$$

in which α_1, α_5, α_6, ... are disposable and have to be determined by matching to the upstream flow. Previous numerical work in this connection [1], [3], [5] has concentrated on obtaining the upstream flow to some reasonable accuracy and then attempting a match. Here we examine the difference equations obtained by differencing in the z-direction only and try to deduce what happens as separation is approached; for simplicity, this is largely explained in terms of a one-mesh-point model, and it is shown that a singularity occurs at which the solution in general has an expansion in even powers of ξ. We consider to what extent the behaviour for a fixed non-zero mesh size h models the behaviour of the boundary-layer equations, and suggest that this illuminates the singularity of the boundary-layer equations at separation. The convergence as $h \to 0$ is investigated numerically for the case with mainstream velocity $U(x) = 1 - x$.

The basic numerical procedure is allied to those used by Leigh [3] and Terrill [5], but differs mainly in the method of solving the non-linear set of difference equations. Here Newton iteration is used, and the resulting set of linear equations solved by an efficient form of Gaussian elimination. The method has been extended to deal with a fifth-order system of partial differential equations which includes compressible flow using Stewartson's transformation and some quasi-three-dimensional flows, in particular, flow past a yawed flat plate with an imposed pressure gradient, which will be considered numerically for the mainstream $(U,V) = (1 - x, 1)$.

For this case the equation for the crossflow component of velocity v is decoupled from the chordwise flow equations, which is the ordinary two-dimensional equation with $U = 1 - x$. A Goldstein-type theory has recently been developed for it by Banks (as yet unpublished), and an excellent match been made with a numerical solution. Details of this match will be presented. This case is of interest here because it turns out that τ_y, the crossflow skin friction, has an expansion of the form

$$\tau_y = b_0 + b_1 \xi_1 + O(\xi^2)$$

with b_0, $b_1 \neq 0$, so that the fact that the difference equations can only have an expansion in even powers of ξ is shown up more sharply. Nevertheless, excellent agreement is obtained in the limit $h \to 0$.

References

[1] Hartree, D. R. A solution of the laminary boundary-layer equation for retarded flow. A.R.C. R. & M. No. 2426. (1939/49).

[2] Goldstein, S. On laminar boundary-layer flow near a position of separation. Q.J.M.A.M. 1, 43. (1948).

[3] Leigh, D. C. F. The laminar boundary-layer equations: a method of solution by means of an automatic computer. Proc. Camb. Phil. Soc. 51, 320. (1955).

[4] Stewartson, K. On Goldstein's theory of laminar separation. Q.J.M.A.M. 11, 399. (1958).

[5] Terrill, R. M. Laminar boundary-layer flow near separation with and without suction. Phil. Trans. A 253, 55. (1960).

The solution was evaluated numerically using the Runge-Kutta method.

In the special case $m = 0$ one obtains the Prandtl-Blasius equation

$$\phi''' + \phi\phi'' = 0 \tag{11}$$

with the boundary condition at the wall

$$\eta^* = 0: \quad \phi = C - 4A, \quad \phi' = 0 \tag{12}$$

Thus longitudinal curvature and boundary layer control have the same influence on the boundary condition. In order to obtain a potential main flow one can deduce from the expression for the vorticity that up to the order A the relation

$$U(x,y) = \frac{U_o(x)}{1 + ky} \tag{13}$$

must hold. This leads to a stream function

$$\psi_1 = \frac{U_o}{k} \ln(1 + ky) \tag{14}$$

which differs from the asymptotic stream function of the boundary layer and does not include the displacement effect. Therefore an additional stream function ψ_2 is introduced which satisfies the condition of irrotationality up to terms of the order A

$$\frac{\partial^2 \psi_2}{\partial \eta^{*2}} = 0 \tag{15}$$

The boundary condition is given by the v-component of the boundary layer solution at the edge of the boundary layer, which may be identified with $\eta^* = 0$. This leads to

$$\psi_2 = -\sqrt{\frac{2}{m+1} U_{o1} x_1 \nu}\ \bar{\delta}_1 \left(\frac{x}{x_1}\right)^{\frac{m+1}{2}} \tag{16}$$

The solutions ψ_1, and ψ_2 show that the co-ordinates η^* and x are optimal co-ordinates in the sense of Kaplun[3]. Thus the solution derived here also describes the main flow accurately up to terms of second order and therefore fulfills all requirements of a second order theory. In [4] ψ_2 was not yet included as it does not influence the numerical results.

The heat transfer problem considering the dissipation function now also can be treated. [4]. Numerical results are obtained which can be applied to curvature as well as boundary layer control.

References

[1] Murphy, J. S. Some effects of surface curvature on laminar boundary layer flow. J. Aeronaut. Sci. 20, 338-344. (1953).

[2] Schultz-Grunow, F., Breuer, W. Laminar boundary layers on cambered walls in: Basic developments in Fluid Mechanics (ed. M. Holt), Vol. 1, pp. 377-436, Academic Press. (1965).

[3] Kaplun, S. The role of co-ordinate system in boundary layer theory. Zeitschrift für angewandte Mathematik and Physik 5, 111-135. (1954).

[4] Schultz-Grunow, F., Henseler, H. Ähnliche Grenzschichtlösungen zweiter Ordnung etc. Wärme- und Stoffübertragung 1, 214-219. (1968).

---

19. SELF-SIMILAR SOLUTIONS OF SECOND ORDER LAMINAR BOUNDARY LAYER EQUATIONS WITH LONGITUDINAL CURVATURE AND BOUNDARY LAYER CONTROL

F. Schultz-Grunow, H. Henseler
Institut für Allgemeine Mechanik an der Technischen Hochschule,
Aachen

Terms up to the order δ/R (δ = boundary layer thickness, R = radius of curvature) or $Re^{-1/2}$ ($R = RU/\nu$) are considered [1,2].

The similarity conditions lead to a class of surfaces with a curvature $k \sim x^{\frac{m-1}{2}}$, where m is arbitrary and x is the arc length of the wall curve. This requires a main flow velocity distribution along the wall according to $U_o \sim x^m$. $m = 0$ corresponds to the evolute of a circle with a sharp leading edge and $m = 1$ to the stagnation point flow at a cylinder.

The boundary layer equations can be simplified considerably by introducing the substitution [2]

$$\eta^* = \frac{1}{2A} \ell n(1 + ky) \tag{1}$$

y denotes the co-ordinate perpendicular to the wall and A the curvature parameter. ($A > 0$: convex wall, $A < 0$: concave wall). This quantity is deduced from the similarity condition $\delta/k = \text{const.}$ leading to the relation $ky = 2A\eta$ with $\eta = y/\delta$.

Introducing a dimensionless stream function $\varphi(\eta^*)$ into the boundary layer equation and eliminating the pressure by crosswise differentiation one obtains the fourth order equation [4].

$$[\varphi''' + (\varphi - 4A)\varphi'' - \beta\varphi'^2]' = 4A[\varphi''' + (\varphi - 4A)\varphi''] \tag{2}$$

which can be integrated once. The integral can be solved by successive approximation putting the right hand side, which is of the small order A, equal zero. Thus the Falkner-Skan equation is obtained, the integral of which leads to

$$(1 + \beta)/\varphi'^2 \, d\eta^* = \varphi'' + \varphi' + \beta\eta^* + C_1 \tag{3}$$

The constant of integration C is determined by the asymptotic behaviour of φ at large η^*, which is found by considering the displacement thickness δ_1, which is defined by

$$\delta_1 = \int_0^\infty \frac{U(s) - u}{U_o} \, dy \tag{4}$$

Introducing the dimensionless quantity $\bar{\delta}_1$,

$$\delta_1 = \sqrt{\frac{2}{m+1} \frac{\nu x}{U_o}} \, \bar{\delta}_1 \tag{5}$$

one obtains

$$\bar{\delta}_1 = \int_0^\infty (1 - \varphi') \, d\eta^* = \eta^* - \varphi(\infty) + C \tag{6}$$

C is the boundary layer control parameter. ($C > 0$: suction, $C < 0$ blowing)

From this the asymptotic expression for the stream function is

$$\varphi(\infty) = \eta^* + C - \bar{\delta}_1 \tag{7}$$

Using this relationship the constant C_1 in (3) can be expressed as

$$C_1 = -\beta(\bar{\delta}_1 - C) \tag{8}$$

and one obtains when substituting $\phi = \varphi - 4A$

$$\phi''' + \phi\phi'' + \beta(1 - \phi'^2) = 4A \frac{\beta}{\beta+1} [\phi'' + \phi\phi' - \eta^* - \bar{\delta}_1] \tag{9}$$

with the boundary conditions

$$\eta^* = 0: \quad \phi = C - 4A, \ \phi' = 0; \quad \eta^* = \infty: \quad \phi' = 1 \tag{10}$$

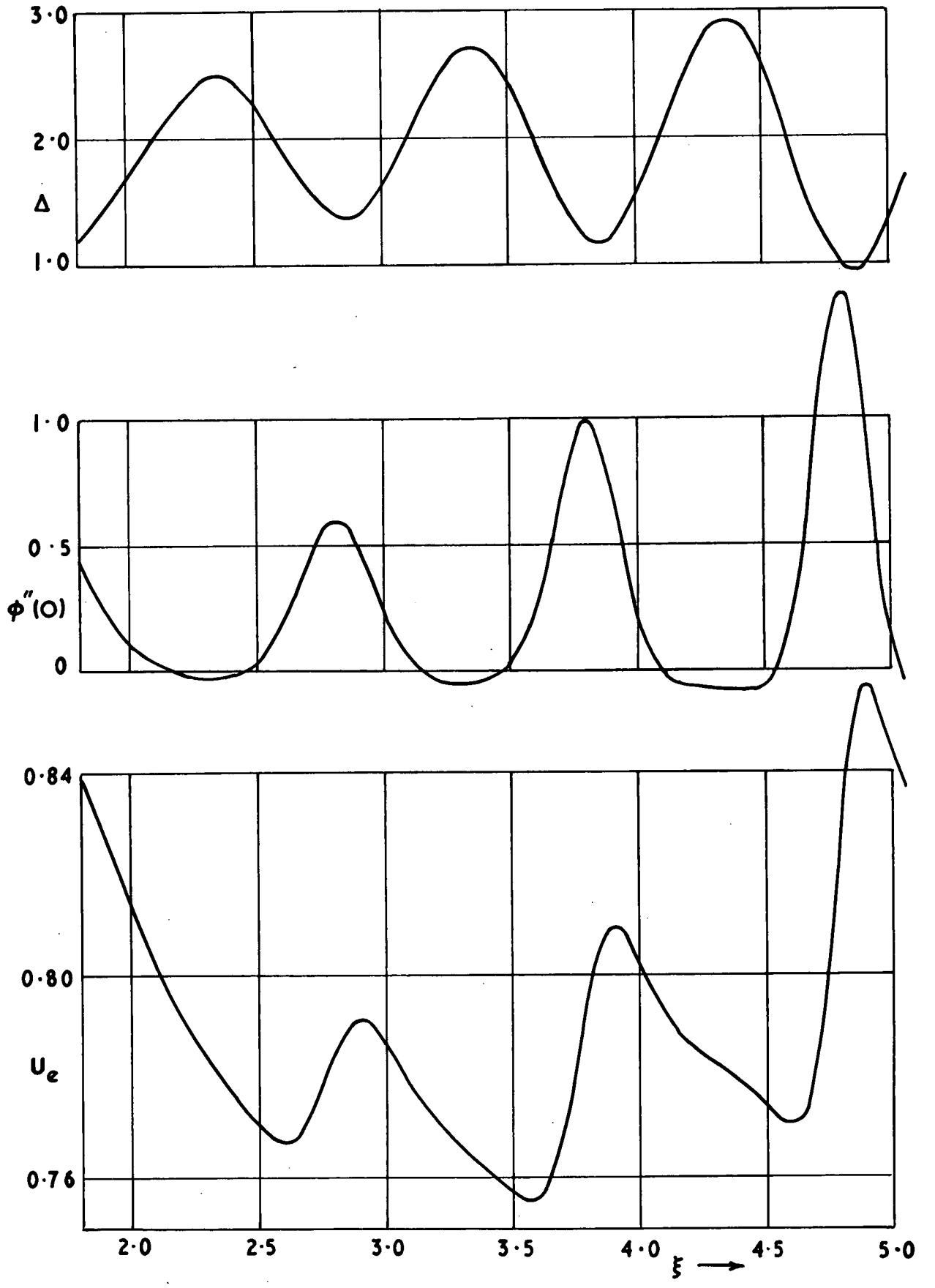

FIG.3 $\Delta(\xi)$ Specified

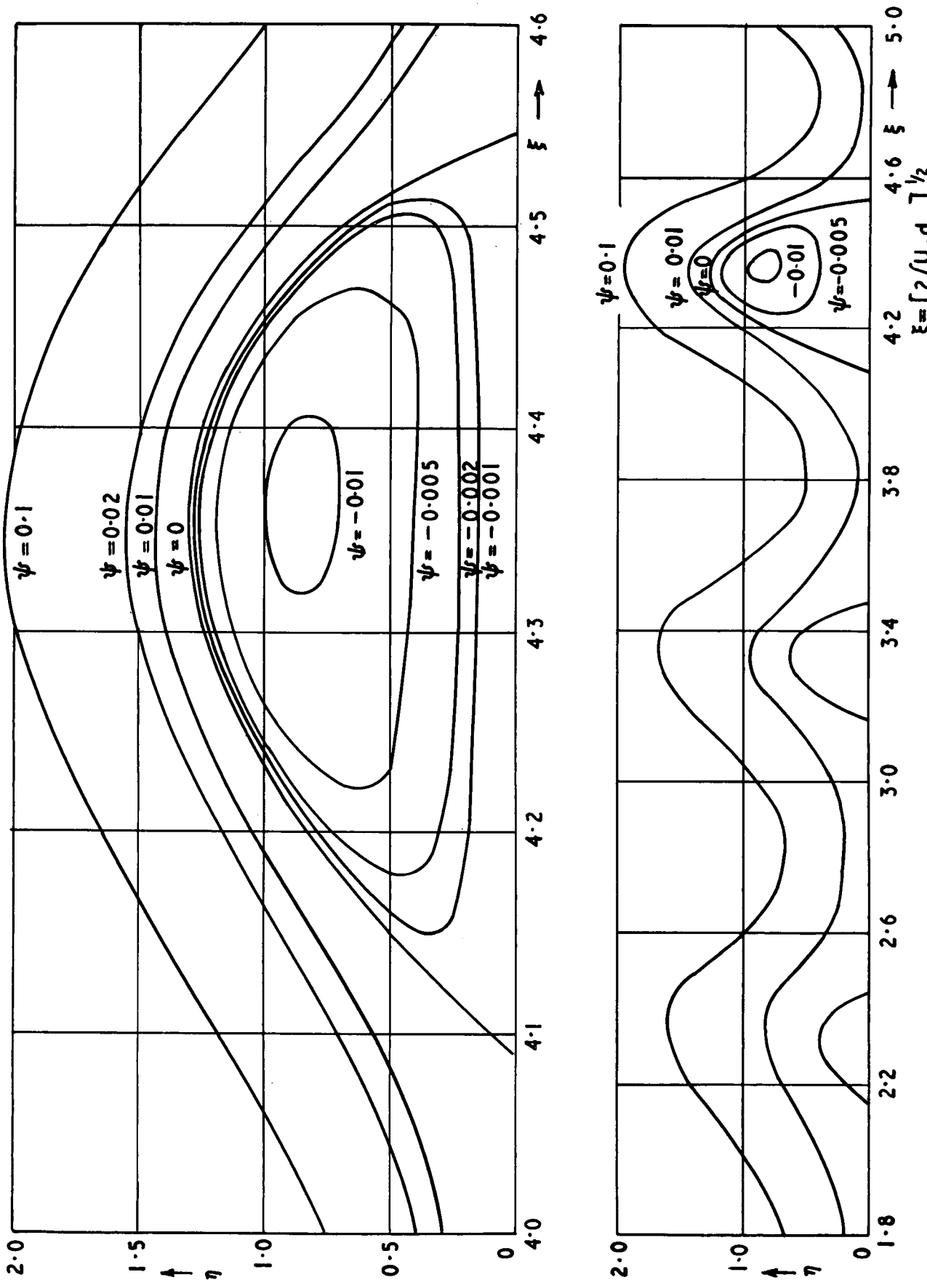

FIG. 2 Streamline pattern

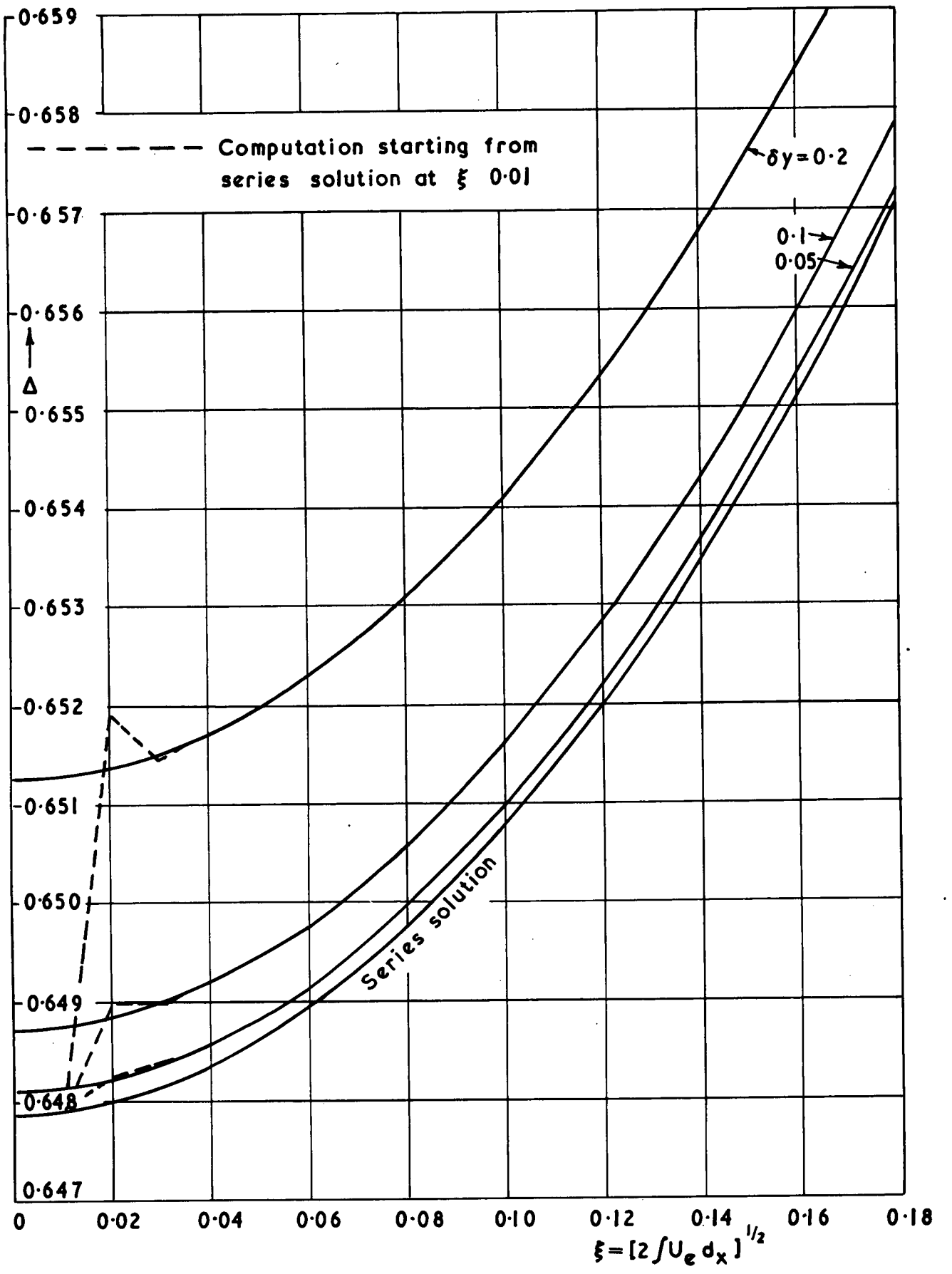

FIG.1 Stagnation region of parabola

References

[1] Catherall, D. Private communication.

[2] Crank, J. and Nicholson, P. A practical method for numerical evaluation of solutions of partial differential equations of the heat conduction type. Proc. Camb. Phil. Soc. Vol. 43, p. 50. (1947).

[3] Sells, C. C. L. Two-dimensional laminar compressible boundary layer programme for a perfect gas. A.R.C. R. & M. 3538. (1966).

[4] Catherall, D. and Mangler, K. W. An indirect method for the solution of the Navier-Stokes equations for laminar incompressible flow at large Reynolds numbers. J. Fluid Mech. Vol. 26, p. 163. (1966).

[5] Cooke, J. C. Numerical solution of Taylor's swirl atomiser problems. RAE Technical Report 66128. (1966). A.R.C. R. & M. 30864.

[6] Richardson, L. F. and Gaunt, J. A. The deferred approach to the limit. Phil. Trans. Roy. Soc. (A) Vol. 226, p. 299. (1926).

[7] Hall, M. G. A numerical method for calculating steady three-dimensional laminar boundary layers. RAE Technical Report 67145. (1967). A.R.C. 29525.

[8] Hall, M. G. A numerical method for calculating unsteady two-dimensional laminar boundary layers. Mg. - Archiv., 38, p. 97. (1969).

4. Refinement

The accuracy of some of our solutions was checked against known results. It was found for instance [2] that if we take $N = 25$ and 50 in succession (N = number of intervals in the η direction) and then use Richardson's h^2-extrapolation [6] the results are often more accurate than those for a computation using $N = 100$. If we went further and used h^4-extrapolation we could obtain better results with $N = 5$, $N = 10$ and $N = 20$ than we could with $N = 100$.

5. Starting the Computation

When starting from a stagnation point it has been found that one can vary the first step size without affecting the result at the end of this step very much. One can see, for instance, that in the first step from $x = 0$ the expression $x u u_x$ expressed in finite difference form does not depend on δx. Being worried about this Catherall and Mangler [4] decided to use a series solution at the start so that they could begin the finite difference procedure a little way downstream with a known starting value. This was later found not only unnecessary but actually a disadvantage because the starting value is a solution of the differential not the difference equation and because it complicates the procedure considerably. It is now believed to be better to start at the stagnation point with the same procedure as used later. Fig. 1 illustrates this well, and it also shows that oscillations damp out very quickly and that the solutions end up the same whatever starting method is used. $\theta = \frac{1}{2}$ was taken in all the computations of Fig. 1.

At $x = 0$ itself the equations become ordinary differential equations which are solved by a procedure identical with that already given, only simpler. Almost any initial guess for the profile will do, and the solution is actually performed by the same computer routine as the later step-by-step method, simply by writing $\theta = 1$ $m = 0$ just for this one computation.

6. Separation

As we proceed downstream, separation may occur and this may modify the external stream. If we insist on keeping to the specified external flow a singularity usually arises, which in incompressible flow is typified by

$$(u_\eta)_o \sim (x_s - x)^{1/2}$$

where x_s is the value of x at separation. What happens in practice is that the number of iterations required for convergence to a specified tolerance starts to increase. We then halve the step size and this enables us to get a little further downstream, when we may need to halve the step again and again; even this fails in the end. By this means we can approach very near to the separation point and we can obtain a very close approximation to its value by plotting x against $(u_\eta)_o^2$. We obtain a line which is very nearly straight and by this means we can find the separation point by finding the value of x which makes $(u_\eta)_o$ vanish. We do the same in the compressible case but the power does not always seem to be $\frac{1}{2}$. We then have to find a power which gives the straightest line. If we choose powers near to this the extrapolated separation point hardly changes anyway, so the exact power is unimportant for this purpose.

Catherall and Mangler [4] by careful adjustment of the external stream were able to avoid the occurrence of a singularity at separation and were even able to continue on to a reattachment point. This was only possible when the separation bubble was embedded deep down inside the layer and very small. Presumably this is because inside the bubble they are marching upstream, and errors grow. If, however, the bubble is small the growth of error is not serious. Fig. 2 shows a series of separation bubbles [2] obtained by suitable adjustment of the external stream. The upper half is a magnification of the last bubble in the lower half. Fig. 3 shows Δ, $(u_\eta)_o$ and U_e for this particular solution.

7. General Three-Dimensional Boundary Layers

We have only just started using the same technique for genuine three-dimensional cases and have so far only dealt with incompressible flow; we have not yet investigated the difficulties which will no doubt arise when starting. This work has been done by Hall [7], who has also used the method for a problem involving two space dimensions and time [8], which has many features similar to a three-dimensional problem. These two references describe the procedure well enough to render detailed description here unnecessary.

$$C = \frac{(S - Hu^2)^{1/2}(B - 1)}{(S - B - Hu^2)} \qquad (18)$$

where B is a constant known from Sutherland's law and the given external stagnation conditions.

The boundary conditions are, for an impermeable wall, $u = 0, \phi = 0$ or $\bar{\phi} = 0$ for $\eta = 0$; $u = 1$, $S = 1$ for $\eta = \eta_o$; together with S or its η derivative known at $\eta = 0$ and a given initial profile at $x = 0$.

This formulation is due to Sells [3].

We do not find it necessary to make any more sophisticated transformation.

The first equation (13) is considered as an equation in u and is evaluated at the point $\{(m + \theta)\,\delta x, n\,\delta\eta\}$ as already described, with the additional complication that it must be linearized and ϕ must be found.

The non-linear terms in (13) are dealt with by Newtonian quasi-linearization, that is, if $u^{(o)}$ is the value of u at one iteration and $u^{(1)}$ is the value at the next then the terms uu_x and u^2 are written

$$(uu_x)^{(1)} = u^{(1)} u_x^{(o)} + u^{(o)} u_x^{(1)} - (uu_x)^{(o)},$$

$$(u^2)^{(1)} = 2u^{(1)} u^{(o)} - (u^2)^{(o)}.$$

The second equation (14) is linear in S, but contains ϕ.

To find $\phi_{m+\theta,n}$ we write equation (15) or (17) in finite difference form, evaluating it at the point $\{(m + \theta)\,\delta x, (n - \tfrac{1}{2})\,\delta\eta\}$; the latter becomes

$$\frac{\bar{\phi}_{m+\theta,n} - \bar{\phi}_{m+\theta,n-1}}{\delta\eta} = \tfrac{1}{2}\{1 + E[(m + \theta)\,\delta x]\}\,\tfrac{1}{2}\{\theta\, u_{m+1,n} + (1 - \theta)\, u_{m,n} + \theta\, u_{m+1,n-1} + (1 - \theta)\, \theta_{m,n-1}\}$$

$$+ (m + \theta)\,\delta x\, \frac{(u_{m+1,n} - u_{m,n}) + (u_{m+1,n-1} - u_{m,n-1})}{2\delta x},$$

with a corresponding simpler form for the former. The boundary condition is $\phi_{m+\theta,0} = 0$. Finding ϕ in this way is basically an integration by the trapezium rule.

Thus the procedure is to guess (or extrapolate) values at the end of the step, find ϕ from equations (15) or (17) as the case may be and solve (13) and (14) for u and S as already described. We then iterate backwards and forwards between the three equations until there is only a very small change or 'tolerance' ε in some representative quantity which may be an expression related to skin friction such as $(u_\eta)_o$ or displacement thickness such as $\Delta(x) = \int (1 - u)\, d\eta$, usually the latter. The iteration is done in strict sequence and not in 'blocks'.

The step sizes are usually such that the number of iterations required is about 6 or so early on, but the number increases slowly. Later it increases more rapidly as separation is approached, when it is necessary to reduce the step size.

No particular difficulty was found in using these methods but in one case [5] the iterations sometimes oscillated and did not appear to be converging or converged very slowly. The answer here was under-relaxation. Thus if $u^{(o)}$ and $u^{(1)}$ are the results at any two stages in the iteration, instead of taking $u^{(1)}$ as the starting point for the next iteration the value

$$\alpha\, u^{(1)} + (1 - \alpha)\, u^{(o)}$$

was taken; usually $\alpha = \tfrac{1}{2}$ was satisfactory. Of course it was necessary to reduce the tolerance ε accordingly.

For the determination of derivatives at the wall it was usual to go one step 'into' the wall so that equation (3) involves one extra equation corresponding to $n = 0$.

Suction or blowing causes no difficulty. Instead of $\phi(0) = 0$ we must have $\phi(0) = w_o(x)$, a function known from the given circumstances of blowing or suction. Either a given heat transfer or a given wall temperature can be dealt with equally easily.

3. Boundary Layer Equations

We write the two-dimensional equations in the usual notation, scaled by a length ℓ, velocity U_∞ and density ρ_∞ in the usual way

$$\rho(u'u'_x + w'u'_z) = -p_x + \frac{\partial}{\partial z}(\mu u'_z) \tag{4}$$

$$\rho(u'h_x + w'h_z) = u'p_x + \mu u'^2_z + \frac{\partial}{\partial z}\left(\frac{1}{Pr} h_z\right) \tag{5}$$

$$\frac{\partial}{\partial x}(\rho u') + \frac{\partial}{\partial z}(\rho w') = 0 \tag{6}$$

and put

$$\rho u' = \psi_z , \quad \rho w' = -\psi_x \tag{7}$$

and then make the transformation

$$\psi = (\mu_s \rho_s x U_e)^{1/2} \phi \tag{8}$$

$$\eta = \left(\frac{U_e}{\mu_s \rho_s x}\right)^{1/2} \int_0^z \rho(z')\, dz' \tag{9}$$

where the subscript s denotes stagnation values. We write

$$\frac{\mu}{\mu_s} = C \frac{h}{H_s} \tag{10}$$

where C is not necessarily a constant, and we make the abbreviations

$$E = \frac{x U_{ex}}{U_e} , \quad F = \frac{H_s}{h_e} E , \quad G = \frac{h_e \rho_e}{H_s \rho_s} , \quad H = \frac{U_e^2}{2H_s} . \tag{11}$$

We also write

$$u' = U_e \phi_\eta = U_e u , \quad S = \frac{h + \frac{1}{2}u'^2}{H_s} \tag{12}$$

and the equations become

$$G \frac{\partial}{\partial \eta}(C u_\eta) = -u_\eta [\tfrac{1}{2}(1 + E)\phi + x \phi_x] + x u u_x + F(u^2 - S) \tag{13}$$

$$G \frac{\partial}{\partial \eta}\left(\frac{C}{Pr} S_\eta\right) = -S_\eta [\tfrac{1}{2}(1 + E)\phi + x \phi_x] + x u S_x - HG \frac{\partial}{\partial \eta}\left\{ \frac{C}{Pr} \frac{\partial}{\partial \eta}(Pr - 1)(u^2 - 1) \right\} \tag{14}$$

$$\phi_\eta = u . \tag{15}$$

Since the factor in square brackets occurs in both equations, and if there is a third (as in three dimensions) it occurs again, some of us use a new $\bar{\phi}$ satisfying

$$\bar{\phi} = \tfrac{1}{2}(1 + E)\phi + x \phi_x \tag{16}$$

which simplifies the first two (or three) equations and replaces the last one by

$$\bar{\phi}_\eta = \tfrac{1}{2}(1 + E) u + x u_x . \tag{17}$$

We take C as a constant or give it its value according to Sutherland's law

18. THE NUMERICAL SOLUTION OF THE LAMINAR BOUNDARY LAYER EQUATIONS FOR AN IDEAL GAS IN TWO AND THREE DIMENSIONS

J. C. Cooke*
K. W. Mangler

1. Introduction

In this paper we intend to concentrate on the implicit finite difference methods developed at the Royal Aircraft Establishment for the calculation of laminar boundary layers for perfect gases, with Prandtl number not far from 1, usually around 0·7.

The method, with experience, has proved capable of solving more and more complicated types of problem, going as far as separation or even beyond it. It has also been applied to three-dimensional boundary layer problems.

We shall illustrate the methods by taking rather simplified equations to illustrate the points we are aiming to stress.

2. The Basic Method

In all cases the external flow is assumed to be known and the usual stretching of the co-ordinate z normal to the wall is done, the stretched co-ordinate being denoted by η whilst the velocities u and v are normalized by their external values U_e and V_e. Boundary layers approach the external flow exponentially; indeed it is true in general that a normalized velocity u approaches its external value 1 in such a way that

$$u(\eta) = 1 + O(e^{-k\eta^2}) \quad \text{as} \quad \eta \to \infty ,$$

where k is some constant. Hence for a given problem the infinite range $0 \leqslant \eta < \infty$ is replaced by the finite range $0 \leqslant \eta \leqslant \eta_o$ where η_o has some value depending on the problem and the transformation. We have often fixed η_o during the whole of the computation, not too large (otherwise there is much wasted work) and not too small (otherwise there is a loss of accuracy). We can check this by looking at the full velocity profiles from time to time during a computation. Catherall [1] has sometimes tested to see if there is a sufficiently small difference between $u(\eta_o) = 1$ and $u(\eta_o - \delta\eta)$. If this grows above a very small value we increase η_o by some fixed amount (say add ten more points). This may have to be done several times during a computation.

It is usual to illustrate the method by consideration of the heat conduction equation

$$u_{\eta\eta} = k(x,\eta)\, u_x \tag{1}$$

in which we divide the range $0 \leqslant \eta \leqslant \eta_o$ into N intervals and express the equation in finite difference form. With an obvious notation equation (1) is evaluated at the point $[(m + \theta)\,\delta x,\ n\delta\eta]$ where $0 < \theta < 1$ and we obtain

$$\frac{\theta(u_{m+1,n+1} - 2u_{m+1,n} + u_{m+1,n-1}) + (1-\theta)(u_{m,n+1} - 2u_{m,n} + u_{m,n-1})}{(\delta\eta)^2} = \frac{u_{m+1,n} - u_{m,n}}{\delta x}\, k\{(m+\theta)\,\delta x, n\,\delta\eta\} . \tag{2}$$

This is most accurate when $\theta = \frac{1}{2}$. If all quantities with subscript m are known it gives an equation of the form

$$a_n u_{m+1,n+1} + b_n u_{m+1,n} + c_n u_{m+1,n-1} = d_n , \quad (1 \leqslant n \leqslant N-1)$$

$$u_{m+1,0} = 0 , \quad u_{m+1,N} = 1 , \tag{3}$$

with a_n, b_n, c_n, d_n, all known. The solution of this equation is easily obtained by inverting a tri-diagonal matrix. The Crank-Nicholson method [2] is equivalent to taking $\theta = \frac{1}{2}$, and in the linear case the procedure is stable if $\frac{1}{2} \leqslant \theta < 1$.

We usually take $\theta = \frac{1}{2}$ but occasionally we have had to vary it.

* Now at University of Bristol.

17. # A NEW, FAST, FINITE-DIFFERENCE PROCEDURE FOR THE SOLUTION OF PARABOLIC DIFFERENTIAL EQUATIONS, WITH SPECIAL REFERENCE TO THOSE OF THE TURBULENT BOUNDARY LAYER

D. B. Spalding
Imperial College, London

Nature of method

The method is an implicit, finite-difference, marching-integration procedure, for solving sets of simultaneous, non-linear, parabolic differential equations, of the type:

$$\left.\begin{matrix} x \geq x_0 \\ 0 \leq \omega \leq 1 \end{matrix}\right\}: \quad \frac{\partial \phi}{\partial x} + (a + b\omega)\frac{\partial \phi}{\partial \omega} = \frac{\partial}{\partial \omega}\left(c \frac{\partial \phi}{\partial \omega}\right) + d \ ,$$

where ϕ is a typical dependent variable; a and b are functions of x, perhaps defined by differential equations involving the local ϕ distribution; and c and d are functions of x, ω and the ϕ's.

In boundary-layer circumstances, ϕ can stand for longitudinal velocity, swirl velocity, stagnation enthalpy, concentration, kinetic energy of turbulent fluctuations, etc.; x is downstream distance, and ω is non-dimensional stream function. The quantities a and b represent the rates of change of the stream functions at the limits $\omega = 0$ and $\omega = 1$; if either of these limits separates the boundary layer from an adjacent shear-free stream, the differential equations for a and b are chosen so as to keep the conditions at the nearest grid point extremely close to the conditions of the main stream. The quantity d represents, according to the significance of ϕ: longitudinal pressure gradient; or kinetic heating; or sources and sinks of material resulting from chemical reaction; or generation and dissipation of the kinetic energy of turbulence; etc.

For computational economy, special practices may be introduced near solid walls, where the longitudinal convection terms become negligible. Appropriate "wall-flux relations", based upon once-for-all exact numerical integrations of the Couette-flow equations, are employed in place of the standard finite-difference relations, for the interval near a solid wall.

The method is, so far, confined to two-dimensional flows, whether plane or axisymmetrical.

Applications made so far

The method has been applied to several physical situations in the last few months (up to September 1967), including:

(i) Free turbulent flows, namely: plane mixing layers, with influence of density variations; axisymmetrical turbulent flows, with influence of density variations brought about by temperature differences, concentration differences, and kinetic heating; plane jets and wakes.

(ii) Turbulent wall jets, especially those encountered in film-cooling situations, with influence of density variations. The radial wall jet, with mass transfer through the wall, is one of the special cases which have been studied.

(iii) Hydrodynamic and thermal development of turbulent boundary layers on smooth walls with influence of pressure gradient and non-uniform wall temperature. The so-called "equilibfium" boundary layers have been given special attention.

(iv) Both laminar and turbulent boundary layers on a flat plate, with influence of temperature difference and kinetic heating on viscosity and density.

(v) Laminar and turbulent flows within round-sectioned pipes and diffusers, with influence of property variations and mass transfer through the walls.

(vi) A turbulent free-convection boundary layer on a vertical flat plate.

The method is found to be fast enough for computer time to impose no serious limitation. About 1000 forward-integration steps are made per minute on an IBM 7090, when three or four equations are solved simultaneously and when the ω range is split into 15 intervals (more are seldom needed). In a typical forward step, the mass flow rate in the boundary layer increases by 5%; so 200 to 500 forward steps are usually enough to complete the calculation of a boundary layer.

Publications, etc.

The method, together with the general Fortran IV computer programme, has been published as a book. The reference is: S. V. Patankar and D. B. Spalding, "Heat and mass transfer in boundary layers", International Textbook Co. Ltd., 158, Buckingham Palace Rd., London, S.W.1.

which are usually roughly equal and opposite and do not exceed one or two degrees except near separation. These inclined characteristics can be crudely thought of as the boundaries of the wake of a disturbance within the boundary layer, so that the notions of hyperbolicity agrees with the usual physical concepts. The V component velocity does not occur in the equations along the inclined characteristics because it is a consequence, rather than a cause, of the changes in U and τ : thus only two of the three characteristic equations need be solved simultaneously, and V follows from the equation along the vertical characteristic which is easily seen from equations (1) and (2) to be

$$-U\frac{dV}{dy}+V\frac{dU}{dy}=\left(U_1\frac{dU_1}{dx}\right)+\frac{d\tau}{dy} \qquad (5)$$

the term in parentheses being of course known. The numerical method is therefore almost trivial and most of our ingenuity has gone on satisfying the boundary conditions (especially the inner boundary condition) and minimising computing time. A typical run, over an x distance of 100 initial boundary layer thicknesses takes about a minute in Kidsgrove Algol on KDF 9, a computer with a 6 μ sec cycle time: writing in user code would reduce this by a factor of 10 or 15, and Fortran runs on IBM 360 or CDC 6600 take only a few seconds.

We specify U and τ at points equally spaced on the y-axis (which is a characteristic, so that V follows from (5)) and use the finite-difference equations along the inclined characteristics to calculate U and τ at $x = \Delta x$, again at equally-spaced points: it is a considerable advantage to keep the mesh points on the vertical characteristic. Since $L \sim y$ near the surface the equations are singular at $y = 0$ (in reality, viscous stresses become important): since $\partial\tau/\partial y$ is not negligible near the surface it is an advantage to approach as near as possible to the singularity, and to our surprise the numerical method can be persuaded to work with adequate (1 percent) accuracy down to one y step from the surface despite the complicated nature of the algebraic boundary conditions; therefore we have not bothered to stretch the co-ordinates, which would give greater accuracy at the expense of complications. The outer boundary condition has given relatively little trouble: we allow the boundary layer to grow by one y step per x step (occasionally doubling the y step to keep the number of points down) and clip off any negative values of τ (or excessive values of U) that are introduced by finite-difference errors.

In the lecture, we shall give details of the extension of the method to compressible heat transfer, in which we use an equation for the heat transfer $\overline{\theta v}$ which is very similar to equation (3) for the momentum transfer $\overline{uv}$: five characteristics appear and the problem is somewhat complicated by the coupling between the velocity and temperature fields caused by density variations. We shall also outline the extension to three-dimensional flow, which is not much more complicated than two-dimensional flow because spanwise diffusion of turbulent energy is negligible (to the boundary layer approximation) so that the characteristics emanating from a point remain lines on a twisted strip rather than forming a conical surface. This behaviour [2] is reminiscent of Raetz's zone-of-influence concept for the laminar boundary layer.

Recently [3], we have programmed an implicit method for the basic two-dimensional method, using first-order differences in the x direction with a logarithmic formula for $\partial U/\partial y$ and a parabolic formula for $\partial\tau/\partial y$: this approach is more convenient than the method of characteristics for problems with large numbers of dependent or independent variables.

The extension to time-dependent flows is analytically straightforward: one adds appropriate terms in $\partial/\partial t$ to the left hand sides of equations (1) and (3), and no further empirical information is needed. Only the numerically trivial case of flow on an infinite accelerating plate has been programmed so far.

A summary of the work is given in Ref. 4.

References

[1] Bradshaw, P., Ferriss, D. H. and Atwell, N. P.
Calculation of boundary layer development using the turbulent energy equation.
J. Fluid Mech. 28, 593. (1967).

[2] Martin, D. W. and Ferriss, D. H.
Analysis of a mathematical model of three-dimensional steady incompressible turbulent boundary layers.
NPL Maths. Report Ma 74. (1969).

[3] Ferriss, D. H. An implicit numerical method for the calculation of boundary layer development using the turbulene energy equation.
NPL Aero Rep. 1295. (1969).

[4] Bradshaw, P. Calculation of boundary layer development using the turbulent energy equation.
IX Summary.
NPL Aero Rep. 1287. (1969).

16. REPRESENTATION OF TURBULENT MIXING BY HYPERBOLIC EQUATIONS

P. Bradshaw and D. H. Ferriss
National Physical Laboratory, Teddington

Conventional hypotheses about the Reynolds shear stress $-\rho\overline{uv}$ are usually direct relations between the shear stress and the local velocity gradient: for instance, the "eddy viscosity" ν_e is defined by $-\overline{uv} = \nu_e \partial U/\partial y$ and the "mixing length" ℓ by $-\overline{uv} = \ell^2(\partial U/\partial y)^2$, and $\nu_e/U_\infty\delta^*$ and ℓ/δ are assumed to be universal functions of y/δ. This sort of local-equilibrium concept is valid only if the distance that a turbulent eddy travels in the course of its lifetime is short compared to any length scale of the mean flow and numerous experiments have shown that this is not so in general. However, in a boundary layer close to the surface (say for $y < 0{\cdot}1\delta$) the mixing length formula, with $\ell = Ky$, (or a corresponding eddy-viscosity formula) is a good approximation, and since at least two-thirds of the rise to free stream velocity occurs between the surface and $y = 0{\cdot}1\delta$ the assumptions made in the outer part of the boundary layer are not too critical unless the boundary layer is changing rapidly. Therefore mixing-length and eddy viscosity methods have been quite popular although they are not very satisfactory for predicting separation, a phenomenon in which the aircraft engineer, in particular, is deeply interested.

If we wish to improve our predictions we must allow for the effect of past history on the shear stress at a given point: we require a differential equation expressing the rate of change of shear stress (along a streamline) as a function of local conditions. Now from the Navier-Stokes equations we can obtain an exact differential equation for the rate of change of turbulent kinetic energy $\frac{1}{2}\rho\overline{q^2} \equiv \frac{1}{2}\rho(\overline{u^2} + \overline{v^2} + \overline{w^2})$ along a streamline as a function of local mean velocity gradient and various local properties of the turbulence, and if we make the hypothesis that there are simple universal relations between the shear stress and the other properties of the turbulence and substitute these relations into the turbulent energy equations, we obtain the desired differential equation for shear stress. The hypothesis of simple relations between the shear stress and the other properties of the turbulence is defended and documented in Ref. 1: here we need only comment that this hypothesis is prima facie more reasonable than the hypotheses of relations between shear stress and mean velocity. The same hypothesis can be applied to the exact differential equation for the rate of change of $-\rho\overline{uv}$ along a mean streamline, but the turbulent energy equation is better understood.

The time-average equations to be solved in the two-dimensional incompressible case are

$$U\frac{\partial U}{\partial x} + V\frac{\partial U}{\partial y} = U_1\frac{dU_1}{dx} + \frac{\partial \tau}{\partial y} \qquad (1)$$

$$\frac{\partial U}{\partial x} + \frac{\partial V}{\partial y} = 0 \qquad (2)$$

$$\frac{1}{2a_1}\left(U\frac{\partial \tau}{\partial x} + V\frac{\partial \tau}{\partial y}\right) = \tau\frac{\partial U}{\partial y} - \frac{\tau^{3/2}}{L} - \frac{\partial}{\partial y}\left(G\tau\tau_{max}^{1/2}\right) \qquad (3)$$

advection — production — dissipation — diffusion

where τ is the kinematic shear stress $-\overline{uv}$ and a_1, L and G are empirical functions: a_1 is a constant, G is a dimensionless function of y/δ and L is a length such that L/δ is a function of y/δ. The mixing-length approach equates the local production and dissipation but ignores both the advection (the rate of change of shear stress along a streamline) and the diffusion term: these terms are small in a boundary layer close to the surface and equation (3) then reduces to the mixing length formula. Equation (3) is not expected to be valid in the viscous sublayer very close to the surface but, fortunately, there is a well-established algebraic relation between U and τ (the logarithmic law) which holds close to the surface but outside the sublayer, and this provides a 'boundary' condition: in addition V is specified at (or very near) the surface. At the outer edge of a boundary layer, or at both edges of a free shear layer, we have $U \to$ constant, $\tau \to 0$.

Equations (1) to (3) are hyperbolic. If the energy diffusion is represented as a gradient process, a second derivative appears in the last term of equation (3) and the equations are parabolic, but with no diffusion at all they are hyperbolic: we chose the present form for the diffusion term as being the most plausible physically without regard to the mathematical consequences. It is natural and convenient to use the method of characteristics: one of the three characteristics is normal to the surface, the other two are inclined to the surface at the angles

$$\tan^{-1}\left\{\frac{V + a_1 G \tau_{max}^{1/2} \pm \sqrt{a_1^2 G^2 \tau_{max} + 2a_1 \tau}}{U}\right\} \qquad (4)$$

References (continued)

[6] Gordon, P. and Scala, S. M. Numerical investigation of the formation of discontinuities in nonisentropic inviscid flows. GE TIS69SD1; also Proceedings of the International Symposium on High Speed Computing in Fluid Dynamics, U.S. Naval Postgraduate School, Monterey, Calif. (August 19-24, 1968). Physics of Fluids Supplement. (November 1969).

[7] Scala, S. M. and Gordon, P. Solution of the Navier-Stokes equations for viscous supersonic flows adjacent to isothermal and adiabatic surfaces. General Electric Company, Space Sciences Laboratory, Document TIS 69SD1001. (April 28, 1969); also, Proceedings of the Symposium on Viscous Interaction Phenomena in Supersonic and Hypersonic Flow, (R. Korkegi - Ed.), to appear in 1970.

Since no laboratory experiments were conducted to verify the results of the numerical solution of the physical problem treated in Ref. [1] , the next study was focused on the following. We wished to see if a steady state (asymptotic) solution of the Navier-Stokes equations would reproduce the classical Becker analytical solution for shock wave structure. Furthermore, we were interested in establishing that the steady state (asymptotic solution) would be achieved utilizing a reasonable amount of computer time. When constant viscosity and thermal conductivity were introduced into the governing equations, we were able to obtain numerical solutions [2] for the time development of the structure of a one-dimensional shock wave which in the asymptotic limit came arbitrarily close to Becker's analytical solution for constant gas properties. Moreover, it was found that the physical elapsed time to achieve a steady state shock wave structure utilizing an adiabatic piston, (and the corresponding computer time), was quite reasonable as measured in terms of cost. After obtaining a number of solutions of the one-dimensional Navier-Stokes equations in cartesian co-ordinates, the authors also investigated the shock formation problem in spherical co-ordinates [3] . In the latter paper a standard explosion was treated and it was discovered that accuracy could not be maintained unless the local computational mesh size was of the order of the local mean free path.

In extending the method to the multi-dimensional case, the authors proceeded to investigate the two-dimensional supersonic viscous flow around a circular cylinder [4,5] . In following nature in two-dimensional problems, we have found it convenient to initiate the flow using a one-dimensional steady flow obtained in our earlier work. This can be likened to a physical experiment in which a model is placed into a shock tube and the flow is subsequently initiated by the passage of a planar shock wave down the tube from the high pressure end.

In Ref. [4] , the stability and convergence criteria were extended to two spatial dimensions and time, and it was again demonstrated computationally that convergence could indeed be obtained. Furthermore, the question of the downstream boundary conditions which we imposed at a finite distance from the body was investigated and it was established that the effects of upstream influence could be made negligibly small by placing the downstream boundary sufficiently far away from the body. In Ref. [5] the same physical problem of the viscous flow around a cylinder was treated, except that the non-equilibrium dissociation of the molecules was calculated. A diffusion equation was introduced with finite reaction rate chemistry in order to calculate the dissociation of the nitrogen molecules into atoms in a self-consistent manner. In both of these papers, only one of the two limiting boundary conditions on surface temperature was considered, namely, the adiabatic wall, (zero heat transfer rate).

In studying viscous problems, the question was raised whether or not the finite difference representation we were using did not introduce artificial viscosity effects. Accordingly, the method was applied to the solution of the Euler equations [Ref. 6] and it was shown that no artificial viscosity effect existed which might mask the true molecular viscosity when the Euler subsystem was coupled to the viscous terms appearing in the complete Navier-Stokes equations.

In our most recent study [Ref. 7] , the other limiting boundary condition on surface temperature was also utilized, namely, the isothermal wall (finite heat transfer rate). The new results for the isothermal and adiabatic limits were compared. In addition, numerical solutions were obtained for the viscous supersonic flow around an isothermal sphere. The structure of the flow field and the new results for the pressure and shear stress distributions and heat transfer rate at the surface of the cylindrical and spherical bodies were obtained.

References

[1] Scala, S. M. and Gordon, P. Reflection of a shock wave at a surface.
TIS R65SD24. (June 1965). Missile and Space Div., General Electric Co.; also
The Physics of Fluids, Vol. 9, No. 6, pp. 1158-1166. (June 1966).

[2] Scala, S. M. and Gordon, P. Asymptotic solutions of the time-dependent Navier-Stokes equations.
Bulletin Americal Physical Society, Vol. 12, p. 851. (1967).

[3] Scala, S. M. and Gordon, P. Spherically-symmetric shock formation according to the Navier-Stokes equations in 'Theoretical investigation of nuclear burst phenomena', GE Final Report,
NOL Contract N60921-7164. (December 1969).

[4] Scala, S. M. and Gordon, P. Solution of the time-dependent Navier-Stokes equations for the flow around a circular cylinder.
AIAA Paper 67-221. (January 1967); also
AIAA Journal, Vol. 6, No. 5, pp. 815-822. (May 1968).

[5] Scala, S. M. and Gordon, P. Solution of the time-dependent Navier-Stokes equations for the flow of dissociating gas over a circular cylinder.
Fluid Physics of Hypersonic Wakes, Proceedings of AGARD, NATO Conference, Fort Collins, Colo. (May 10-12, 1967); also, TIS R67SD56, General Electric Co.

15. SOLUTION OF THE TIME-DEPENDENT NAVIER-STOKES EQUATIONS FOR SUPERSONIC FLOWS

Sinclaire M. Scala[1] and Paul Gordon[2]
General Electric Company
Valley Forge Space Technology Center

In the past, aerodynamicists have simplified the theoretical treatment of determining the flow field around a hypersonic vehicle by developing special methods for treating the various viscous and relatively inviscid zones of the flow, including the shock wave, the shock layer, the boundary layer and the wake. Although each of the earlier approaches started with the Navier-Stokes equations, with few exceptions, different sets of assumptions were then introduced and the resulting simplified equations were integrated employing different analytical or numerical techniques such as separation of the variables, similarity solutions, series solutions and the method of characteristics.

Thus, in the past, the total flow field has been obtained by means of "patchwork". The contiguous flow regions have not usually been treated self-consistently. Moreover, in many cases, it was assumed that an independent knowledge of certain critical parameters was available, say from a flow visualization experiment, (e.g. the shock shape or the length and shape of the near wake region). Consequently, none of the aforementioned techniques is satisfactory if one wishes to calculate the complete compressible, viscous, thermally conducting, non-equilibrium flow around a vehicle, without either knowing or assuming a significant part of the solution.

It is therefore desirable to have available an established procedure for calculating viscous flow fields in which patchwork techniques are not employed, and where one does not require experimental results to construct a solution. That is, one should be able to solve the complete Navier-Stokes equations numerically without introducing assumptions which oversimplify the problem and without depending on the availability of data which may not necessarily exist.

During the past five years, the authors have been active in the development and extension of numerical procedures for the calculation of flow fields based on the solution of the time-dependent Navier-Stokes equations including compressibility, viscosity, diffusion and other real gas effects. The treatment of such flows implies that one will include in the governing system of partial differential equations the specific effects of compressibility, viscous dissipation, thermal conductivity, diffusion and chemical reactions. It was desirable that a method be developed which could be used not only to include any or all of the aforementioned real gas effects, but could also be used to compute the flow in an arbitrary multi-dimensional curvilinear co-ordinate system.

There are at least two compelling reasons for utilizing the time-dependent form of the Navier-Stokes equations. One, is simply that in many practical problems, the transient solution is the one of interest rather than the steady state solution, (which may be the trivial solution, or may even be non-existent). Two, even when the steady state solution is the one desired, it appears necessary to retain some form of the time dependence of the equations. For example, each iterative step of a relaxation method, such as the one proposed years ago by Thom and Apelt, for solving the Navier-Stokes equations, can also be interpreted as a fictitious time-dependent path, in which the vanishing of the residuals corresponds to the transient approach to the steady state solution.

This idea of following a time-dependent path to the steady state was investigated more directly by Peaceman and Rachford in the solution of a generalized elliptic equation (e.g., the multi-dimensional heat conduction equation) by retaining a physically meaningful time-dependent term and actually solving the parabolic partial differential equation for a long elapsed time.

The idea of retaining the time derivatives, i.e., "following nature", in flow field problems was presented by Crocco as a means of obtaining the steady state solution of the Navier-Stokes equations. In his pioneering paper, Crocco presented the rationale for introducing a time-dependent term which would in some sense follow nature and vanish identically in the asymptotic limit as the steady state solution is approached.

In extending Crocco's ideas, we decided to treat the complete time-dependent form of the Navier-Stokes equations, rather than introduce fictitious time derivatives. In our first paper on this subject[1], numerical solutions were presented for the complete time-dependent compressible Navier-Stokes equations for the one-dimensional motion produced by a piston. A planar piston was accelerated into a stationary gas and the formation of the resulting compression wave, and its subsequent reflection at a wall, was followed in time. The gas model utilized for molecular nitrogen specified that the molecules had a constant specific heat, and that the viscosity and thermal conductivity coefficients were proportional to the square root of the local absolute gas temperature. During the evolution of the finite difference procedure, the authors experimented with various numerical methods including the purely explicit scheme, and the Dufort-Frankel method as applied to the viscous terms; the Lax method and characteristic methods such as envisaged by Courant, Isaacson and Rees were applied to the inviscid terms. In Ref. [1], the authors derived stability and convergence criteria and showed computationally that convergence was achieved when these criteria were satisfied.

---

[1] Manager, Environmental Sciences Laboratory.

[2] Manager, Scientific Computations and Applied Mathematics.

MACH	RE	XSTP	BLH	WALL
2.8	550.	2.0	0.410	AD

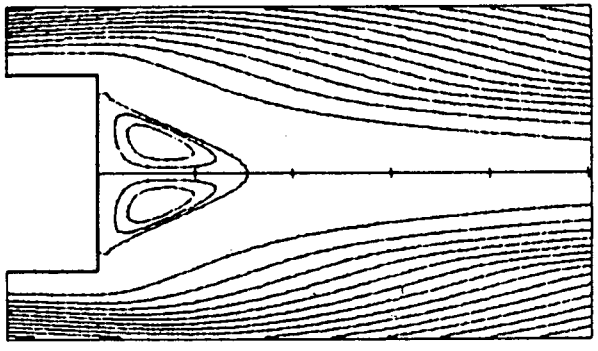

STREAM FN

MACH	RE	WALL	XSTP	BLH	MAX	MIN	DEL
2.8	550.	AD	2.0	0.41	1.008	0.028	0.075

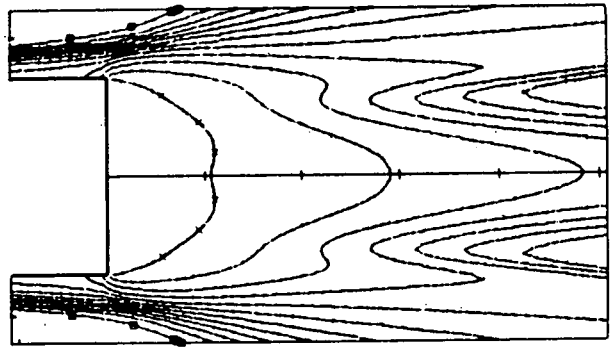

DENSITY

MACH	RE	WALL	XSTP	BLH	MAX	MIN	DEL
2.8	550.	AD	2.0	0.41	2.620	0.655	0.151

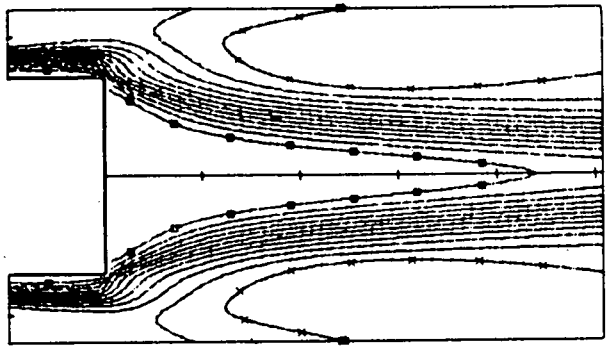

INTERNAL ENERGY

MACH	RE	WALL	XSTP	BLH	MAX	MIN	DEL
2.8	550.	AD	2.0	0.41	1.010	0.069	0.072

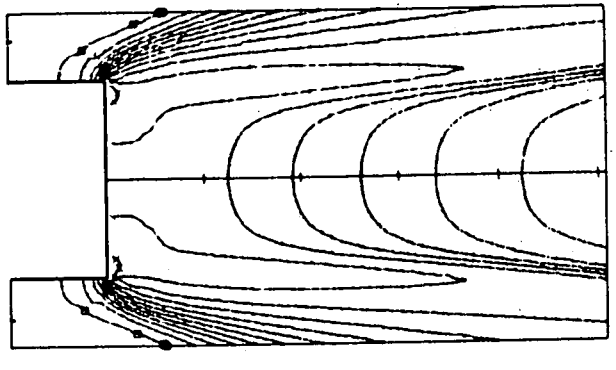

PRESSURE

Since the one-dimensional linearized Navier-Stokes equations, when written in matrix form, have the same appearance as equation (*), a scheme that is stable for the Navier-Stokes equations should be stable for (*) . In addition, at the present, we know of no scheme that is stable for (*) , that has not proved stable when naturally extended and used for the Navier-Stokes system of equations, in either one or two dimensions. The advantage of using (*) is that stability criteria (from the von Neumann necessary condition) are rather easily derived, whereas for the linearized Navier-Stokes equations the conditions are sometimes hard to find. It seems safe, therefore, when examining difference schemes, to limit oneself initially to the consideration of schemes that are stable for (*).

The time difference scheme that we have used is given below for equation (*), where we use the notation

$$u(x,t) = u(j\Delta x,\ n\Delta t) = u_j^n$$

$$\hat{u}_j^{n+1} - u_j^n = -\frac{a\Delta t}{2\Delta x}\,(u_{j+1}^n - u_{j-1}^n) + \nu\,\frac{\Delta t}{\Delta x^2}\,(u_{j+1}^n - 2\hat{u}_j^{n+1} + u_{j-1}^n)$$

$$u_j^{n+1} - u_j^n = -\frac{a\Delta t}{2\Delta x}\,(\hat{u}_{j+1}^{n+1} - \hat{u}_{j+1}^{n+1}) + \nu\,\frac{\Delta t}{\Delta x^2}\,(\hat{u}_{j+1}^{n+1} - 2u_j^{n+1} + \hat{u}_{j-1}^{n+1})$$

with the stability condition $a\Delta t < \Delta x$.

This two step scheme has the advantage that both steps have the same difference form. This allows the boundary conditions to be applied in the same manner for each step.

In the calculations a uniform rectangular mesh was used with the length of the mesh cell in the direction of the centreline twice the length in the normal direction. There were approximately 2000 grid points in the field. A check calculation with the mesh size approximately halved was performed and the results compared favourably.

Solutions were obtained for a range of Reynolds numbers (based on the base half-height and the inflow conditions) less than 1000 at Mach numbers between 2 and 4. Both the cases of an adiabatic wall and a constant wall temperature were computed. The important features of the flow, such as the expansion around the corner, the separation of the boundary layer, the re-circulation region, the recompression, and the formation of the wake shock are illustrated in the results. Also shown are the changes in the solution with the variation of the Reynolds number, the Mach number, and the wall temperature condition.

References

[1] Brailovskaya, I. Yu. A difference scheme for numerical solution of the two-dimensional non-stationary Navier-Stokes equations for a compressible gas. Soviet Physics-Doklady, 10, 107-110. (August 1965).

Additional References published since the September 1967 AGARD Seminar.

[2] Allen, J. S. Ph.D. Thesis, Princeton University (1968).

[3] Allen, J. S. and Cheng, S. I. Numerical solutions of the compressible Navier-Stokes equations for the laminar near wake, submitted to the Physics of Fluids. (1969).

[4] Cheng, S. I. Accuracy of difference formulation of Navier-Stokes equations. Proc. of the First International Symposium of High Speed Computing in Fluid Dynamics, sponsored by IUTAM, (1968), to appear in The Physics of Fluids.

---

14. NUMERICAL SOLUTIONS OF THE COMPRESSIBLE NAVIER-STOKES EQUATIONS FOR THE LAMINAR NEAR-WAKE IN SUPERSONIC FLOW †

J. S. Allen* and S. I. Cheng**
Princeton University, Princeton, New Jersey

Numerical solutions of finite difference approximations to the compressible Navier-Stokes equations have been calculated for the steady flow of a supersonic stream and boundary layer over a rectangular base. The configuration represents a model problem for the laminar near wake of a slender blunt-based body. Typical results are shown in Figs. 1-4.

The incoming flow is placed upstream of the corner of the base. On the body the no-slip condition is applied to the velocity components and a specified wall temperature or an adiabatic wall condition is applied to the internal energy. The flow field is assumed to be symmetric about a centreline running through the base. Along the top boundary a simple wave condition, simulating the effect of a fluid of infinite extent, is used.

The difference approximations are derived from the integral form of the conservation laws which are written in a Cartesian co-ordinate system for a calorically perfect gas with a Prandtl number equal to one. Constant coefficients of viscosity and heat conductivity are used. The steady state solutions are obtained from an iteration scheme that is based essentially on a difference approximation to the unsteady equations.

To formulate the difference equations the flow field is divided into uniform rectangular mesh cells, where the centres of the cells form a set of grid points. The approximations to the spatial derivatives are derived from the integral form of the conservation laws for each mesh cell. This results in centred difference equations with a formal discretization error of the order of the grid size squared. An important advantage of the integral formulation is the conceptual aid it gives in applying boundary conditions on a body surface. Wall boundaries are placed along cell edges, rather than through grid points, and the boundary conditions are applied directly to the flux terms. This procedure was found to be of crucial importance to the success of the computations. Wall boundary conditions that were not formulated in strict accordance with the integral conditions of the conservation laws were found to lead quickly to non-physical results (e.g. negative densities).

The boundary conditions on the top and outflow boundaries of the computational grid, both of which are assumed to lie in the flow field (and as such are not natural boundaries of the flow), require special attention. The outflow boundary was placed far enough downstream so that the outflow was almost entirely supersonic. An extrapolation procedure where, at each time step, the values on the boundary were obtained by smoothly extrapolating the values at the interior points has proved satisfactory.

For the top boundary a simple wave condition has been developed. The inflow above the boundary layer is assumed to be a uniform supersonic stream of infinite extent. Therefore, in the steady state the waves in the outer inviscid flow, resulting from the expansion around the base, should be simple waves, and the outward running family of characteristics should be straight lines with the flow properties constant along them. A boundary condition based on these considerations was used in the unsteady calculations. Values of the variables on the top boundary were obtained by directly extrapolating, along the quasi-steady characteristic directions, the values from the interior row of grid points below the boundary. As a result, in the steady state solution, the values of the variables along the top boundary are consistent with the simple wave condition.

To find the solution to the steady difference equations we used an explicit time difference scheme which we have formed by modifying a scheme due to Brailovskaya [1]. The modification removes the Reynolds number from the stability condition and results in an approximation to different unsteady equations. Limited numerical tests have indicated improved rates of convergence for this scheme compared with the original and with other schemes [2]. This is especially true when the local Reynolds number attains low values in parts of the flow field.

In choosing a stable time difference scheme for the compressible Navier-Stokes equations we found it extremely helpful to study first the application of various difference schemes to the linearized form of Burgers' equation (denoted as equation (*)).

$$\frac{\partial u}{\partial t} + a\frac{\partial u}{\partial x} = \nu\frac{\partial^2 u}{\partial x^2} \qquad (*) \qquad a,\ \nu \geq 0,\ \text{constants}$$

---

†This research was partially supported by the Aerospace Research Laboratories, Office of Aerospace Research, United States Air Force under Contract AF 33616-67-C-1065 and made use of computer facilities supported in part by National Science Foundation Grant NSF-GP579.

*Present address: Department of Aerospace Engineering, The Pennsylvania State University, University Park, Pennsylvania.

**Professor, Department of Aerospace and Mechanical Sciences.

References

[1] Hirt, C. W. Jour. Comp. Phys. 2, 339. (1938)

[2] Gentry, R. A., Martin, R. E., and Daly, B. J. Jour. Comp. Phys. 1, 87. (1966).

[3] Butler, T. D. To be published in Phys. of Fluids.

[4] Harlow, F. H. Methods in computational physics.
Vol. 3, B. Alder, S. Fernbach, and M. Rotenberg, Eds: Academic Press, N.Y. (1964).
Amsden, A. A., Los Alamos Scientific Laboratory Report LA-3466. (1966).

[5] Harlow, F. H. and Welch, J. E. Phys. of Fluids 8, 2182. (1965),
Harlow, F. H., Welch, J. E., Shannon, J. R., and Daly, B. J.,
Los Alamos Scientific Laboratory Report, LA-3425. (1965).

[6] Harlow, F. H. and Nakayama, P. I. Phys. Fluids, 10, 2323. (1967).
Harlow, F. H. and Nakayama, P. I. Los Alamos Scientific Laboratory Report LA-3854. (1968).
Harlow, F. H. Los Alamos Scientific Laboratory Report LA-3947. (1968).
Harlow, F. H. and Hirt, C. W. Los Alamos Scientific Laboratory Report LA-4086. (1969).
Hirt, C. W. To be published in the Proceedings of the International Symposium on High-Speed computing in Fluid Dynamics held at Monterey, California, August 1968.

13. COMPUTER STUDIES OF TIME-DEPENDENT FLOWS*

C. W. Hirt
University of California, Los Alamos Scientific Laboratory
Los Alamos, New Mexico

This paper presents a discussion of finite difference approximations to the full, time-dependent, Navier-Stokes equations. The methods described here are developed from an Eulerian viewpoint. A fluid is visualized as flowing through a network of stationary rectangular cells, and for each cell of the network, values are assigned for the average mass, momentum, and energy. These values are advanced in time by calculating net fluxes, through cell surfaces.

In this paper the basic Eulerian approach is introduced by considering a simple linear convection equation. Several alternative finite difference approximations are compared. They lead to the important result that truncation errors associated with a finite difference approximation are good indicators of computational stability and accuracy [1]. This result is quite general and has important consequences for approximations of the Navier-Stokes equations.

The approximations used for the linear convection equation can be developed readily into finite difference approximations for the full Navier-Stokes equations. An example of this is illustrated by the Fluid-In-Cell (FLIC) method [2]. The FLIC method can be applied to a variety of aerodynamic problems. Two typical examples are the calculation of hypersonic flow about a cone and the calculation of an interaction between a blast wave and a bow shock on a blunt nosed projectile.

Extensions of the FLIC method are possible in many directions. One interesting extension was developed in a study of hypersonic flow about the sharp leading edge of a flat plate [3]. This study involved a coupling of the continuum Navier-Stokes equations with boundary conditions derived from a molecular model. The molecular model simulated partial slip and temperature jump boundary conditions.

The FLIC method is not suitable for multimaterial problems, since it has no provision for recording the positions of material interfaces. In FLIC, every cell is treated as homogeneous, and average masses are fluxed through cell boundaries. These processes produce smeared interfaces, which can significantly affect the results of a calculation. A way out of this problem is to replace continuous mass distributions by particles having discrete masses. Flux calculations are replaced by calculations of particle movement, and material interfaces are maintained by labelling the type of material that each mass particle belongs to. This idea forms the basis of the Particle-In-Cell (PIC) method [4]. The PIC method is illustrated by a calculation of hypersonic wake flow, and by a calculation of the hypervelocity impact of a projectile on a plate.

The FLIC and PIC methods represent two ways of calculating time-dependent flows of compressible fluids. For incompressible fluids special techniques must be employed to satisfy the incompressibility condition. One computing scheme is described, the Marker-And-Cell (MAC) method [5], which satisfies this condition by solving a Poisson equation for the pressure at each step in time. The technique is illustrated by application to the investigation of hydraulic jump formation.

It has already been noted that the truncation error analysis applied to the linear convection equation is quite general. In particular, it can be applied to finite difference approximations of the Navier-Stokes equations. It is easy to see, in fact, that diffusion-like truncation errors must occur. These errors can overshadow real viscosity effects unless an upper bound is set on the Reynolds number of a calculation. The actual value of the upper bound depends on the particular difference scheme used and on the particular problem under study. This and related restrictions must be carefully observed when using finite difference approximations. In many cases the results for a fictitiously low Reynolds number, however, can closely approximate true high-Reynolds-number flows.

An exciting new contribution to numerical fluid dynamics is the attempt to calculate turbulent flows. It would appear out of the question to resolve the detailed motion of a turbulent fluid. However, it now seems possible to simulate the effects of turbulence on the mean motion of a fluid by coupling the Navier-Stokes equations, including a Reynolds stress, to a set of turbulence transport equations [6]. This approach looks quite promising and is now under active investigation.

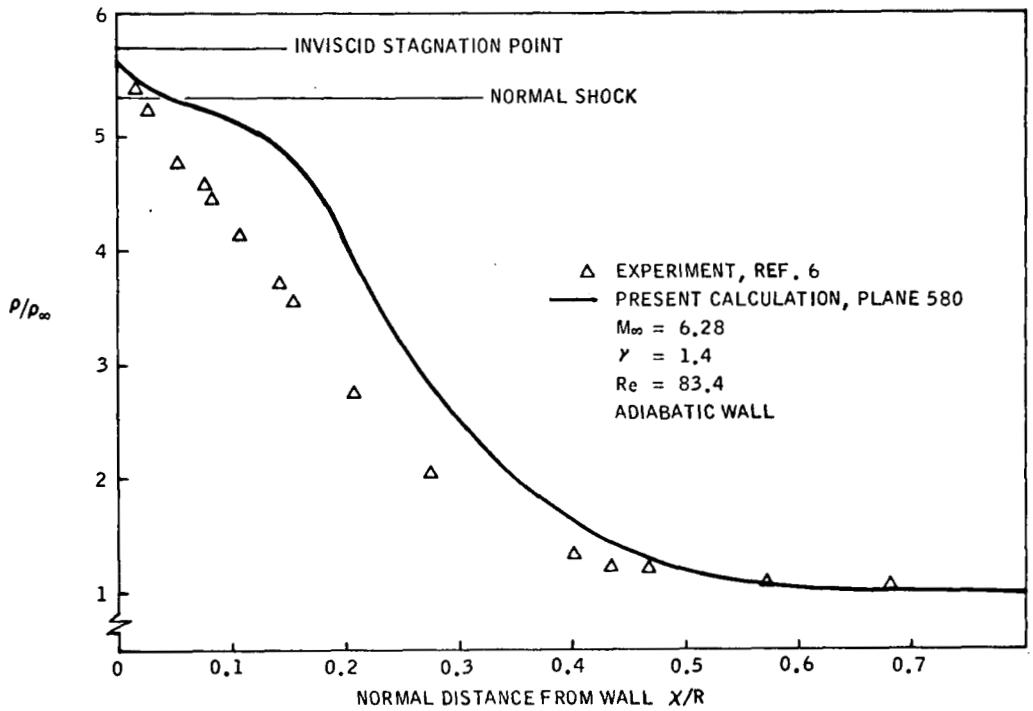

Figure 5. Stagnation line density profile (0° ray).

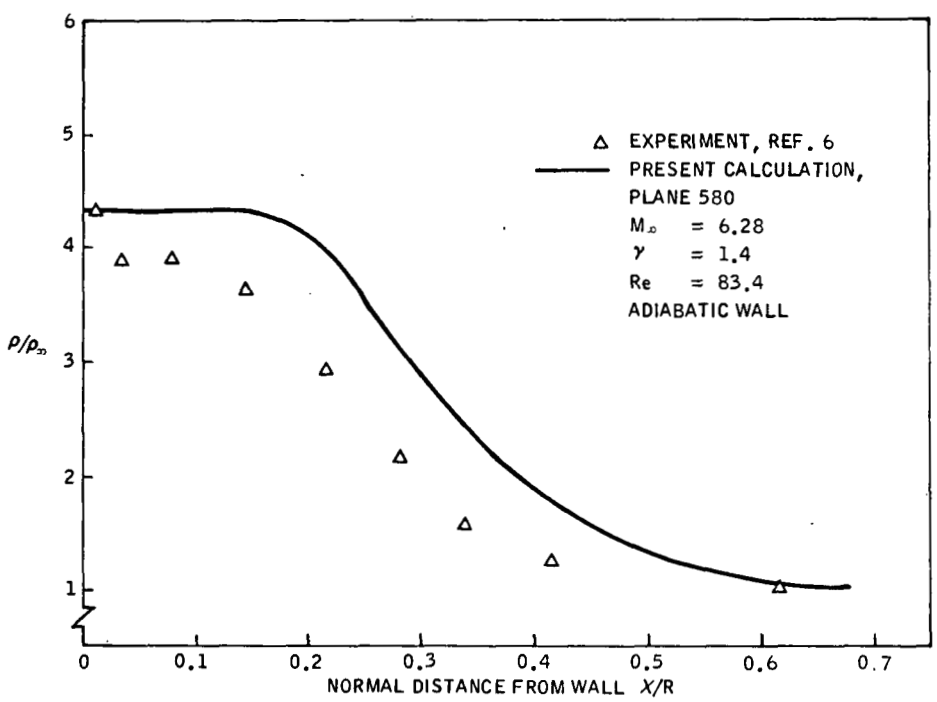

Figure 6. Density profile along the 30° ray.

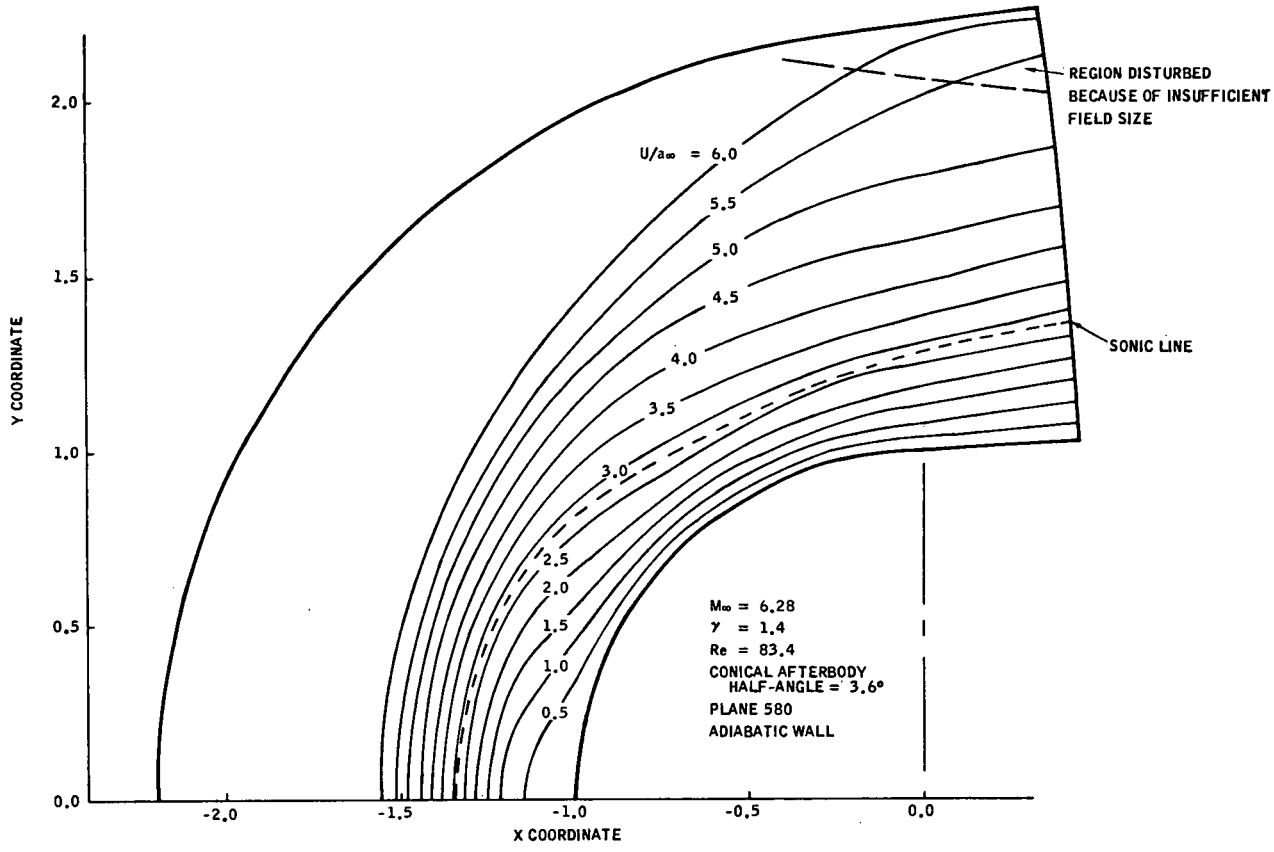

Figure 3. Total velocity contours for the viscous flow about a sphere with conical afterbody.

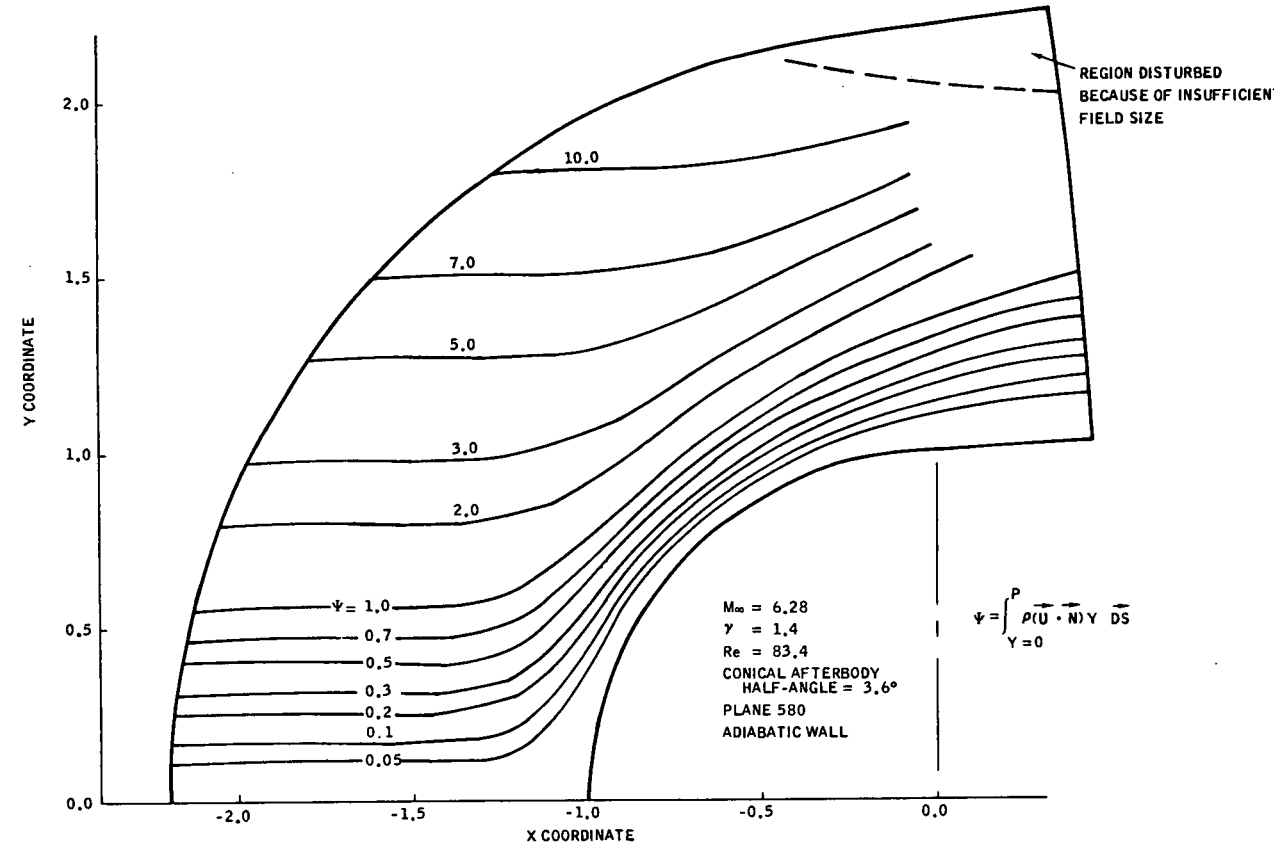

Figure 4. Streamlines for the viscous flow about a sphere with conical afterbody.

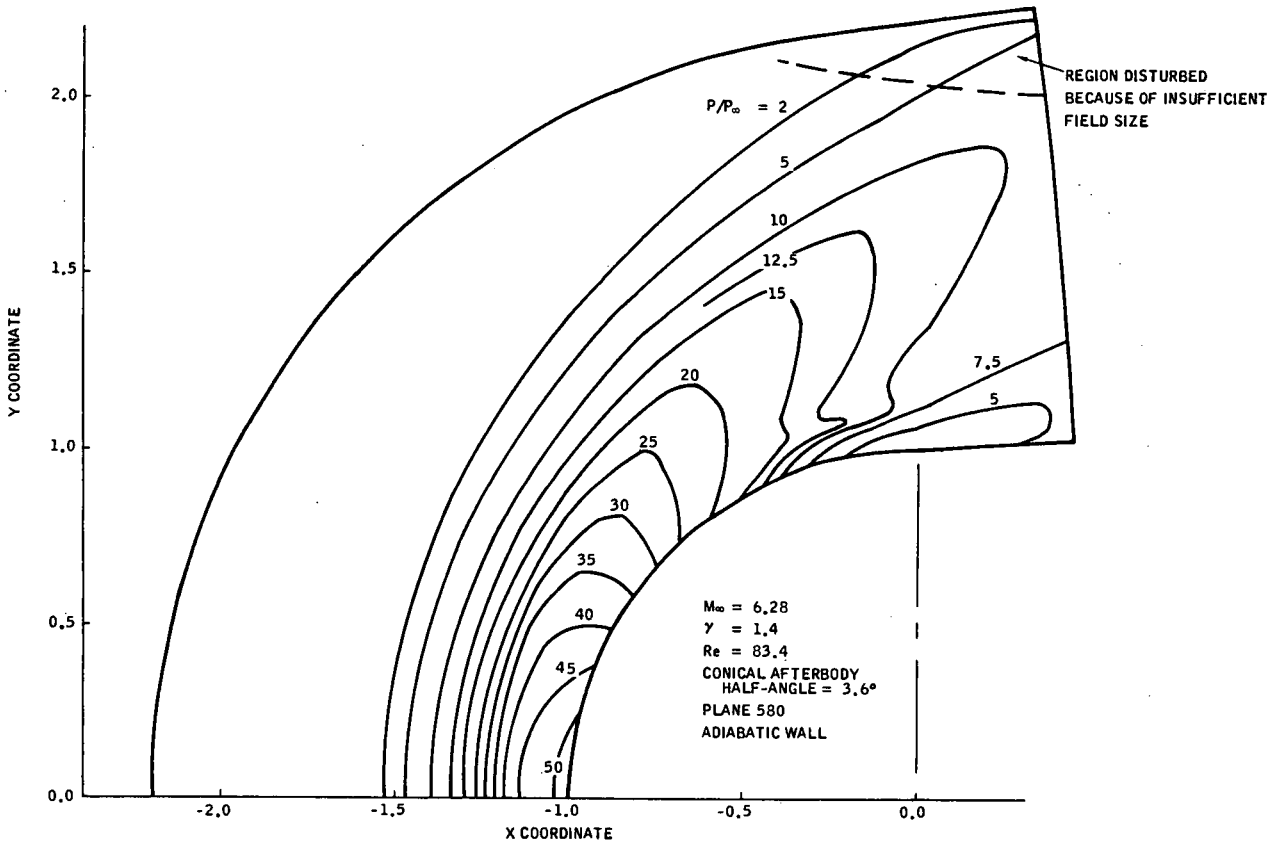

Figure 1. Isobars for the viscous flow about a sphere with conical afterbody.

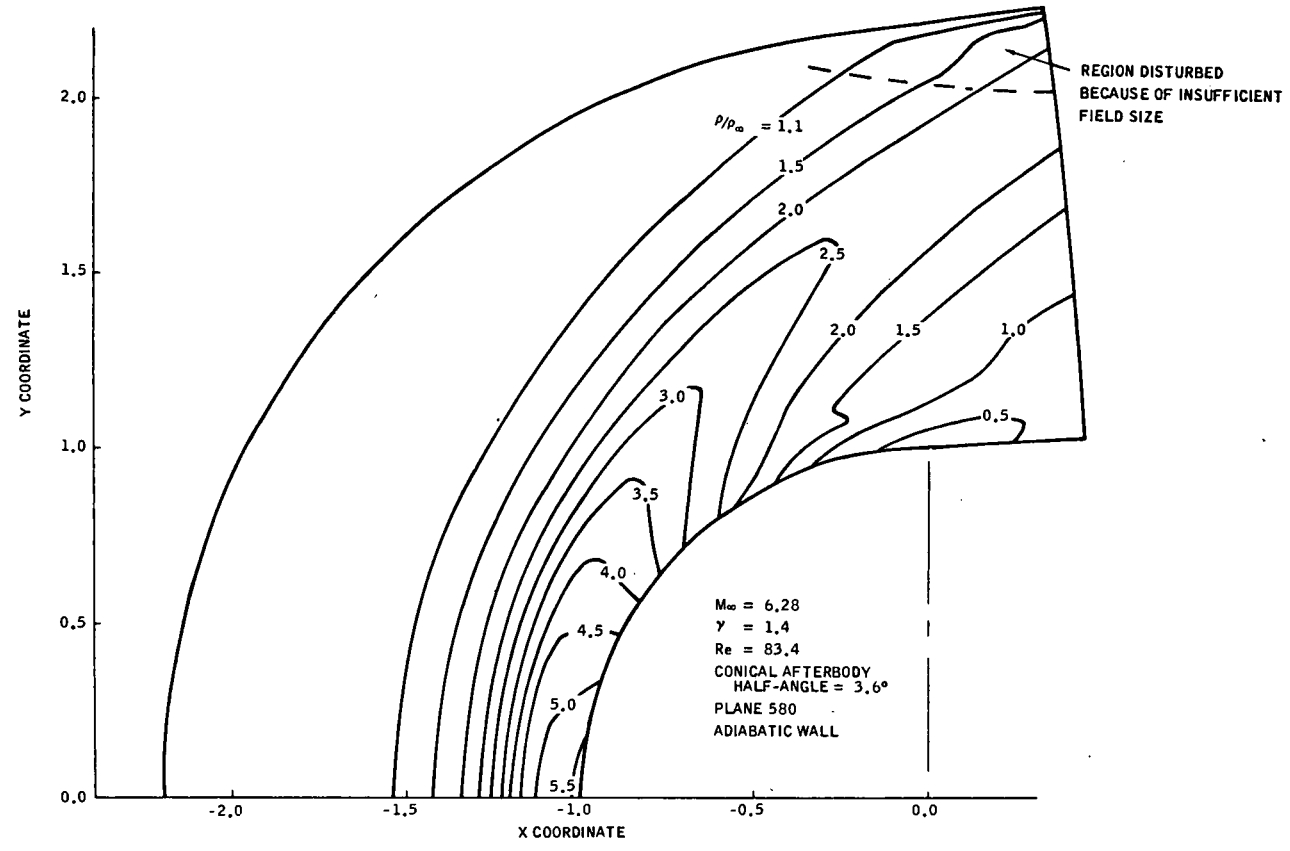

Figure 2. Density contours for the viscous flow about a sphere with conical afterbody.

12. RAREFIED HYPERSONIC FLOW OVER THE FORWARD PART OF A BLUNTED CONE*

R. J. Magnus and W. H. Gallaher
The Convair Division of General Dynamics
San Diego, California, U.S.A.

The calculation of the Mach 6•28, Re 83•4 airflow about a spherically blunted 3•6 degree half angle cone frustum by numerical means based on the unsteady Navier-Stokes equations has been attempted.

About 850 mesh points in systems of body-oriented orthogonal curvi-linear co-ordinates (spaced each 3•6 degrees along the sphere and spaced 0•05 sphere radii normal to the body) have been used to cover the field.

The calculation was started with uniform parallel flow and adiabatic-wall no-slip boundary conditions imposed along the body. Conditions at points of the field were altered by amounts calculated using finite-difference approximations to the unsteady equations. To try to hasten convergence to a steady state, the solution was advanced in the timelike direction as far as permissible based upon local limits on the stability of the difference scheme employed.

Drift in free-stream properties because of the truncation errors of the difference scheme and the use of curvi-linear co-ordinates was suppressed by re-assigning free-stream conditions to field points at which changes did not exceed preassigned threshold values. Rigorous convergence to a stationary state was not achieved when the calculation was halted, because of expense, after 580 passes through the field. The pressure, density, and total velocity contours and the streamlines after 580 passes are shown in Figs. 1 to 4. From the state of the field when calculations were suspended and the time step limits of the difference scheme used, it has been estimated that from 800 to 3600 timelike calculation steps (depending upon the particular streamline being followed) would be necessary to follow the convection of a particle through the shock layer.

The calculated density distributions along the stagnation streamline and 30° ray are compared to measurements obtained by Wainwright [1] ahead of a $T_w = T_o$ spherical model in Figs. 5 and 6.

Reference

[1] Wainwright, J. B. Experimental investigation of the density flow field in the stagnation region of a blunt body in high speed rarefied flow. Celestial Research Corp., Rep. BD-339-101, Nov. 1966, AD-646743.

• This work uses a computer program developed under sponsorship of the Air Force Flight Dynamics Laboratory, Research and Technology Division, Air Force Systems Command, USAF, Contract AF33(615)-5156. See Magnus, R. J. and Gallaher, W.H., "Development of a Program for Calculating Viscous Supersonic Flow over Blunted Cones," Air Force Flight Dynamics Laboratory, AFFDL TR68-28, January 1968 AD-836553.

which is a difference approximation to the differential equation

$$U_t = F_x + \frac{\Delta x}{2} F_{xx}$$

Thus again we have a scheme which introduces an artificial viscosity of $O(\Delta x)$.

Consider now the case finite ε . For $\varepsilon = O(1)$ any of the above mentioned schemes would yield a legitimate solution since the artificial viscosity is an order of magnitude smaller than the real viscous term. However, if $\varepsilon = O(\Delta x) = O(\Delta t)$, then the real and artificial viscosities are of the same order of magnitude. For still smaller ε , the artificial viscosity dominates the real one. It seems that in neither case will the difference scheme furnish a legitimate solution.

Another possible difference scheme uses the real viscous terms to ensure numerical stability. The simplest of these schemes has the following form:

$$U_o^i = U_o^o + \frac{\Delta t}{2\Delta x}(F_{+1}^o - F_{-1}^o) + \frac{\varepsilon \Delta t}{\Delta x^2}(U_{+1}^o + U_{-1}^o - 2U_o^o)$$

In order for this scheme to remain stable, the following condition must be satisfied:

$$|\alpha| \frac{\Delta t}{\Delta x} \leq \frac{2\varepsilon \Delta t}{\Delta x^2} \leq 1$$

The condition $\alpha \frac{\Delta t}{\Delta x} \leq 1$ is recognized as the Courant-Friedrichs-Lewy (C.F.L.) condition. For the case of the Navier-Stokes equations this condition becomes:

$$\frac{\Delta t}{\Delta x} \leq (q + a)^{-1}$$

where q is the magnitude of the fluid velocity vector and a is the speed of sound.

The term $\Delta x/\varepsilon$ represents a Reynolds number referred to the mesh size, $Re_{\Delta x}$. Provided that the C.F.L. condition is satisfied, the stability condition restricts the use of this difference scheme to $Re_{\Delta x} \leq \frac{2}{|\alpha|}$ which is of order one. Thus the scheme is feasible only for very low Reynolds numbers.

Another method which was proposed in Ref. 1 uses the second order term, U_{tt} , in the Taylor series to ensure stability. This term, however, is approximated in such a fashion that it should vanish simultaneously with the first order terms in the approach to steady state. Thus no artificial viscosity is introduced; however, this scheme has not been sufficiently tested.

The condition $Re_{\Delta x} = O(1)$ is unnecessarily restrictive. An estimate based on boundary layer concepts[1] shows that sufficient resolution is achieved if

$$\Delta\eta \, Re_{\Delta\eta} = O(1)$$

where $\Delta\eta$ is the mesh size normal to the surface using boundary layer type co-ordinates. For larger Reynolds numbers, say of order 10^4 , it becomes necessary to separate the flow field into viscous and inviscid regions so that it becomes manageable on present day computers.

However, for any of the above mentioned explicit schemes, the small mesh size in the viscous region would require a correspondingly small time step. Implicit schemes, on the other hand, seem out of question for the full Navier-Stokes equations. Consequently, alternate methods are now being studied which exhibit some of the stability properties of the implicit schemes but allow calculations in a fashion similar to those used for explicit schemes.

Reference

[1] Freudiger, F. A., Gallaher, W. H. and Thommen, H. U. Numerical calculation of low Reynolds number flow over a blunt wedge with rearward facing step. Office of Aerospace Research, ARL 67-0151. (July 1967).

11.

INTEGRATION OF THE UNSTEADY NAVIER-STOKES EQUATIONS BY FINITE DIFFERENCES [1]

Hans U. Thommen[2]

A number of investigators have recently developed methods for integrating the Navier-Stokes equations numerically. Some authors base their approach on the unsteady equations and find steady state flowfields as asymptotic solutions for large times. This paper deals with this approach; an attempt is being made to estimate the limits of applicability of such methods.

Rather than discussing the full Navier-Stokes equations we will consider the simpler, scalar equation introduced by Burgers for the study of some aspects of turbulent flow. Using subscripts to denote partial differentiation, the Burgers equation is written in the form [3]

$$U_t = F_x(U) + \varepsilon\, U_{xx} = \alpha(U)U_x + \varepsilon\, U_{xx} \tag{1}$$

We assume that the parameter ε is small; it plays the role of the reciprocal of the Reynolds number in the Navier-Stokes equations. The difference approximation to equation (1) is based on a Taylor expansion of U. If the expansion is performed about the point (x,t), we have:

$$\begin{aligned} U(x,t+\Delta t) &= U(x,t) + \Delta t\, U_t(x,t) + \frac{\Delta t^2}{2!} U_{tt}(x,t) + O(\Delta t^3) \\ &= U(x,t) + \Delta t\, [F_x + \varepsilon\, U_{xx}] + \frac{\Delta t^2}{2!} \Big\{ (\alpha\, F_x)_x \\ &\quad + \varepsilon\, [(\alpha\, U_{xx})_x + F_{xxx} + \varepsilon\, U_{xxxx}] \Big\} + O(\Delta t^3) \end{aligned} \tag{2}$$

where we have replaced the time derivatives with spatial derivatives using equation (1). Let us first consider the inviscid case, $\varepsilon = 0$. This case was treated by Lax and Wendroff by using centred differences to approximate F_x. In this case it is necessary to include the second order term, $(\alpha\, F_x)_x$, in order to have a stable difference scheme. This term then represents an artificial viscosity term in the asymptotic, steady state solution, as can be seen by rewriting equation (2) in the form:

$$U(x,t+\Delta t) - U(x,t) = \Delta t \left\{ F_x + \frac{\Delta t}{2} (\alpha\, F_x)_x \right\} + O(\Delta t^3)$$

As the left-hand side tends to zero, the difference approximation approaches the steady state solution to the modified differential equation

$$F_x + \frac{\Delta t}{2} (\alpha\, F_x)_x = 0$$

with an artificial viscosity term of $O(\Delta t)$. The same is true if non-centred differences are used for F_x and the Taylor series is truncated after the first term. Using the abbreviation $U(x + m\Delta x,\ t + \ell\, \Delta t) = U^{\ell}_{m}$, a scheme used by several authors is of the form:

$$U^1_0 = U^0_0 + \frac{\Delta t}{\Delta x} \left[F^0_{+1} - F^0_0 \right]$$

This equation can be written in the form

$$U^1_0 = U^0_0 + \frac{\Delta t}{2\Delta x} \left[F^0_{+1} - F^0_{-1} \right] + \frac{\Delta t}{2\Delta x} \left[F^0_{+1} - 2F^0_0 + F^0_{-1} \right]$$

---

[1] Work reported in this paper was supported by the U.S. Air Force under contract AF 33 (615)-3989

[2] Professor of Mechanical Engineering, Southeastern Massachusetts University, North Dartmouth Massachusetts 02747

[3] Burgers considered the case $\alpha = dF/dU = -U$

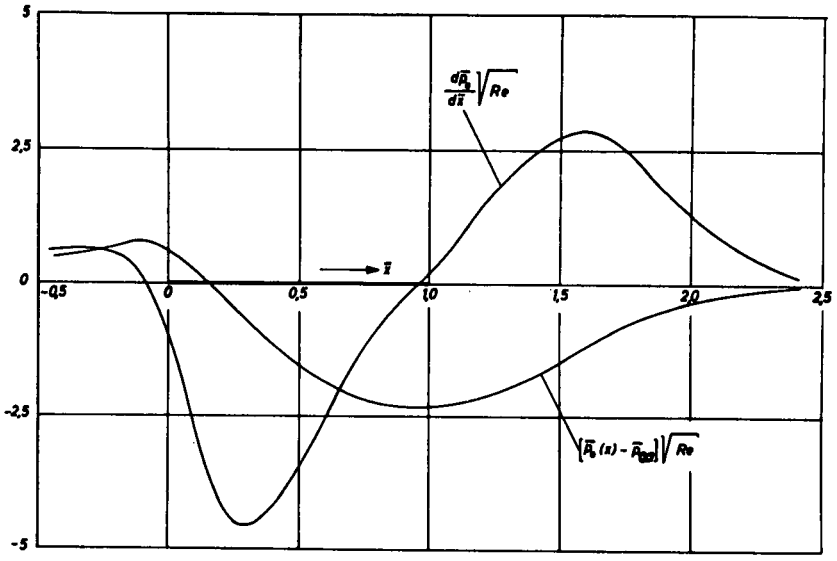

Fig. 7 Pressure gradient and pressure distribution along the plate axis (y = o) at large Re-numbers

$\bar{p}_o = p_o/\rho U^2$

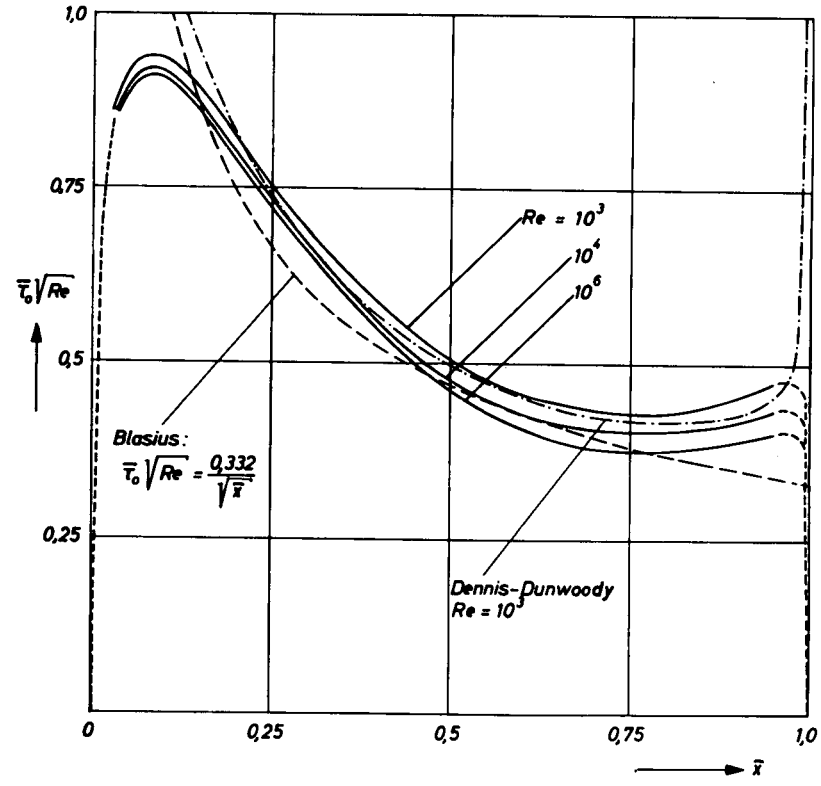

Fig. 8 Distribution of local skin friction $\bar{\tau}_o = \frac{\tau_o}{\rho U^2} \equiv c_f$ along the plate.

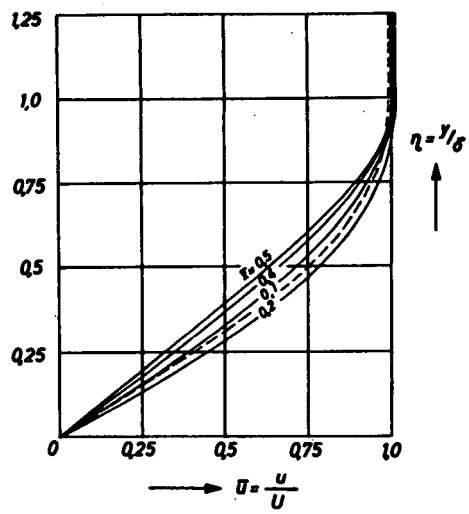

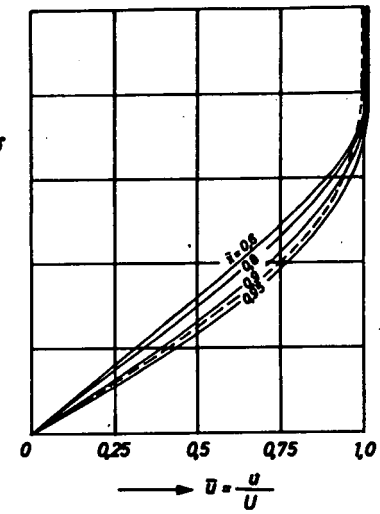

Fig. 1 Velocity profiles at the plate

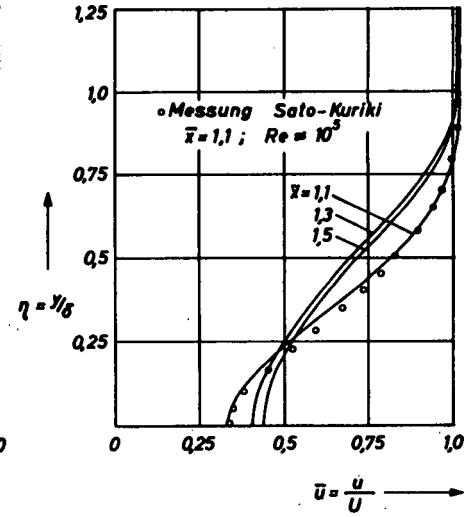

Fig. 2 - in the wake

at $Re = \frac{U \cdot L}{\nu} = 10^4$

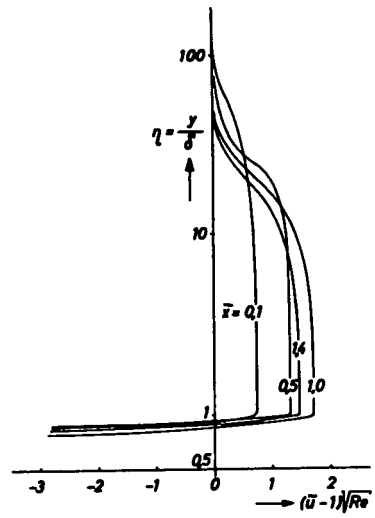

Fig. 3 Decay of velocity disturbance outside the boundary layer, Re = 10^4

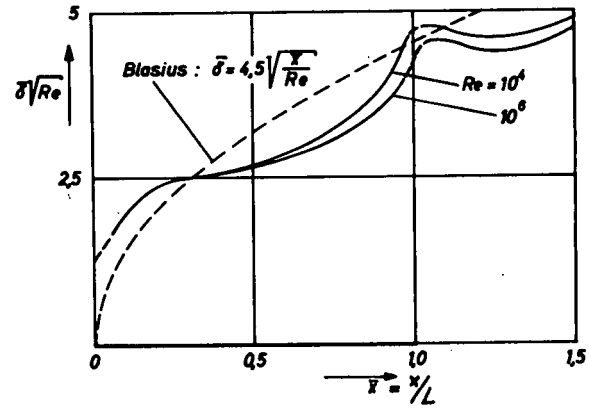

Fig. 4 Boundary-layer thickness $\bar{\delta} = \delta/L$

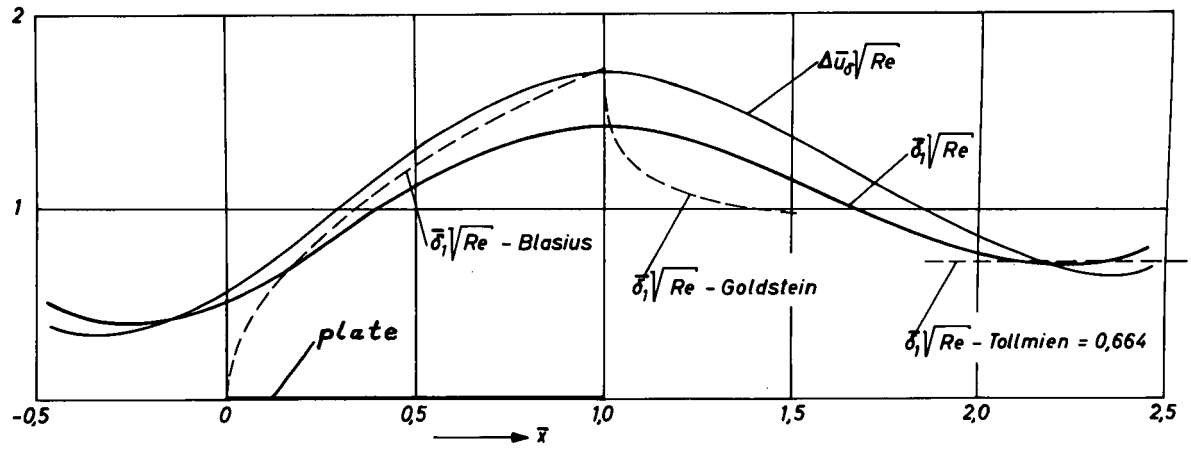

Fig. 5 Displacement thickness $\bar{\delta}_1 = \delta_1/L$ and velocity overshoot

$\Delta\bar{u}_\delta = \frac{u_\delta - U}{U}$ at large Re-numbers.

The use of the method of integral relations for the numerical solution of the Navier-Stokes equations was shown by an approximate calculation of the laminar flow over a flat plate of finite length at large Reynolds numbers [1]. The calculations were extended to regions upstream and downstream of the plate, as well. The numerical solution of the system - it consisted of four non-linear differential equations of the third order in this case - did not offer fundamental difficulties. The singularities at the leading and trailing edge occurring in other methods did not appear. The results, some of them shown in Figs. 1 to 8, are in good agreement with other work and supply some new information: especially on the existence of the velocity overshoot and its maximum value $\Delta u_\delta = u_\delta - U$ at $y = \delta$, where δ is exactly defined, and on the distribution of skin friction. The calculations are not very good in regions in front of the plate and in the wake for reasons given in [1]. So displacement thickness δ_1 should tend steadily to zero there, forming an apparent body with cusp-nosed leading edge. As a surprising result c_f has a tendency to vanish at the leading and trailing edge, which seems to be physically reasonable.

The advantage of the method may be seen in its transparency to physical understanding and in its relatively small calculation effort. Application to turbulent flow is possible.

References

[1] Gerking, L. Ein Verfahren zur Lösung der Navier-Stokesschen Gleichungen mit Integralbedingungen und seine Anwendung auf die Strömung um eine endlich lange ebene Platte. Diss. Universität Karlsruhe. (1967).

[2] Gerking, L. Ergebnisse aus Integralbedingungen zur Navier-Stokesschen Gleichung. Deutsche Luft- und Raumfahrt, Mitt. 68-33. (1938).

[3] Gerking, L. Integralbedingungen für reibungsbehaftete inkompressible Strömungen. Ing. Archiv. (To be published 1969).

10.

AN APPROXIMATE METHOD FOR THE SOLUTION OF THE NAVIER-STOKES EQUATIONS USING INTEGRAL RELATIONS AND ITS APPLICATION TO THE FLOW OVER A FLAT PLATE OF FINITE LENGTH

L. Gerking
University of Karlsruhe

The method of integral relations, known as a successful method in boundary-layer theory, has been applied in a modified form to the solution of the complete Navier-Stokes equations. By multiplying the vorticity equation with powers of the distance from the body, followed by integration across the whole flow field vertical to the incident flow, a set of an infinite number of ordinary differential equations is obtained. These are for two-dimensional incompressible flow:

$$\int_{-\infty}^{\infty} y^n \frac{\partial u\omega}{\partial x}\,dy + \int_{-\infty}^{\infty} y^n \frac{\partial v\omega}{\partial y}\,dy = \nu \int_{-\infty}^{\infty} y^n \left(\frac{\partial^2\omega}{\partial x^2} + \frac{\partial^2\omega}{\partial y^2}\right) dy \qquad (1)$$

$n = 0,1,2 \ldots$

for axisymmetrical incompressible flow:

$$\int_{-\infty}^{\infty} r^n \frac{\partial w\omega}{\partial z}\,dr + \int_{-\infty}^{\infty} r^n \frac{\partial u\omega}{\partial r}\,dr = \int_{-\infty}^{\infty} r^n \left(\frac{\partial^2\omega}{\partial z^2} + \frac{\partial^2\omega}{\partial r^2} + \frac{1}{r}\frac{\partial\omega}{\partial r} - \frac{\omega}{r^2}\right) dr \qquad (2)$$

$n = 1,2,3 \ldots$

for two-dimensional compressible flow: $\left(\text{with } q = \frac{u^2 + v^2}{2}\right)$

$$\int_{-\infty}^{\infty} y^n \frac{\partial\rho u\omega}{\partial x}\,dy + \int_{-\infty}^{\infty} y^n \frac{\partial\rho v\omega}{\partial y}\,dy + \int_{-\infty}^{\infty} y^n \left(\frac{\partial\rho}{\partial x}\frac{\partial q}{\partial y} - \frac{\partial\rho}{\partial y}\frac{\partial q}{\partial x}\right) dy \qquad (3)$$

$$= \int_{-\infty}^{\infty} y^n \left\{ \frac{\partial^2\mu\omega}{\partial y^2} + \frac{\partial^2\mu\omega}{\partial x^2} - 2\frac{\partial^2}{\partial y^2}\left(\mu\frac{\partial v}{\partial x}\right) + 2\frac{\partial^2}{\partial x^2}\left(\mu\frac{\partial u}{\partial y}\right) - 2\frac{\partial^2}{\partial y\,\partial x}\left[\mu\left(\frac{\partial u}{\partial x} - \frac{\partial v}{\partial y}\right)\right]\right\} dy$$

$n = 0,1,2 \ldots$

For flows in pipes and channels the integration is extended from one wall to the other. While the integrals exist in two-dimensional incompressible flow, by virtue of the exponential decay of vorticity ω, this has not yet been proved for the two other flow types.

Assumptions for the unknown functions have to be made with respect to y or r, respectively, to solve these equations, e.g. for ω in set (1):

$$\omega(x,y) = [a_0(x) + a_1(x)\,y]\, e^{-a_2(x)\,y^2} \qquad (4)$$

With a suitable assumption for the velocity profile $u(x,y)$ - v then follows from continuity equation - the integro-differential equations are transformed into ordinary differential equations, which serve to determine the unknown x-dependent parameters $a_0(x)$, $a_1(x)$ etc. Improvements for better approximation of the exact solution will lead to more parameters in the assumptions, and by consequence more equations have to be solved.

It is reasonable to start calculation with the first equations, because they have a physical meaning. So the second equations of the sets are momentum equations. They give the total change of momentum in planes vertical to the incident flow, supplying expressions for lift and drag. Some physical statements of basic interest may be derived from these integro-differential conservation laws, which refer not only to the momentum transfer, but with the third equations to the moment of momentum, and furthermore to the conservation of mass and energy [2,3]. Above all it can be shown that overshoots in velocity occur in every incompressible two-dimensional and axisymmetrical flow at some distance from the wall of a body placed into an infinitely large flow field of uniform velocity U. This holds as well for the infinitely thin flat plate of finite length at zero incidence, for

$$\int_{-\infty}^{\infty} (u - U)\,dy = 0 \qquad (5)$$

by consequence of mass conservation.

Notation

U_∞	Vitesse de l'écoulement à l'infini.
L	Longueur caractéristique de l'obstacle.
R	Nombre de Reynolds basé sur les conditions à l'infini.
ψ	Fonction de courant.
x	Abscisse curviligne d'un point de la paroi.
y	Distance normale à la paroi.
$\bar{x} = \frac{x}{L}$ $\bar{y} = \frac{y\sqrt{R}}{L}$ $\bar{\psi} = \frac{\psi\sqrt{R}}{LU_\infty}$	Variables couche limite
$\tilde{x} = \frac{xR^\delta}{L}$ $\tilde{y} = \frac{yR^\delta}{L}$ $\tilde{\psi} = \frac{\psi R}{LU_\infty}$	Variables Navier-Stokes
$\tau_f = \frac{2\rho_\infty U_\infty^2}{\sqrt{R}}\,\alpha(\bar{x})$	Frottement à la paroi
$\left(\frac{dp}{dx}\right)_e = \frac{6\rho_\infty U_\infty^2}{L}\,\beta(\bar{x})$	Gradient de pression extérieur.

Conclusion

L'hypothèse II étant très peu restrictive (elle élimine seulement les solutions conduisant à des vitesses infinies au point de separation comme $1/\rho^p$ avec $p > 1$), on peut dire que tout est basé sur la validité de l'hypothèse I.

Reprenant alors les deux questions soulevées au début, on peut apporter les éléments de réponse suivants:

1) Si l'hypothèse I est satisfaite, la solution de Prandtl est régulière au point de séparation ($\alpha = 1$). On peut alors penser qu'il n'existe pas de zone Navier-Stokes et, effectivement, l'ordre de grandeur de cette zone serait telle que $\delta = \frac{1}{2}$ d'apres (3), c'est-à-dire du meme ordre que l'epaisseur de la couche limite, ce qui est impossible, ainsi qu'on peut le montrer facilement à partir des résultats de [6] ; les équations de la couche limite sont alors valables au voisinage du point de decollement et, de plus, l'angle de séparation est soit d'ordre $1/\sqrt{R}$, soit égal à $\pi/2$ (point d'arrêt).

2) Si l'hypothèse I n'est pas satisfaite, l'étude présentée ici ne permet pas d'eliminer la solution singulière de Goldstein [1], pour laquelle $\alpha = \frac{1}{2}$; on a alors $\delta = 3/5$, valeur compatible avec les résultats de [6]. Il existe donc, dans cette hypothèse, une zone Navier-Stokes d'ordre de grandeur $LR^{-3/5}$.

Signalons, pour terminer, deux travaux récents qui viennent appuyer la thèse 1); Il s'agit, d'une part, d'un calcul numérique de Catherall et Mangler [8] qui montre que les équations de la couche limite sont capables de conduire à des solutions régulières, avec décollement, et, d'autre part, d'une etude théorique de Guiraud [9], qui aboutit à des conclusions analogues, à partir d'un modèle linéaire où l'équation de la chaleur joue le rôle de celle de Prandtl, et l'équation de Laplace, celle de Navier-Stokes.

References

[1] Goldstein, S. Quart. Jour. of Mech. and Appl. Math. 1, p. 43. (1948).

[2] Dean, W. R. Proc. Camb. Phil. Soc., 46. (1950).

[3] Stewartson, K. Quart. Jour. of Mech. and Appl. Math. 11, p. 399. (1958).

[4] Kaplun, S. Fluid mechanics and singular perturbations. Academic Press, New York-London. (1967).

[5] Brown, S. N. and K. Stewartson Laminar separation. dans Annual Review of Fluid Mechanics, 1, Palo Alto, Calif. (1969).

[6] Francois, C. Comptes rendus t. 267 - série A, p. 429. (1968).

[7] Francois, C. La Recherche Aérospatiale No. 121. (1967).

[8] Catherall, D. and Mangler, K. W. Journ. Fluid Mech. 26, No. 1, p. 163. (1966).

[9] Guiraud, J. P. Comptes rendus t. 268, série A, p. 239. (1969).

9.

ETUDE DU DECOLLEMENT SUR PLAQUE PLANE

Claude Francois
O.N.E.R.A., Paris

Le décollement de la couche limite laminaire en un point O d'une paroi où le rayon de courbure est modéré soulève les deux questions importantes de la validité des équations de Prandtl au voisinage de O et de la présence éventuelle d'une singularité en ce point. De nombreux auteurs se sont penchés sur ces questions, parmi lesquels il faut mentionner Goldstein[1], Dean[2], Stewartson[3] et Kaplun[4]. Il convient également de citer le remarquable article de synthèse dû récemment à Brown et Stewartson [5].

Le travail présenté ici, limité au cas incompressible et bidimensionnel, est basé sur l'idée que l'étude du seul voisinage de la paroi permet de linéariser les équations et de construire ainsi plus facilement la solution; on peut, en effet, montrer que lorsque la distance à la paroi tend vers zéro, l'écoulement est dominé par les effets visqueux. Il s'ensuit que, partout où il existe une couche limite, la solution, écrite dans le système de variables couche-limite, admet, au voisinage du corps, un développement de la forme (1):

$$\psi = \alpha(\bar{x})\,\bar{y}^2 + \beta(\bar{x})\,\bar{y}^3 + \ldots \qquad (1)$$

où $\alpha(\bar{x})$ représente le frottement à la paroi et $\beta(\bar{x})$ le gradient de pression extérieur.

S'il existe des zones où il est nécessaire de revenir aux équations de Navier-Stokes complètes, on retrouve, près du corps, l'équation de Stokes (2) écrite dans le système de variables Navier-Stokes.

$$\tilde{\Delta}(\tilde{\Delta}\,\tilde{\psi}) = 0 \qquad (2)$$

Désignant par $\alpha(\bar{x}) \sim \bar{x}^{\alpha}$ le comportement du frottement au voisinage du point de séparation O, l'étude du raccord couche limite ↔ zone Navier-Stokes, présentée dans [6], conduit à la conclusion que cette dernière région a pour dimension caractéristique $LR^{-\delta}$ avec:

$$\delta = \frac{3}{2(\alpha + 2)} \qquad (3)$$

On doit alors rechercher des solutions de (2), vérifiant la condition d'adhérence du fluide à la paroi (qui, à cette échelle, est un plan), et se comportant lorsque $x \to \infty$ comme $\tilde{y}^2\,\tilde{x}^{\alpha}$; pour ce faire, on écrit la solution de (2) sous la forme (4);

$$\tilde{\psi} = f(z) + \bar{f}(\bar{z}) + \bar{z}\,g(z) + z\,\bar{g}(\bar{z}) \qquad (4)$$

où $z = \tilde{y} + i\tilde{x}$, $\bar{z} = \tilde{y} - i\tilde{x}$, f et g désignant deux fonctions arbitraires et $\bar{f},\bar{g}$ leurs fonctions conjuguées.

La détermination de $f,g,\bar{f},\bar{g}$, envisagée en détail dans [7] utilise les techniques développées par Muskhelishvili et conduit à la solution (5);

$$\left.\begin{aligned}
\tilde{\psi} &= \tilde{\psi}_1 + \tilde{\psi}_2 \\
\psi_1 &= 4\,\mathrm{Re}\left\{\tilde{y}\,\frac{dP_1}{dz} + (2\tilde{y} + i\tilde{x})\,\frac{Q_1}{z^2} - \frac{\tilde{y}}{z}\,\frac{dQ_1}{dz}\right\} \\
\psi_2 &= 2\,\mathrm{Im}\left\{\tilde{y}\left(\frac{dP_2}{dz} - \frac{1}{z}\,\frac{dQ_2}{dz} + \frac{Q_2}{z^2}\right) - P_2\right\}
\end{aligned}\right\} \qquad (5)$$

Dans ces expressions P_1,Q_1,P_2,Q_2 désignent quatre polynômes arbitraires de la variable z^2 et Re { }, Im { } sont respectivement les parties réelles et imaginaires des parenthèses.

La solution (5) est obtenue sous réserve que soient satisfaites les hypothèses suivantes:

Hypothèse I: $f,g,\bar{f},\bar{g}$ sont holomorphes dans le demi plan $\tilde{y} > 0$ et de degré fini à l'infini.

Hypothèse II: $f',\bar{f}',g,\bar{g}$ vérifient, au point O, une condition de Holder du type:

$$\left|\Phi(z)\right| \leq \frac{C}{z^{p}}$$

(C = constante réelle positive et p constante réelle, inférieure à 1).

L'examen de (5) montre alors qu'il n'existe aucune solution présentant une ligne de séparation unique issue de O, et ayant le comportement voulu lorsque $|\vec{x}| \to \infty$ excepté si $\alpha = 1$ (Cf. [7]).

AGARD Conference Proceedings No.60 North Atlantic Treaty Organization, Advisory Group for Aerospace Research and Development NUMERICAL METHODS FOR VISCOUS FLOWS Published May 1970 83 pages This paper contains extended abstracts of papers presented at a Seminar organised by the Fluid Dynamics Panel of AGARD in September 1967 on this subject. Contents are divided into three sections: Solutions of the Navier-Stokes equations. Numerical methods for turbulent boundary layers. Solutions of the higher order boundary layer problems.	518.12:532.516	AGARD Conference Proceedings No.60 North Atlantic Treaty Organization, Advisory Group for Aerospace Research and Development NUMERICAL METHODS FOR VISCOUS FLOWS Published May 1970 83 pages This paper contains extended abstracts of papers presented at a Seminar organised by the Fluid Dynamics Panel of AGARD in September 1967 on this subject. Contents are divided into three sections: Solutions of the Navier-Stokes equations. Numerical methods for turbulent boundary layers. Solutions of the higher order boundary layer problems.	518.12:532.516
AGARD Conference Proceedings No.60 North Atlantic Treaty Organization, Advisory Group for Aerospace Research and Development NUMERICAL METHODS FOR VISCOUS FLOWS Published May 1970 83 pages This paper contains extended abstracts of papers presented at a Seminar organised by the Fluid Dynamics Panel of AGARD in September 1967 on this subject. Contents are divided into three sections: Solutions of the Navier-Stokes equations. Numerical methods for turbulent boundary layers. Solutions of the higher order boundary layer problems.	518.12:532.516	AGARD Conference Proceedings No.60 North Atlantic Treaty Organization, Advisory Group for Aerospace Research and Development NUMERICAL METHODS FOR VISCOUS FLOWS Published May 1970 83 pages This paper contains extended abstracts of papers presented at a Seminar organised by the Fluid Dynamics Panel of AGARD in September 1967 on this subject. Contents are divided into three sections: Solutions of the Navier-Stokes equations. Numerical methods for turbulent boundary layers. Solutions of the higher order boundary layer problems.	518.12:532.516

AGARD Conference Proceedings No.60
North Atlantic Treaty Organization, Advisory Group for Aerospace Research and Development
NUMERICAL METHODS FOR VISCOUS FLOWS
Published May 1970
83 pages

This paper contains extended abstracts of papers presented at a Seminar organised by the Fluid Dynamics Panel of AGARD in September 1967 on this subject. Contents are divided into three sections:

Solutions of the Navier-Stokes equations.

Numerical methods for turbulent boundary layers.

Solutions of the higher order boundary layer problems.

518.12:532.516

AGARD Conference Proceedings No.60
North Atlantic Treaty Organization, Advisory Group for Aerospace Research and Development
NUMERICAL METHODS FOR VISCOUS FLOWS
Published May 1970
83 pages

This paper contains extended abstracts of papers presented at a Seminar organised by the Fluid Dynamics Panel of AGARD in September 1967 on this subject. Contents are divided into three sections:

Solutions of the Navier-Stokes equations.

Numerical methods for turbulent boundary layers.

Solutions of the higher order boundary layer problems.

518.12:532.516

AGARD Conference Proceedings No.60
North Atlantic Treaty Organization, Advisory Group for Aerospace Research and Development
NUMERICAL METHODS FOR VISCOUS FLOWS
Published May 1970
83 pages

This paper contains extended abstracts of papers presented at a Seminar organised by the Fluid Dynamics Panel of AGARD in September 1967 on this subject. Contents are divided into three sections:

Solutions of the Navier-Stokes equations.

Numerical methods for turbulent boundary layers.

Solutions of the higher order boundary layer problems.

518.12:532.516

AGARD Conference Proceedings No.60
North Atlantic Treaty Organization, Advisory Group for Aerospace Research and Development
NUMERICAL METHODS FOR VISCOUS FLOWS
Published May 1970
83 pages

This paper contains extended abstracts of papers presented at a Seminar organised by the Fluid Dynamics Panel of AGARD in September 1967 on this subject. Contents are divided into three sections:

Solutions of the Navier-Stokes equations.

Numerical methods for turbulent boundary layers.

Solutions of the higher order boundary layer problems.

518.12:532.516

8. A NEW PROCEDURE FOR THE NUMERICAL SOLUTION OF THE ELLIPTIC EQUATIONS OF SIMULTANEOUS HEAT, MASS, AND MOMENTUM TRANSFER

D. B. Spalding
Imperial College, London

Nature of method

The method is a finite-difference, successive-substitution procedure, suitable for solving sets of simultaneous, non-linear, elliptic differential equations, of the type:

$$G.\ \text{grad}\ \phi = \text{div}\ (\Gamma_\phi\ \text{grad}\ \phi) + S_\phi$$

where: G is the mass-flux vector, obtainable by differentiating the stream function (which also obeys an equation of the above form, though simpler); ϕ is any dependent variable, such as vorticity, stagnation enthalpy, swirl velocity, concentration, kinetic energy of turbulent fluctuations, etc.; Γ_ϕ is an appropriate diffusion coefficient, dependent in any way on local conditions; and S_ϕ stands for a source or sink of the relevant property. The method is so far, confined to two-dimensional flows, whether plane or axisymmetrical.

Of several novelties in the method, the crucial one is the derivation of the difference equations from the differential ones by integration over a small region surrounding the grid point, coupled with the assumption that fluid crossing a boundary of this region carries the properties prevailing at the upstream grid point. (The label "tank-and-tube formulation" has been used, and is suggestive). Other novelties concern the handling of the boundary condition for vorticity, and the use of under-relaxation when large density variations are present.

Most of the novelties have been introduced so as to procure, first of all, unfailing convergence of the substitution procedure, and, secondly, high accuracy with modest computer time. Both objectives have been achieved, the first more completely than the second.

Applications made so far

The method has been applied to several physical situations in the last few months (up to September, 1967), including:

(i) Uniform-property laminar flows, namely: the flow of heat, vorticity and material in a square cavity with a moving lid; and the flow which arises when a jet impinges at right angles on to a wall. Reynolds numbers up to 10^8 have been used without divergence, even with coarse grids (10 x 10).

(ii) A non-Newtonian flow, namely: the flow of material and heat induced in a polymer, passing through the spiral passage of a screw extruder.

(iii) A turbulent impinging-jet flow. The Kolmogorov-Prandtl model of turbulence has been used; this necessitates the solution of the partial differential equation for the kinetic energy of turbulent fluctuations.

(iv) Flow in an axisymmetrical combustion chamber in which fuel and air enter through separate orifices at one end; mixing and combusion occur in the chamber; and combustion products flow out through the other end. The air enters with a swirling motion, so four simultaneous equations have to be solved in this case; the dependent variables are: stream function, vorticity, swirl velocity, and temperature. A solution is obtained, typically, in four minutes on an IBM 7090 computer.

Publications

The method is described in detail in a book by A. D. Crosman, W. M. Pun, A. K. Runchal, D. B. Spalding and M. Wolfshtein entitled "Heat and mass transfer in recirculating flows". This book will be published by Academic Press during June, 1969.

$$\lambda(x,\phi) = \sum_{n=1}^{\infty} g_n(x)\,\mu_n(\phi) \tag{14}$$

and then, by standard methods of orthogonal functions equation (11) is reduced to

$$\frac{dg_i}{dx} - \frac{(i-1)}{x}\,g_i = f_i(x), \quad (i = 1,2,3,\ldots), \tag{15}$$

where

$$f_i = -\frac{i}{4}\sum_{j=1}^{\infty}\left[A_{i,j}(x)\,\frac{dg_j}{dx} + \frac{2}{x}\{A_{i,j}(x) + B_{i,j}(x)\}\,g_j\right]$$

with

$$A_{i,j}(x) = \int_{-\infty}^{\infty} x\,\frac{\partial \Psi'}{\partial \phi}\,\mu_i(\phi)\,\mu_j(\phi)\,d\phi$$

$$B_{i,j}(x) = \left(\frac{j+1}{2}\right)^{i/2}\int_{-\infty}^{\infty} x^2\,\frac{\partial \Psi'}{\partial x}\,\mu_i(\phi)\,\mu_{j+i}(\phi)\,d\phi\ .$$

This method is suggested by the fact that at the limit point $z = 0$, the solution to equation (11) actually reduces to one of the modes (8).

Initial conditions for the functions $g_i(x)$ can be stated so that the system of equations (15) can be integrated to a given degree of precision using step-by-step methods. As each step of the solution is completed, the function $\lambda(x,\phi)$ can be computed and $\Psi'(x,\phi)$ determined from (12) by numerical integration. For example, in the case of any flow symmetrical about $\theta = 0$, the function $\lambda(x,\phi)$ is an odd function of ϕ and only the odd modes of (9) are involved. In this case a set of boundary conditions is

$$g_1(0) = 1,\ g_1(0) = 0, \quad (i = 3,5,7,\ldots)\ .$$

For general asymmetrical flows the problem is a little more complicated. All modes are present and a component generating from the fundamental solutions (8) with $n = 2$ must be included. This includes a further arbitrary constant, dependent upon the lift coefficient.

For small enough x, series solutions of the system of equations (15) and the equation (12) can be obtained. The general solution of (15) can be written

$$g_i(x) = x^{i-1}\int^{z'} t^{-(i-1)} f_i(t)\,dt + C_n\,x^{i-1}\ , \tag{16}$$

where the C_n are arbitrary constants determined from the initial conditions. A method of successive approximation is used to generate solutions for each $g_i(x)$ in the form of series

$$g_i(x) = \sum p_i^{(r,s)}\,x^r(\log x)^s\ , \tag{17}$$

where the $p_i^{(r,s)}$ are numerical coefficients. There is a corresponding series for $\Psi'(x,\phi)^i$

$$\Psi'(x,\phi) = \sum F^{(r,s)}(\phi)\,x^r(\log x)^s\ , \tag{18}$$

where the $F^{(r,s)}(\phi)$ are numerical functions of ϕ. It is hoped to publish full details of the results which have been obtained.

References

Filon, L. N. G. Proc. Roy Soc. A. 113, 7. (1926).
Imai, I. Proc. Roy Soc. A. 208, 487. (1951).
Chang, I. D. J. Math. Mech. 10, 811. (1961).
Kawaguti, M. J. Phys. Soc. Japan 8, 747. (1953).
Keller, H. B. and Takami, H. Numerical solution of non-linear differential equations. D. Greenspan Ed., J. Wiley (New York), p. 115. (1966)

It can be shown that equation (5) has a set of fundamental solutions at the limit point $z = 0$, As $z \to 0$, its limiting form is

$$2z\frac{\partial \chi}{\partial z} + \frac{\partial^2 \chi}{\partial \phi^2} - (1 + \phi^2)\chi = 0 \ . \tag{7}$$

By separation of variables, fundamental solutions of (7) are found to be

$$\chi_n = A_n z^{n+1} \mu_n(\phi) \ , \ (n = 0,1,2,\ldots) \tag{8}$$

where the functions μ_n satisfy

$$\mu_n'' + (2n + 1 - \phi^2)\mu_n = 0 \ , \tag{9}$$

primes denoting differentiation with regard to ϕ . The solutions of (9) are known to be

$$\mu_n = e^{-\phi^2/2} H_n(\phi)/\delta_n^{1/2} \ ,$$

where $H_n(\phi)$ are the Hermite polynomials and $\delta_n = 2^n n!(\pi)^{1/2}$ and is so chosen that

$$\int_{-\infty}^{\infty} \mu_n^2 \, d\phi = 1 \ .$$

The functions $\mu_n(\phi)$ are orthogonal in the range $(0,\infty)$ for ϕ . Finally it may be shown that if ζ is to have the correct behaviour as $z \to 0$ then $A_0 = 0$, and the leading term at $z = 0$ is

$$\chi_1 = A_1 z^2 \mu_1(\phi) \ .$$

Substitution of this in (6) leads to the limit point solution for Ψ

$$\Psi \sim -\frac{C_D}{\sqrt{\pi}} \int_0^{\phi} e^{-t} \, dt \ , \tag{10}$$

where C_D is the drag coefficient on the immersed body, in terms of which A_1 can be expressed by integrating the total stresses round a large contour in the fluid. It also turns out that all physical parameters of the solution can be removed from the basic equations and from the boundary conditions by making the substitutions

$$z = \frac{k}{2\alpha} x, \ \chi = A_1 \lambda z^2 \ , \ \Psi = \alpha \Psi' \ ,$$

where $\alpha = C_D/\pi^{1/2}$. Thus ultimately (6) and (7) become

$$\frac{\partial^2 \lambda}{\partial \phi^2} + \left(2 + \tfrac{1}{2}x\frac{\partial \Psi'}{\partial \phi}\right)x\frac{\partial \lambda}{\partial x} - \tfrac{1}{2}x^2\frac{\partial \Psi'}{\partial x}\frac{\partial \lambda}{\partial \phi} + \left(3 - \phi^2 + x\frac{\partial \Psi'}{\partial \phi} + \tfrac{1}{2}x^2\phi\right)\frac{\partial \Psi'}{\partial x}\lambda = 0 \tag{11}$$

and

$$\frac{\partial^2 \Psi'}{\partial \phi^2} = \delta_1^{1/2} \lambda e^{-\phi^2/2} \ . \tag{12}$$

For small enough z , the physical range $(-\pi, \pi)$ for the co-ordinate θ corresponds to the range $(-\infty, \infty)$ for ϕ and the boundary conditions are

$$\left.\begin{aligned} &\lambda(0,\phi) = \mu_1(\phi), \ \lambda(x,-\infty) = \lambda(x,\infty) = 0 \ , \\ &\frac{\partial \Psi'}{\partial \phi}(x,-\infty) = \frac{\partial \Psi'}{\partial \phi}(x,\infty) = 0 \ . \end{aligned}\right\} \tag{13}$$

It is possible to integrate the two equations (11) and (12) numerically subject to the conditions (13). It is also possible to reduce (11) to a set of ordinary differential equations by the following procedure. Put

7. A NUMERICAL METHOD FOR CALCULATING TWO-DIMENSIONAL WAKES

S. C. R. Dennis
University of Western Ontario

It is known that it is possible to obtain a solution of the Navier-Stokes equations for the steady two-dimensional motion of an incompressible fluid which is valid at large distances from a body submerged in the fluid. The problem was considered by Filon (1926) and subsequently developed by Imai (1951) and I. D. Chang (1961). These solutions are to some extent arbitrary since they contain unknown constants. However, the constants can be definitely fixed when the lift and drag on the body are known and then the solution is completely determined. In recent times some use has been made of Imai's solution by Kawaguti (1953) and Keller and Takami (1966) in computing numerical solutions of the flow past a circular cylinder. Thus solutions of this kind are of practical, as well as theoretical, interest. The main difficulty in obtaining solutions by purely analytical methods is that successive approximations, on which the methods usually depend, rapidly build up in complexity. In the present paper a method is considered in which the analysis is developed partly analytically and partly numerically. By employing numerical analysis, successive approximations to the Navier-Stokes equations can be carried much farther.

All quantities are assumed to be dimensionless. Let (ξ,θ) represent modified polar co-ordinates, the variable ξ being related to the polar distance r by the equation $\xi = \log r$. Then the equations governing steady motion are known to be, in terms of the stream function ψ and vorticity magnitude ζ,

$$\nabla_1^2 \psi + r^2\zeta = 0 \tag{1}$$

$$\nabla_1^2 \zeta = \frac{R}{2}\frac{\partial(\psi,\zeta)}{\partial(\theta,\xi)} \tag{2}$$

where $\nabla_1^2 = \partial^2/\partial\xi^2 + \partial^2/\partial\theta^2$ and $R = Ud/\nu$ is the Reynolds number based on a representative length d. If the external flow is a steady stream parallel to $\theta = 0$, the stream function of the potential flow is $r \sin\theta$ and it is customary to work in terms of a perturbation stream function Ψ such that

$$\psi = \Psi + r \sin\theta . \tag{3}$$

The first approximation to the vorticity of the outer flow is obtained by substituting (3) in (2) and neglecting products of derivatives of Ψ and ζ, assumed small. This is the Oseen solution and from it can be deduced the fact that, for large r, the vorticity is essentially confined to a narrowing region of the (ξ,θ)-plane distributed about the axis $\theta = 0$ with breadth (in the angle θ) proportional to $r^{-1/2}$. This gives rise to an expanding parabolic vorticity wake in the (x,y)-plane. For this reason, Imai employed a transformation of the Cartesian form of the equations to a system of parabolic co-ordinates and then used methods of the complex variable to obtain approximations to the equations.

In the present method a different procedure is adopted. The form of the vorticity wake at large distances indicates that one should scale the co-ordinate θ with respect to the breadth of the wake. At the same time it is convenient to identify $r = \infty$ with the origin of a new co-ordinate z, and also introduce a change in the variable ζ. Thus the change of variables

$$z = r^{-1/2}, \quad \theta = 2kz\phi, \quad \zeta = \chi e^{-\phi^2/2}, \tag{4}$$

are made, where $k = (2/R)^{1/2}$. If these are substituted in (2) it is found that certain terms may be omitted if z^2/R is small, and equation (2) becomes

$$\left(2 + \frac{z}{k}\frac{\partial\Psi}{\partial\phi}\right)z\frac{\partial\chi}{\partial z} + \frac{\partial^2\chi}{\partial\phi^2} - \frac{z^2}{k}\frac{\partial\Psi}{\partial z}\frac{\partial\chi}{\partial\phi} - \left(1 + \phi^2 - \frac{z^2\phi}{k}\frac{\partial\Psi}{\partial z}\right)\chi = 0 . \tag{5}$$

The perturbed stream function Ψ satisfies the same equation (1) as ψ. If z^2/R is small, the equation for Ψ is

$$\frac{\partial^2\Psi}{\partial\phi^2} + \frac{8}{Rz^2}e^{-\phi^2/2}\chi = 0 . \tag{6}$$

These are the two basic equations from which the solution at large distances (or for large enough R) is derived.

6. ECOULEMENT PLAN D'UN FLUIDE VISQUEUX INCOMPRESSIBLE AUTOUR D'UN OBSTACLE S'ETENDANT A L'INFINI AVAL

Robert Legendre
Ingénieur Général du Génie Maritime
Directeur Technique de l'O.N.E.R.A., Paris

La méthode d'approximations successives utilisée ne fait pas appel à la théorie de la couche limite et ne fixe aucun ordre de grandeur pour le nombre de Reynolds rapporté à une dimension caractéristique de l'obstacle ou pour le nombre de Reynolds rapporté a l'abscisse curviligne.

Dans l'équation portant sur la fonction de courant, déduite des équations de Navier-Stokes, le Laplacien du Laplacien est séparé et les autres termes sont supposés connus d'après les approximations précédentes. Une fonction de Green convenable, satisfaisant à la condition d'adhérence intègre l'equation ainsi simplifiée. La première approximation doit être celle de Blasius.

Un artifice est utilisé pour que la singularité à l'infini de la fonction de courant, qui est très compliquée, ne compromette pas la convergence de l'intégrale fournissant la nouvelle approximation. Il suffit de substituer au calcul de la fonction de courant celui d'une correction et toutes les approximations successives sont asymptotiques à l'approximation de Blasius à l'infini.

Reference

The complete text has been published by ONERA, TP no. 505. (1967).

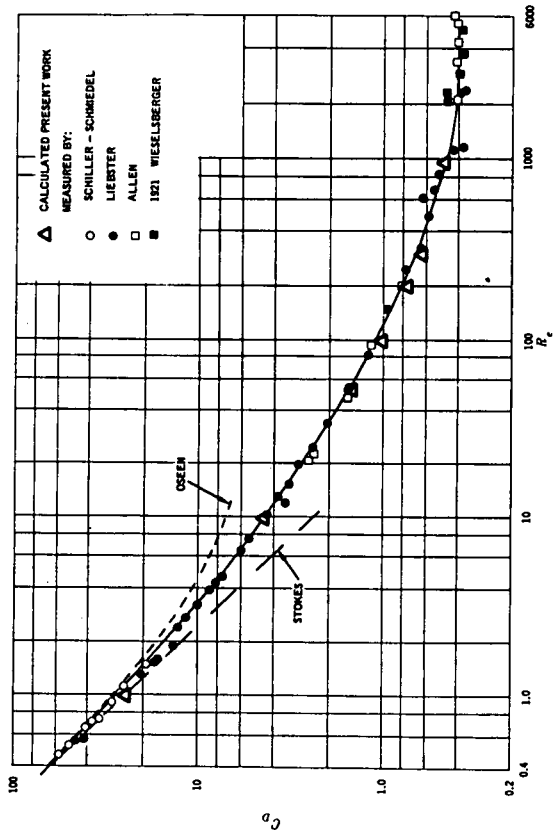

Drag Coefficient C_D versus Reynolds Number R_e (of Sphere)

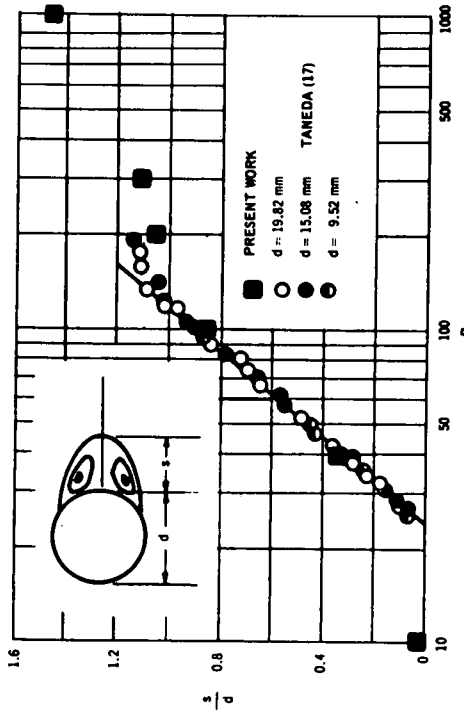

Plot of s/d Against Log R_e (Sphere)

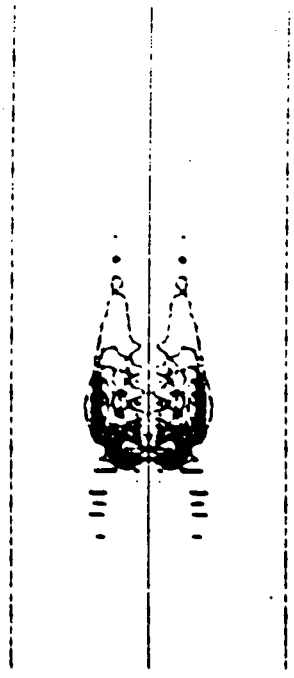

ISODINES CONST. FLOW MOVING WALL

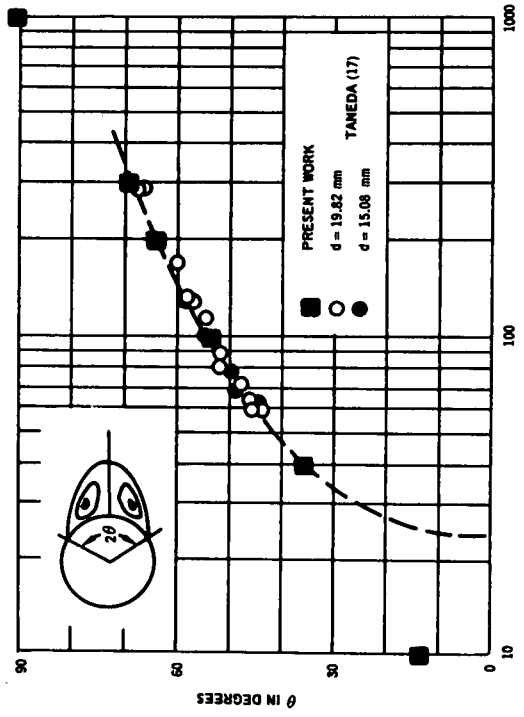

Position of the Separation (on Sphere)

computational accuracy. The wake side of the flow field is particularly sensitive to the outflow boundary condition. Computational accuracy is more critically tested by comparison with experimental data of the characteristics of the recirculatory wake. The angular location θ_s of the separation point and the length s/d of the recirculatory wake from our calculations did compare favourably with Taneda's data. (Fig. 3,4).

Taneda extrapolated the s/d vs. Re curve and inferred the absence of the recirculatory wake at $Re \lesssim 24$. The data of Nisi and Porter showed the first appearance of the recirculatory wake at $Re \sim 8$ or 9. Our calculation at $Re = 10$ indicated a small crescent shaped recirculatory wake one cell thick. No firm statement could be made in this regard.

Papers Published since September 1967 AGARD Seminar

Rimon, Y. Ph.D. Thesis (Princeton University). Also available as ARL Report No. ARL 69-0063, Wright Patterson Air Force Base, Dayton, Ohio. (1967).

Rimon, Y. and Cheng, S. I. Numerical solution of a uniform flow over a sphere at intermediate Reynolds numbers.
Physics of Fluids, Vol. 12, No. 5, p. 949. (May 1969).

Cheng, S. I. Accuracy of difference formulation of Navier-Stokes equations.
Proceedings of the First International Symposium of High Speed Computing in Fluid Dynamics, sponsored by IUTAM, 1968. To appear in Physics of Fluids.

Rimon, Y. Numerical solution of the incompressible time-dependent viscous flow past a thin oblate spheroid.
Proceedings of the First International Symposium of High Speed Computing in Fluid Dynamics, sponsored by IUTAM, 1968. To appear in Physics of Fluids.

5.

NUMERICAL SOLUTION OF TIME-DEPENDENT INCOMPRESSIBLE VISCOUS FLOWS OVER A DISK OR A SPHERE[1]

Y. Rimon[2] and S. I. Cheng[3]
Princeton University, Princeton, N.J.

The Navier-Stokes equations for the axi-symmetric flow of an incompressible fluid over a disk or a sphere were solved by a finite difference method for $10^3 \geq Re \geq 1$. Time-dependent stream function-vorticity formulation was adopted with a centred difference scheme of second order accuracy both in time DuFort-Frankel) and in space. For the disk case, we encountered difficulties in implementing boundary conditions with the velocity components defined at the mid-points of the mesh cells. For the sphere case, all dependent variables were defined on mesh points. Linearized stability criteria guided the selection of an empirical stability relation between time and space increments. This was satisfactory even when a local, large disturbance was introduced after initial stage of the computation. In the initial stage, however, time increments much smaller than those suggested by the linearized stability criteria must be used to keep the fractional change of the vorticity over a time step small everywhere. The initial flow field was taken as the inviscid flow as if the body were impulsively started from rest. At lower Reynolds numbers ($Re \lesssim 10$ for the sphere case) the inviscid solution was totally inadequate, and the Stokes solution was used instead.

The flow is contained in a pipe moving with the speed of the uniform or the mean flow entering the pipe. The pipe to obstacle diameter ratio is about eight. No-slip boundary condition was used on the solid obstacle. The periodic inflow-outflow boundary condition, although convenient, is not desirable on physical grounds. With a constant uniform inflow, the boundary condition of out-flow becomes a serious problem. Not only that computational instability could result from apparently reasonable out-flow conditions but that the structure of the wake flow obtained from stable computations was significantly influenced by the different choices of the out-flow boundary conditions. The condition that the streamlines leaving the downstream boundary are parallel to the axis of symmetry was found satisfactory based on comparison of calculated results with experimental data.

The disk was one cell thick and four cells diameter located on axial and radial co-ordinate lines with sharp corners. Around these corner points, different difference treatments led to significantly different flow fields. Without knowing the analytic nature of the flow singularity or a detailed description of the flow field from experiments around such sharp corners, we could not make a judicious choice. It is futile to hope that our approximate treatment of such corner points might localize the errors to within their immediate vicinity. Under the circumstances, even with many more points representing the disk surface, the results could at best be of qualitative value. All the contour plots of streamlines, vorticity lines and streaklines so obtained did look quite reasonable. At higher Reynolds numbers, ($Re = 300$), lines of equal vorticity broke away as closed loops, displaying the characteristics of the shedding of ring vortices from the rear of the recirculatory wake (Fig. 1). The Strouhal number of the shedding is about 1·5, somewhat higher than but of the correct order of magnitude as the experimental values.

With the details of the flow field in the vicinity of the disk possibly in substantial error, the drag on the disk could not be determined from surface stresses. The momentum balance over a large closed contour enclosing the disk did yield drag coefficients of reasonable magnitudes, but inevitably distorted by the approximate boundary conditions on the pipewall and on the downstream outflow boundary.

The calculations for the uniform flow over a sphere was aimed at obtaining quantitative results. The sphere surface was described by unit radius $r = 1$, or $z = o$, where $z = \ell n\ r$ was introduced in the spherical polar co-ordinate (r,θ,ϕ). Equal divisions in the (z,θ) plane put many more mesh points in the physical region near the sphere where large gradients of flow properties were expected. The fractional variations of the dependent variables over any cell were thus kept reasonably small and smooth over the entire field. The numerical solution was well behaved to permit the evaluation of the pressure and the shear stress on the spherical surface for drag determination.

The numerical solution was left free to choose its own large time behaviour within the restriction of axisymmetry. For all the cases computed, the flow field approached a "steady state" even for $Re \gtrsim 300$ when the physical wake was known to be time dependent with "periodic" shedding of asymmetric horseshoe like vortices. The computation for the case of $Re = 10^3$ was thus deliberately continued long after the "steady state" was apparently reached. The steady state persisted despite the accumulation of axisymmetric disturbances. It thus appears that the breakdown of the steady sphere wake is due to asymmetric disturbances.

The computed drag coefficient C_D agree well with the standard drag curve over the entire Reynolds number range 1 to 10^3 (Fig. 2). The agreement beyond $Re \gtrsim 300$ is clearly fortuitous. The drag coefficient, being an integrated property, may not be sensitive to the variations in the detailed structure of the flow field so that the temporal average of the sphere drag with extensive asymmetric shedding of vortices remain materially the same as that calculated from an axisymmetric steady configuration. Accordingly, the agreement of the drag coefficient is not likely a meaningful indication of

---

[1]This work was supported under contract AF 33617-67-C-1065 U.S.A.F.

[2]Present address: Naval Ship Res. and Dev. Center, Washington, D.C.

[3]Professor, AMS Department, Princeton University, Princeton, N.J.

4. DIFFERENCE APPROXIMATION SOLUTIONS OF THE ACCELERATION OF A SPHERE IN A VISCOUS FLUID*

Paul Michael
Brookhaven National Laboratory
Upton, New York

Difference approximation techniques have been applied to the time dependent Navier-Stokes equation in order to calculate the accelerated motion of a sphere in an incompressible viscous fluid. A distinctive feature of the work reported here is that the velocity of the sphere (or equivalently the velocity of the fluid past a stationary sphere) and hence the boundary condition is a function of time. Attention has been focused upon the problem of a body starting from rest being acted upon by a constant external force (i.e. gravity) and retarded by drag forces. A pair of dimensionless quantities will determine the motion. One is the ratio of densities of the fluid and the sphere, the other is akin to the Grashoff number that is used in the description of convective flows. This latter parameter is essentially the ratio of the accelerating force to the viscous force; in this work it is defined as $a_o r_o^3 / \nu^2$ where a_o is the acceleration that the body would have in the absence of drag forces, r_o is the sphere radius, and ν is the kinematic viscosity.

The Navier-Stokes equation was written in spherical co-ordinates with the stream function and the vorticity as dependent variables. Values of the stream function and vorticity were defined on a mesh that has constant spacing in angle and is graded exponentially with increasing radius. Central differences were used for the approximation of spatial derivatives; the time derivative was treated by using an implicit method which is equivalent to taking central differences in time. The difference equations were solved by iteration with the aid of a CDC 6600 digital computer. Drag forces were calculated by considering the viscous dissipation of energy and the change of the kinetic energy of the disturbed fluid; this avoids difficulties that occur in the numerical calculation of the pressure.

Calculations have been done for various density ratios and Grashoff numbers. Results to be presented include the resulting Reynolds number as a function of the distance travelled by the sphere, flow configurations and information pertaining to the formation of the region of separated flow.

*Work performed under the auspices of the United States Atomic Energy Commission.

3. NUMERICAL SOLUTIONS OF THE NAVIER-STOKES EQUATIONS FOR TIME DEPENDENT FLOW PAST A CIRCULAR CYLINDER

Albin A. Szewczyk, Professor
Heat Transfer and Fluid Mechanics Laboratory
University of Notre Dame
Notre Dame, Indiana

David C. Thoman
Bendix Aerospace Division
South Bend, Indiana

and

John Kopfer, Research Assistant
Heat Transfer and Fluid Mechanics Laboratory
University of Notre Dame
Notre Dame, Indiana

The work describes the numerical integration of the complete Navier-Stokes equations for the time dependent two-dimensional flow of a viscous incompressible fluid over circular cylinders. Solutions for the Reynolds number range of 1 to 3×10^5 for the flow over stationary and rotating cylinders will be presented. In addition, the particular aspects of the study which we feel are of prime importance and will be discussed are: 1. The wide Reynolds number range covered without calculational instabilities and 2. The fine boundary layer definitions achieved.

Recent attempts have been made to extend the explicit finite difference technique to high Reynolds number flow conditions. These attempts have achieved only limited success. The main limitation has been the occurrence of numerical instabilities associated with the non-linear terms of the vorticity transport equation. In addition, the very thin boundary layers which occur at high Reynolds numbers require extremely small cells if adequate description of the flow development is to be achieved. This theoretical work represents a quantitative attempt to generalize the explicit finite difference method to curved body shapes and extend the method to high Reynolds numbers.

Since cell structure is of prime importance, a systematic variation of cell size in space and with Reynolds number provide cell patterns consistent with the structure of the solutions sought. In the low Reynolds number range, we divide the main flow region into rectangular cells. Boundary cells are formed of partial rectangular cells. The cell structure is so chosen that small cells are used in regions where high velocity gradients are anticipated and large cells used in regions of small gradients. Thus, the increments of the independent space variable are at all locations small compared to the local structure of the expected solutions. An explicit forward difference form was used for the vorticity transport equation. The employment of partial cells at the obstacle surface in conjunction with variable grid permits considerations of complex obstacle geometries. For high Reynolds numbers, i.e. thin boundary layers, we describe a hybrid co-ordinate system introduced to overcome the shortcomings of the rectangular mesh approach. In this system cylindrical co-ordinates are used near the cylinder and rectangular co-ordinates are used in the outer flow region. The two regions are solved simultaneously together with the interface cells between the two regions. Cells of very small radial extent are used very close to the body. The cell widths are varied with the particular Reynolds number being investigated.

Detailed descriptions of the boundary layer development as well as wake development were obtained. Results of the runs are presented in the form of digitally plotted streamlines, streaklines, vorticity and pressure contours. Pressure distributions on the cylinder surface, stagnation points and separation points are presented for various Reynolds numbers as well as drag, lift, and Strouhal numbers. These results are compared with published experimental and analytical values.

In addition, secondary vortex formations are compared with available flow visualization studies. Finally, recent data on the length of the stationary vortex pair attached to the downstream portion of the cylinder will be discussed and compared with the current available literature for various Reynolds numbers.

$$\underline{v}^{o} = \sum_{\nu=1}^{N} \zeta_\nu \underline{v}_\nu \,, \quad \zeta_\nu = \frac{\lambda^2}{\lambda_o^2} z_\nu$$

$$\underline{v}^{k+1} = \sum_{\nu=1}^{N} \zeta_\nu \underline{v}_\nu + R(\lambda_o)(\hat{L}(\lambda)-\hat{L}(\lambda_o))\underline{v}^k + R(\lambda_o)T(\lambda;\underline{v}^k) \,,$$

moreover $\lim_{|z|\to o} \|\tilde{\underline{v}}\| = 0$. $\underline{v}^*$ is a power series in $z_1, \ldots, z_N$, which converges for small values of $|z|$. Introducing this series in (5) one obtains a system of transcendental equations for the determination of z.

For the case $N = 1$ of a single eigenvalue detailed studies of the branching equation have been made. This case occurs when σ is chosen so that K_1 has the eigenvalue λ_o and all other kernels K_n have eigenvalues λ_n: $|\lambda| > \lambda_o$ (e.g. if σ is chosen in the minimum of the neutral eigenvalue curve in linear stability theory). In this case $\tilde{\underline{v}}$ is a power series in ζ. Moreover, the components of $\tilde{\underline{v}} = \{\tilde{u}_n, \tilde{v}_n, \tilde{w}_n\}$ have the form $\zeta^n F_\nu(r; |\zeta|^2)$, $\nu = 1,2,3$, where F_ν is a power series in $|\zeta|^2$ with coefficients depending on r. The branching equation (5) now writes:

$$0 = z\left\{\frac{\tau}{\lambda_o^2} + \sum_{\substack{\nu=1 \\ \mu=o}}^{\infty} b_{\nu\mu} |z|^{2\nu} \tau^\mu\right\} . \tag{6}$$

This equation has, besides $z = 0$, a continuum of solutions, since only $z_o = |z|$ is determined by (6). The general solution is of the form $z = z_o e^{i\alpha}$ with arbitrary α. But the special dependence of the components of $\tilde{\underline{v}}$ on z show that all these solutions of (2) generate solutions of the original boundary value problem which are transformed into each other by a translation in z-direction. The branching solution is unique up to translations in z-direction.

It follows from the results of Velte[1] that there is a first non-vanishing coefficient $b_{\nu o}$ and that $b_{\nu o}$ is negative. Therefore, there are no real branching solutions for $\lambda < \lambda_o$.

For special cases ($r_1 = 2$, $r_1 >> 1$) b_{1o} has been shown to be negative by numerical calculations and error analysis. Then, $\|\tilde{\underline{v}}\|$ behaves like $\sqrt{-\tau/b_{1o}\lambda_o^2}$ near λ_o.

References

[1] Velte, W. Stabilität und Verzweigung stationärer Lösungen der Navier-Stokesschen Gleichungen beim Taylor-Problem. Arch.Rat.Mech.Anal. 22, pp.1-14. (1967).

[2] Judovich, V. I. Secondary flows and fluid instability between rotating cylinders. PMM 30, pp.822-833. (1966).

[3] Vainberg, M. M., Trenogin, V. A. The methods of Lyapunov and Schmidt in the theory of non-linear equations and their further development. Russ.Math.Surv. 17, pp.1-60. (1962).

[4] Kirchgässner, K. Berechnung der Verzweigungslösungen eines hydrodynamischen Randwertproblems. ZAMM, 46, Sonderheft. (1966).

[5] Kirchgässner, K. Verzweigungslösungen eines stationären hydrodynamischen Randwertproblems. Habilitationsschrift, Universität Freiburg. (1966).

[6] Judovich, V. I. Free convection and bifurcation. PMM 31, pp. 101-111. (1967).

[7] Cörtler, H., Kirchgässner, K., Sorger, P. Branching solutions of the Benard-problem. Festschrift zum 60. Geburtstag von Prof. Sedov, in Druck.

$$\|\underline{v}\| := \sup_n \{n \cdot \mathrm{Max}(\|u_n\|_o, \|v_n\|_o, \|w_n\|_o) + \mathrm{Max}(\|u_o\|_o, \|v_o\|_o, \|w_o\|_o)\} .$$

It can be shown that (1) is an equation in B:

$$\underline{v} = L(\lambda)\underline{v} + T(\lambda;\underline{v}) . \tag{2}$$

L is a linear, completely continuous operator, T a quadratic operator, both acting in B. By estimates of the Greens functions entering (1), one obtains for any pair $\underline{v}^1, \underline{v}^2 \in B$:

$$\|T(\lambda;v^1) - T(\lambda;\underline{v}^2)\| \leq c(\|\underline{v}^1\| + \|\underline{v}^2\|)\ \|\underline{v}^1 - \underline{v}^2\| . \tag{3}$$

Therefore, L is the Fréchet-derivative of the operator defined by the right side of (2).

The linearized equation $\underline{v} = L(\lambda)\underline{v}$ has a positive eigenvalue $\lambda_o(\sigma)$, as is known from linear stability theory (cf. [1]). Let the (geometric) multiplicity be N. Then, there is a biothorgonal sequence $\underline{v}_\nu \in B$, $\underline{w}_\mu \in B^*$ (dual space of B)

with $$[\underline{w}_\mu, \underline{v}_\nu] = \delta_{\nu\mu}; \quad \nu, \mu = 1, \ldots, N$$

where $\underline{v}_\nu$, $\underline{w}_\mu$ are eigenelements of $L(\lambda_o)$ and $L^*(\lambda_o)$ (adjoint operator) respectively. $[\underline{w},\underline{v}]$ denotes the value of the functional $\underline{w} \in B^*$ in $\underline{v} \in B$.

We introduce the new variables $z_\mu := [\underline{w}_\mu, \underline{v}]$ and the linear operators P, L:

$$P\underline{v} := \sum_{\nu=1}^{N} z_\nu \underline{v}_\nu , \quad \underline{v} \in B$$

$$\hat{L}(\lambda) := L(\lambda) - \frac{\lambda^2}{\lambda_o^2} P .$$

$E - \hat{L}(\lambda_o)$ has a bounded inverse $R(\lambda_o)$ (Lemma of Schmidt [3]), (E = identity). Since $R(\lambda_o)$ $P\underline{v} = 0$, equation (2) can be written in the form:

$$\underline{v} = \frac{\lambda^2}{\lambda_o^2} P\underline{v} + R(\lambda_o)(\hat{L}(\lambda)-\hat{L}(\lambda_o))\underline{v} + R(\lambda_o)T(\lambda;\underline{v}) . \tag{4}$$

It is easily seen that the following relations hold:

$$[\underline{w}_\mu, R(\lambda_o)\underline{v}] = [\underline{w}_\mu, \underline{v}]$$

$$[w_\mu, \hat{L}(\lambda)\underline{v}] = 0 , \quad \underline{v} \in B .$$

Application of $\underline{w}_\mu$ to (4) yields the branching equations:

$$\begin{aligned} 0 &= \frac{\tau}{\lambda_o^2} z_\mu + [\underline{w}_\mu, T(\lambda;v)] , \quad \mu = 1, \ldots, N . \\ \tau &= \lambda^2 - \lambda_o^2 . \end{aligned} \tag{5}$$

The system (4) and (5) is equivalent to (2).

4. Numerical Methods and Results

Equation (4) can be solved iteratively. For small values of $|z|$ and $|\tau|$, $z = \{z_1, \ldots, z_N\}$, the right side of (4) defines by (3) in the sphere $S(P\underline{v};\delta)$, a Lipschitz bounded operator with a constant q with $q < 1$ for sufficiently small z, τ and δ. S is mapped into itself. By the contraction mapping principle, (4) has in S a unique solution $\underline{v}(r;z)$ which is the limit of the sequence:

2. AN ANALYTIC METHOD FOR THE CALCULATION OF BRANCHING SOLUTIONS OF HYDRODYNAMIC BOUNDARY VALUE PROBLEMS

Klaus Kirchgässner
Institut für Angewandte Mathemetik und
Mechanik der DVL, Freiburg

1. Abstract

It is a well established fact that the Couette flow between rotating cylinders becomes unstable if the Reynolds number exceeds a certain critical value λ_o. For $\lambda > \lambda_o$ a new steady flow pattern exists. It has been proven by Velte [1] and Judovich [2] independently that for $\lambda > \lambda_o$, and λ sufficiently close to λ_o, at least one new stationary solution of the corresponding non-linear boundary value problem exists which bifurcates from the Couette solution. The proof in both cases based on topological arguments was not a constructive one.

In this paper the method of Schmidt-Lyapunov [3] is applied to determine the number of branching solutions and to give an iterative procedure for the calculation of these solutions (cf. [4],[5]). The method can be applied to other bifurcation problems in hydrodynamic stability theory ([6],[7]).

2. Basic Equations

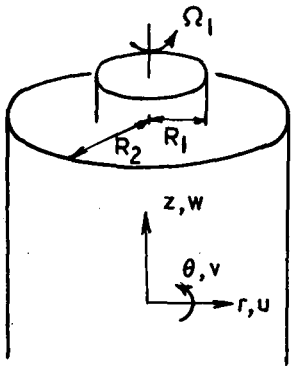

Figure 1

In Fig. 1 the Taylor model and the cylinder-co-ordinate-system used are described.

For small values of the Reynolds number $\lambda = \dfrac{R_1(R_2 - R_1)\Omega_1}{\nu}$ (ν = kinematic viscosity), the Couette solution $\underline{V}, P$ is unique. New steady solutions $\underline{v}, q$ of the Navier-Stokes equations which are independent of the angle θ are written in perturbation form ($\underline{u} = \{u,v,w\}$):

$$\underline{v}(r,z) = \underline{V}(r) + \underline{u}(r,z), \quad q(r,z) = P(r) + p(r,z) .$$

The basic equations for $\underline{u}, p$, obtained from the Navier-Stokes equation in cylinder co-ordinates together with the boundary conditions: $\underline{u} = 0$ for $r = r_1$ and $r = r_2$, ($r_\nu = R_\nu/(R_2 - R_1)$; $\nu = 1,2$) constitute a non-linear boundary value problem which can be transformed by means of the formal Fourier-expansions

$$\underline{u}(r,z) = \sum_{n=-\infty}^{\infty} \underline{u}_n(r) e^{-in\sigma z}, \quad p(r,z) = \sum_{n=-\infty}^{\infty} p_n(r) e^{-in\sigma z},$$

$$\sigma = 2\pi/L, \quad \underline{u}_n := \{u_n, v_n, w_n\}$$

$$\underline{u}_{-n} = \underline{u}_n^{\bullet} \text{ (conjugate complex of } \underline{u}_n)$$

elimination of the pressure and use of Green's functions into an infinite system of integral equations (cf. [5]):

$$\begin{aligned} u_n &= \lambda^2 K_n u_n + \lambda f_n(\underline{u}) \\ v_n &= -2a\lambda G_n u_n + \lambda g_n(\underline{u}) \\ w_n &= 2\,2in\sigma\lambda H_n v_n + \lambda h_n(\underline{u}), \quad n = 0,1, \ldots \end{aligned} \tag{1}$$

$K_o \equiv 0$. K_n, G_n, H_n are continuous kernels, f_n, g_n, h_n quadratic functionals in $\underline{u}$.

3. Function Space and Branching Equation

Let $\underline{v} = \{u_n, v_n, w_n;\ n = 0,1, \ldots\}$ be a sequence of functions continuous in $I := \{r;\ r_1 \le r \le r_2\}$, for which

$$\lim_{n\to\infty} n\{\|u_n\|_o, \|v_n\|_o, \|w_n\|_o\} = 0$$

where $\|u_n\|_o := \max_I |u_n(r)|$. These sequences form a Banach space with the norm

$u_\infty \to 0$, $\mathcal{F}$ has asymptotically the direction of the flow at infinity, and that $\mathcal{F}$ is asymptotically independent of the shape or size of Σ.

If u_∞ is large, smooth solutions continue to exist [Leray 1933], and in three dimensions they are known to tend continuously to u_∞ at infinity [Finn 1959, 1965; Ladyzhenskaia 1961; Fujita 1961]. However, the asymptotic structure of these solutions has not been clarified, and uniquess has not been established.

6. Stationary Solutions as Limits of Time Dependent Solutions

It is natural to expect that stationary flows past an obstacle can be obtained as limits of time dependent solutions, obtained by accelerating the obstacle from rest. The problem seems, however, to be difficult mathematically, owing to changing conditions at infinity. Tentative results have been obtained by Heywood (dissertation, Stanford University). In the case of motions which yield zero net force on Σ (e.g., rotation of a surface of revolution about its axis), Heywood solved the problem completely for small data.

1.

RECENT RESULTS IN THE MATHEMATICAL THEORY OF THE NAVIER-STOKES EQUATIONS

Robert Finn
Stanford University

Although the general mathematical theory of these equations is still in a somewhat fragmentary state, a number of striking and illuminating results is available. I shall describe some of them in this report.

1. The Initial Value Problem; Bounded Domain

Consider a bounded region $\mathfrak{D}$ filled with fluid which adheres at the boundary. The fluid is disturbed initially and then left free. If the disturbance is small, a unique smooth solution exists for all time, and the velocity field tends exponentially in time to zero [Kiselev and Ladyzhenskaia 1957; Kato and Fujita 1962; G. Prodi 1962; Shinbrot and Kaniel 1966]. For an arbitrary disturbance, it is known that at least one "solution" $u(x,t)$ exists in a generalized sense for all time [Leray 1934; E. Hopf 1951, Kato and Fujita 1962; Shinbrot and Kaniel 1966]. Its uniqueness has not been shown; however, each such $u(x,t)$ is a strict solution for all t except for a small (zero Lebesgue measure) bounded set. In particular, it is a strict solution for all sufficiently large t. Its kinetic energy satisfies an inequality $K < K_0 e^{-\alpha t}$, where K_0 and α are the same for all possible "solutions". There is speculation that the exceptional set consists of values of t at which energy can concentrate to produce local flow singularities and possibly bifurcations; precise information on this point is however not available.

For two-dimensional flows, no such exceptional set can occur. The equations admit a unique strict solution for all time [Ladyzhenskaia 1959; Lions and Prodi 1959].

Detailed studies of regularity properties of solutions can be found in Serrin (1962) and in Kaniel and Shinbrot (1967).

2. The Interior and Periodic Stationary Problems; Bifurcation

If $\mathfrak{D}$ is chosen as above, then for an (essentially) arbitrary given distribution of velocities on its bounding surface Σ, there corresponds at least one smooth time independent solution [Leray 1933; Ladyzhenskaia 1959; Fujita 1961]. This is the case even for data which experimentally could lead to turbulent solutions. Taylor instability provides an example of experimentally observed non-uniqueness of periodic stationary solutions. Although Taylor showed the appearance of multiplicities in the solutions of the perturbation equations, the first demonstrations that this occurs for the (non-linear) Navier-Stokes equations were given (independently) by Velte (1966), and by Iudovitch (1965). Both authors used abstract methods, based on the notion of topological degree of mappings in function space. Recently Rabinowitz obtained bifurcative solutions constructively for rectangular Bénard cells (Boussinesq approximation), and even showed that in that case new solutions appear in a neighbourhood of every eigen-value of the linearized equations. The appearance of time dependent bifurcations has not yet been shown, nor has the stability of the stationary solutions been investigated.

3. Connections with Boundary Layer Theory

Let $u(x)$ be a stationary solution of the Navier-Stokes equations in a two-dimensional region adjacent to a wall. If $u(x)$ exhibits qualitative characteristics of a boundary layer profile on a suitable entrance line, then it will be approximated downstream by the (unique) solution of the Prandtl equations having the same initial profile [Nickel 1963; Fife 1965]. The proof, although far from obvious, is in principle remarkably simple, the central tool being the maximum principle for parabolic equations. Further, any laminar solution of the Navier-Stokes equations adjacent to a wall will develop the indicated properties downstream if the pressure gradient is favourable [Fife 1966]. Fife also showed that a boundary layer cannot be expected to develop under all conditions.

4. Connections with Ideal Flows

Let $v(x;t)$ be a solution of the Euler equations defined in all of two-dimensional space, and let $u(x;t)$ be the (uniquely determined) solution of the Navier-Stokes equations, such that $u(x;0) = v(x;0)$. Then $|u(x;t) - v(x;t)| \to 0$ uniformly in x and in any interval $[0,T]$, $T < \infty$, as the Reynolds number $\to \infty$ [Golovkin 1966; McGrath 1967]. The corresponding situation in three dimensions seems ambiguous, particularly in view of the uncertainty about uniqueness of $u(x;t)$.

5. Stationary Flows Past an Obstacle

If, for given obstacle Σ and given fluid, the vector u_∞ is sufficiently small, there is a time-independent solution $u(x)$ of the Navier-Stokes equations defined in the exterior Ω of Σ, vanishing on its surface, and tending to u_∞ at infinity [Finn 1965; Finn and Smith 1967]. The solution exhibits the physically expected wake region behind the obstacle, and is asymptotic at infinity to a particular solution of Oseen's equations. In three dimensions, it is unique among all solutions satisfying a qualitative estimate at infinity. In two dimensions, uniqueness has been proved only among small solutions. In both cases, there holds $\mathcal{F} \cdot u_\infty = \int_\Omega (\mathrm{def}\, u)^2 \, dx$, where $\mathcal{F}$ is the force exerted on Σ in the flow. Thus, the (drag) force in the direction u_∞ cannot vanish. In two dimensions, there holds in addition $\lim_{|u_\infty| \to 0} \frac{\mathcal{F}}{\mu |u_\infty|} \log \frac{1}{|u_\infty|} = 4\pi \frac{u_\infty}{|u_\infty|}$. One concludes in particular that as

Part II - Solutions of the higher-order boundary-layer problem

LIST OF CONTENTS

(Items marked with an asterisk * are in their original unrevised form)

Comments on Part II of the Teddington Seminar (September 20th and 21st, 1967)

SOLUTIONS OF HIGHER-ORDER BOUNDARY LAYER PROBLEMS

M. R. Legendre, France

The two last days of the Seminar were mainly devoted to the discussion of the first and higher-order boundary layer approximations.

In this more classical field, there is less influence of the new methods for "numerical experiment" although the progress of high speed digital computers is important for an improvement of accuracy and gives the possibility to take into account the intricate phenomena which appear at hypersonic speeds.

When there is no risk of separation, it is quite clear that it is possible now to obtain good first-order approximations and to improve them methodically. Of the challenging problem of separation, which was dealt with already during my AGARD meetings, it must be said that it remains beyond the scope of computational techniques, although interesting approaches are already made.

The Seminar in Teddington was very useful in giving an account of the state-of-the-art and giving a starting point for reflexions on what remains to be done.

Comments on Part I of the Teddington Seminar (September 18th and 19th, 1967)

SOLUTIONS OF THE NAVIER-STOKES EQUATIONS

Prof. W. R. Sears, U.S.A.

In my opinion the first two days of the Seminar at Teddington achieved their objectives admirably and have been of great value. These were the days deovted to discussions of numerical solutions of the full equations of fluid flow, the Navier-Stokes equations.

This is a subject of tremendous importance to fluid-mechanicists today. It is clear to any alert observer that the subject of fluid mechanics, including aerodynamics, is being profoundly changed by the advent of high-speed digital computers. Flow-field calculations that were previously outside the scope of any reasonable undertaking are, or soon may be, reduced to routine practice in engineering design. As a result, ingenious techniques of approximation, developed over the decades, such as the inviscid fluid, boundary layers, strip theories, etc., may have much less significance as design tools in the future, even though their conceptual importance is not diminished. One imagines that the aerodynamicist of the future, faced with problems of flow around wings and bodies and through ducts and jets, as always, may have at his disposal a whole new realm of information as important to him as experimentation; namely, the "numerical experiment".

Nevertheless, as one who has attempted to organize meetings to permit fluid mechanicists to discuss these matters, the writer has sometimes encountered some frustrating attitudes. Even overlooking the few traditionalists who refuse to admit that computing machines exist, it has been difficult to get fluid mechanicists to discuss numerical computation rather than fluid mechanics. The idea that the computing machine is, in effect, something more than a faster desk-calculator has sometimes been difficult to put across.

The sessions of September 18th and 19th in Teddington were therefore surprising and very gratifying. The participants were nearly all specialists in this new, difficult, and rapidly developing art: the numerical modelling of fluid flow fields. The subject discussed and debated was, almost exclusively, numerical analysis. The context was, to be sure, fluid mechanics, but the points argued were matters like truncation errors, techniques of difference approximations to differential equations, error accumulation, and computational stability. There were also papers relating to the pure-mathematical basis of this subject (although, as usual, the practitioners of the art appear to have run far ahead of the rigorous proofs that would guarantee their work). A most intriguing feature of the meeting, and one that may be a forecast of many more debates in the future, was discussion of the questions: Is computational instability ever related to fluid-mechanical instability? What is the significance of computations carried out at Reynolds numbers above the value for stable laminar flow? What are the computational evidences of turbulence?

The progress achieved in the subject in the last several years is most impressive. Just a few years ago it could be said that no Navier-Stokes flow field had ever been calculated for flow past a smooth obstacle; the phenomena of boundary layer, separation, and wakes had never been "discovered" by a Navier-Stokes calculation. At this Seminar it became clear that this is no longer true. To be sure, most of the cases worked out to date are those for which the answers are already known: they have been test cases for the techniques. It seems certain that the next step will be to calculate cases for which the answers are not known - there are many of these in practical aerodynamics, where knowledge beyond the scope of boundary-layer theory is desired and is not available.

In summary, the first half of the Seminar seems to have attained its goals. The right people were there, debate was lively, and the right subjects were discussed.

Introduction

In 1967 the Fluid Dynamics Panel of AGARD decided to hold, in addition to the formal Specialists' Meetings for the year, a special Seminar on 'Numerical Methods for Viscous Flows'. This took place at the National Physical Laboratory, Teddington, from September 18th to 21st, 1967, and was attended by about 100 delegates from most of the member countries of NATO.

Thirty three lectures were given, together with informal discussions and a final session in which numerical results for some examples in hypersonic boundary layer theory, set in advance, were obtained by various methods and the results compared. The speakers were not required to write formal papers, only extended abstracts to be issued in advance, and it was not originally intended to publish any form of proceedings. However, the success of the Seminar and the wide interest it aroused has led to a large number of requests for information about it, and so the Panel has now decided to publish a volume containing the authors' abstracts for their papers. The opportunity has been taken of asking the authors to revise their contributions, thus allowing them to update the material and references; though of course this volume does not necessarily present a really up-to-date picture of the 'state of the art'.

The Seminar was divided into two principal parts, dealing respectively with methods for the full Navier-Stokes equations and with methods involving the approximations of boundary layer theory, either in its first or higher orders. It was also felt that the theory of turbulent boundary layers, involving as it does the solution of partial differential equations for the turbulence and boundary layer development, had reached a state when numerical methods of solution could usefully be discussed, and accordingly two additional papers (16 and 17) were included on this topic. After the meeting two members of the Programme Committee, Prof. W. Sears and M. R. Legendre, were asked to review the principal technical contributions; and their reviews follow this Introduction.

Members of the Programme Committee were:

Dr. R. Sedney, U.S.A. (Chairman)
M. P. Carrière, France
Dr. J. Lukasiewicz, U.S.A.
Dr. R. C. Pankhurst, U.K.
Prof. J. A. Steketee, Netherlands

SUMMARY

This paper contains a collection of extended abstracts of papers presented at the Seminar on Numerical Methods for Viscous Flows, organised by the Fluid Dynamics Panel of AGARD at the National Physical Laboratory, Teddington, UK in September 1967. The contents are divided into three sections, dealing respectively with

Solutions of the Navier-Stokes equations

Numerical methods for turbulent boundary layers

Solutions of the higher order boundary layer problem.

Contributions were received from five NATO countries.

RESUME

Le présent ouvrage constitue un recueil de sommaires étendus des exposés présentés au National Physical Laboratory, Teddington, UK en septembre 1967 dans le cadre du programme de conférences sur "Les Méthodes Numériques pour les Ecoulements Visqueux" organisé par la Commission de la Dynamique des Fluides de l'AGARD.

Les matières traitées se divisent en trois parties, couvrant respectivement les sujets suivants:

- Solutions des équations Navier-Stokes
- Méthodes numériques pour couches limites turbulentes
- Solutions du problème de la couche limite d'ordre supérieur.

Des contributions ont été reçues de cinq pays membres de l'OTAN.

518.12:532.516

Printed by Technical Editing and Reproduction Ltd
Harford House, 7-9 Charlotte St, London. W1P 1HD

AGARD Conference Proceedings No.60

NORTH ATLANTIC TREATY ORGANIZATION

ADVISORY GROUP FOR AEROSPACE RESEARCH AND DEVELOPMENT

(ORGANISATION DU TRAITE DE L'ATLANTIQUE NORD)

NUMERICAL METHODS FOR VISCOUS FLOWS

Abstracts of papers presented at a Seminar held by the Fluid Dynamics Panel of AGARD at the National Physical Laboratory, Teddington, U.K., 18-21 September 1967

Edited by R. C. Lock (N.P.L.)

1967

NATIONAL DISTRIBUTION CENTRES FOR AGARD PUBLICATIONS

AGARD publications are distributed to NATO Member Nations through the National Distribution Centres listed below.

BELGIUM
General J.DELHAYE
Coordinateur AGARD - V.S.L.
Etat Major Forces Aériennes
Caserne Prince Baudouin
Place Dailly, Bruxelles 3

CANADA
Director of Scientific Information Services
Defence Research Board
Department of National Defence - 'A' Building
Ottawa, Ontario

DENMARK
Danish Defence Research Board
Østerbrogades Kaserne
Copenhagen Ø

FRANCE
O.N.E.R.A. (Direction)
29, Avenue de la Division Leclerc
92. Châtillon-sous-Bagneux

GERMANY
Zentralstelle für Lüftfahrdokumentation
und Information
Maria-Theresia Str. 21
8 München 27
Attn: Dr Ing. H.J.RAUTENBERG

GREECE
Hellenic Armed Forces Command
D Branch, Athens

ICELAND
Director of Aviation
c/o Flugrad
Reykjavik

ITALY
Aeronautica Militare
Ufficio del Delegato Nazionale all' AGARD
3, P. le del Turismo
Roma/Eur

LUXEMBOURG
Obtainable through BELGIUM

NETHERLANDS
Netherlands Delegation to AGARD
National Aerospace Laboratory, NLR
Attn: Mr A.H.GEUDEKER
P.O. Box 126
Delft

NORWAY
Norwegian Defense Research Establishment
Main Library, c/o Mr P.L.EKERN
P.O. Box 25
N-2007 Kjeller

PORTUGAL
Direccao do Servico de Material
da Forca Aerea
Rua de Escola Politecnica 42
Lisboa
Attn: Brig. General Jose de Sousa OLIVEIRA

TURKEY
Turkish General Staff (ARGE)
Ankara

UNITED KINGDOM
Ministry of Technology Reports Centre
Station Square House
St. Mary Cray
Orpington, Kent BR5 3RE

UNITED STATES
National Aeronautics and Space Administration (NASA)
Langley Field, Virginia
Attn: Report Distribution and Storage Unit

★ ★ ★

If spare copies are not available at these centres, microfiche or hard copy (printed facsimile, or reproduction from microcopy) may be purchased from:

Clearinghouse for Federal
Scientific and Technical
Information (CFSTI)
Springfield
Virginia 22151, USA

ESRO/ELDO Space
Documentation Service
European Space Research Organization
114, Avenue de Neuilly
92, Neuilly-sur-Seine, France

The request for microfiche or hard copy of an AGARD document should include the AGARD serial number when available, title, author (or editor) and publication date; if known, the NASA Accession Number should also be quoted.

Full bibliographical references and abstracts of the newly issued AGARD publications are given in the following bi-monthly abstract journals with indexes:

Scientific and Technical Aerospace Reports (STAR) published by NASA,
Scientific and Technical Information Facility,
P.O. Box 33, College Park,
Maryland 20740, USA

United States Government Research and Development Report Index (USGDRI), published by the Clearinghouse for Federal Scientific and Technical Information, Springfield,
Virginia 22151, USA

Printed by Technical Editing and Reproduction Ltd
Harford House, 7-9 Charlotte St. London, W1P 1HD